NONLINEAR DYNAMICS AND SYSTEMS THEORY

An International Journal of Research and Surveys

Volume 19   Number 2   2019

CONTENTS

Nonlinear Dynamics and Systems Theory

An International Journal of Research and Surveys

INSTRUCTIONS FOR CONTRIBUTORS

(1) General. Nonlinear Dynamics and Systems Theory (ND&ST) is an international journal devoted to publishing peer-refereed, high quality, original papers, brief notes and review articles focusing on nonlinear dynamics and systems theory and their practical applications in engineering, physical and life sciences. Submission of a manuscript is a representation that the submission has been approved by all of the authors and by the institution where the work was carried out. It also represents that the manuscript has not been previously published, has not been copyrighted, is not being submitted for publication elsewhere, and that the authors have agreed that the copyright in the article shall be assigned exclusively to InforMath Publishing Group by signing a transfer of copyright form. Before submission, the authors should visit the website:

http://www.e-ndst.kiev.ua

for information on the preparation of accepted manuscripts. Please download the archive Sample_NDST.zip containing example of article file (you can edit only the file Samplefilename.tex).

(2) Manuscript and Correspondence. Manuscripts should be in English and must meet common standards of usage and grammar. To submit a paper, send by e-mail a file in PDF format directly to

Professor A.A. Martynyuk, Institute of Mechanics,
Nesterov str.3, 03057, MSP 680, Kiev-57, Ukraine
e-mail: journalndst@gmail.com

or to one of the Regional Editors or to a member of the Editorial Board. Final version of the manuscript must typeset using LaTex program which is prepared in accordance with the style file of the Journal. Manuscript texts should contain the title of the article, name(s) of the author(s) and complete affiliations. Each article requires an abstract not exceeding 150 words. Formulas and citations should not be included in the abstract. AMS subject classifications and key words must be included in all accepted papers. Each article requires a running head (abbreviated form of the title) of no more than 30 characters. The sizes for regular papers, survey articles, brief notes, letters to editors and book reviews are: (i) 10-14 pages for regular papers, (ii) up to 24 pages for survey articles, and (iii) 2-3 pages for brief notes, letters to the editor and book reviews.

(3) Tables, Graphs and Illustrations. Each figure must be of a quality suitable for direct reproduction and must include a caption. Drawings should include all relevant details and should be drawn professionally in black ink on plain white drawing paper. In addition to a hard copy of the artwork, it is necessary to attach the electronic file of the artwork (preferably in PCX format).

(4) References. Each entry must be cited in the text by author(s) and number or by number alone. All references should be listed in their alphabetic order. Use please the following style:

Journal: [1] H. Poincare, Title of the article. *Title of the Journal* **volume**
(issue) (year) pages. [Language]

Book: [2] A.M. Lyapunov, *Title of the Book.* Name of the Publishers, Town, year.

Proceeding: [3] R. Bellman, Title of the article. In: *Title of the Book.* (Eds.).
Name of the Publishers, Town, year, pages. [Language]

(5) Proofs and Sample Copy. Proofs sent to authors should be returned to the Editorial Office with corrections within three days after receipt. The corresponding author will receive a sample copy of the issue of the Journal for which his/her paper is published.

(6) Editorial Policy. Every submission will undergo a stringent peer review process. An editor will be assigned to handle the review process of the paper. He/she will secure at least two reviewers' reports. The decision on acceptance, rejection or acceptance subject to revision will be made based on these reviewers' reports and the editor's own reading of the paper.

NONLINEAR DYNAMICS AND SYSTEMS THEORY

An International Journal of Research and Surveys
Published by InforMath Publishing Group since 2001

CONTENTS

NONLINEAR DYNAMICS AND SYSTEMS THEORY

An International Journal of Research and Surveys

Impact Factor from SCOPUS for 2017: SNIP – 0.707, SJR – 0.316

Nonlinear Dynamics and Systems Theory (ISSN 1562–8353 (Print), ISSN 1813–7385 (Online)) is an international journal published under the auspices of the S.P. Timoshenko Institute of Mechanics of National Academy of Sciences of Ukraine and Curtin University of Technology (Perth, Australia). It aims to publish high quality original scientific papers and surveys in areas of nonlinear dynamics and systems theory and their real world applications.

AIMS AND SCOPE

Nonlinear Dynamics and Systems Theory is a multidisciplinary journal. It publishes papers focusing on proofs of important theorems as well as papers presenting new ideas and new theory, conjectures, numerical algorithms and physical experiments in areas related to nonlinear dynamics and systems theory. Papers that deal with theoretical aspects of nonlinear dynamics and/or systems theory should contain significant mathematical results with an indication of their possible applications. Papers that emphasize applications should contain new mathematical models of real world phenomena and/or description of engineering problems. They should include rigorous analysis of data used and results obtained. Papers that integrate and interrelate ideas and methods of nonlinear dynamics and systems theory will be particularly welcomed. This journal and the individual contributions published therein are protected under the copyright by International InforMath Publishing Group.

PUBLICATION AND SUBSCRIPTION INFORMATION

Nonlinear Dynamics and Systems Theory will have 4 issues in 2019, printed in hard copy (ISSN 1562–8353) and available online (ISSN 1813–7385), by InforMath Publishing Group, Nesterov str., 3, Institute of Mechanics, Kiev, MSP 680, Ukraine, 03057. Subscription prices are available upon request from the Publisher, EBSCO Information Services (`mailto:journals@ebsco.com`), or website of the Journal: `http://e-ndst.kiev.ua`. Subscriptions are accepted on a calendar year basis. Issues are sent by airmail to all countries of the world. Claims for missing issues should be made within six months of the date of dispatch.

ABSTRACTING AND INDEXING SERVICES

Papers published in this journal are indexed or abstracted in: Mathematical Reviews / MathSciNet, Zentralblatt MATH / Mathematics Abstracts, PASCAL database (INIST–CNRS) and SCOPUS.

Optimal Voltage Controller using T-S Fuzzy Model for Multimachine Power Systems

A. Abbadi, F. Hamidia, A. Morsli and A. Tlemcani [*]

Electrical Engineering and Automatic Research Laboratory LREA, Electrical Engineering Department, University of Medea, Algeria

Abstract: This paper presents an LMI approach to optimal fuzzy control based on the quadratic performance function to enhance the transient stability and achieve voltage regulation for multimachine power systems. First, the dynamic model of the power system has been modeled by Takagi-Sugeno fuzzy systems using the method of sum of products of linearly independent functions. The optimal fuzzy controller proposed is designed by solving the minimization problem that minimizes the upper bound of a given quadratic performance function. The stability conditions are represented in terms of LMIs. The proposed controller is applied to a two-machine three-bus power system. Simulation results illustrate the performance of the developed approach regardless of the system operating conditions.

Keywords: *multimachine power system; T-S fuzzy model; optimal fuzzy control; Lyapunov stability; linear matrix inequalities (LMI).*

Mathematics Subject Classification (2010): 03B52, 93C42, 94D05.

1   Introduction

System stability is the most important issue for power systems; traditionally, transient and voltage instability have been the most widespread stability problems. They concern the maintenance of the synchronism between generators as well as a steady acceptable voltage under normal operating and disturbed conditions.

Modern power systems are highly complex and nonlinear, and their operating conditions can vary over a wide range, therefore, the nonlinear characteristics of the power system and, hence, the nonlinear dynamic model of the system should be used in the analysis of transient stability and voltage regulation.

---

  [*] Corresponding author: `mailto:h_tlemcani@yahoo.fr`

One of many design techniques developed for modeling and control of nonlinear systems is the Takagi-Sugeno (T-S) one [1–7]. The approach mainly consists of three stages. The first stage is the fuzzy modeling for nonlinear controlled objects. There are two major ways in fuzzy modeling. One is the fuzzy model identification [2,3] using input-output data. The other is the fuzzy model construction (fuzzy IF-THEN rules) based on the idea of sector nonlinearity. The second stage is the fuzzy control rule derivation that mirrors the rule structure of a fuzzy model. It is realized by the so-called parallel distributed compensation (PDC) [4–6]. The third stage is the fuzzy controller design, i.e., the determination of feedback gains stated in terms of linear matrix inequalities (LMI) [5]; the stability is investigated using the quadratic Lyapunov function. Generally, such a design focuses on the stability issue only and does not satisfy certain performance criteria and constraints in an optimal fashion.

In the control design, it is often of interest to synthesize a controller to satisfy, in an optimal fashion, certain performance criteria and constraints in addition to stability [5].

In the linear case, the optimization problem is resolved by determining an optimal feedback of a Ricatti equation [8–10] . This type of controller is known under the name of a linear quadratic regulator problem (LQR). For the nonlinear systems, the problem requires the resolution of the Hamilton-Jacobi-Bellman (HJB) equation which represents a partial derivative equation [11, 12].

In the field of the power system stability, Kharaajoo in [13] has used an aproximative solution of the HJB equation to enhance the transient stability and achieve voltage regulation of a single-machine infinite-bus power system. The global control law is represented by the average of two control laws weighted by a sensitivity indicator such that the closed-loop power system is transiently stable when subjected to a fault, and restores the steady pre-fault voltage value after the disturbance. The analytical solution of this HJB equation was very difficult to be found, so an approximate method using the Taylor series expansion is used.

As the Takagi-Sugeno (T-S) fuzzy system is an efficient approach to model the nonlinear systems, Tanaka [5] proposed an alternative approach to nonlinear optimal control based on fuzzy logic. The optimal fuzzy control methodology presented is designed by solving a minimization problem that minimizes the upper bound of a given quadratic performance function. In strict sense, this approach is a suboptimal design. One of the advantages of this methodology is that the design conditions are represented in terms of LMIs.

This paper presents an optimal fuzzy controller design via convex optimization techniques based on LMIs to enhance the transient stability and achieve voltage regulation of multimachine power systems. The DFL technique has been used to linearize and decouple a nonlinear n-machine power system to n independent DFL compensated models. Then these compensated models are described by continuous-time T-S models. The fuzzy system is stabilized by the PDC fuzzy controller based on the minimization of the upper bound of a quadratic performance function.

To begin with, in Section 2, the background materials concerning the T-S fuzzy model and model-based fuzzy controller are introduced. In Section 3, the optimal fuzzy controller design is presented. The equivalent T-S fuzzy model of the multimachine power system is developed in Section 4. In Section 5, the control scheme proposed is implemented in a two-machine three-bus power system and simulation results are provided to demonstrate the performance of the proposed optimal voltage controller. Finally, conclusions are drawn in Section 6.

2   T-S Fuzzy Model and Control

2.1   T-S fuzzy model

A nonlinear system can be approximated by a T-S fuzzy model. The T-S model consists of a set of IF-THEN rules. Each rule represents the local linear input-output relation of the nonlinear system and has the following form:

Plant Rule i:

$$\begin{cases} \qquad \text{If } z_1(t) \text{ is } M_{i,1}.... \text{ and } z_p(t) \text{ is } M_{i,p}, \\ \text{then } \dot{x}_i = A_i x(t) + B_i u(t), i = 1, 2, ..., r. \end{cases} \tag{1}$$

Here $z(t) = \{z_1(t), ..., z_p(t)\}$ are known as premise variables, i.e., the nonlinear terms appeared in the system equations. Those premise variables are usually functions of the state variables. Also, $M_{i,j}$ is the fuzzy set, r is the number of model rules, A_i and B_i are the system and input matrices, respectively. It is assumed that (A_i, B_i) is a controllable pair. Also, x(t) is the system state vector, and u(t) is the input vector. The overall system dynamics is then described as

$$\dot{x} = \sum_{i=1}^{r} h_i(z(t))(A_i x(t) + B_i u(t)). \tag{2}$$

2.2   T-S model-based fuzzy control

The concept of PDC, following the terminology of [5], is utilized to design fuzzy state-feedback controllers on the basis of the T-S fuzzy models (1). In the PDC design, each control rule is designed from the corresponding rule of a T-S fuzzy model. The designed fuzzy controller shares the same fuzzy sets with the fuzzy model in the premise parts. For the fuzzy models (1), we construct the following fuzzy controller via the PDC:

Control rule i:

$$\begin{cases} \text{If } z_1(t) \text{ is } M_{i,1}....... \text{ and } z_p(t) \text{ is } M_{i,p}, \\ \qquad \text{then } u(t) = -K_i x(t), i = 1, 2, ..., r, \end{cases} \tag{3}$$

where K_i is a linear state feedback gain for the i-th subsystem. The overall fuzzy controller is represented by

$$u(t) = -\sum_{i=1}^{r} K_i x(t), \quad i = 1, 2, ..., r. \tag{4}$$

Substituting equation(4) into equation (2), the fuzzy control system (FCS) can be represented by (closed-loop)

$$u(t) = -\sum_{i=1}^{r}\sum_{i=j}^{r} h_i(z(t))h_j(z(t))(A_i - B_i K_j)x(t). \tag{5}$$

3   Optimal Fuzzy Controller Design

This section presents an optimal fuzzy controller design which consists in the determination of the control laws that minimize the upper bound of the following quadratic performance function:

$$J = \int_0^\infty (x^T(t)Wx(t) + u^T(t)Ru(t))dt, \tag{6}$$

where W and R are assumed to be a semi-positive definite matrix and a positive definite matrix, respectively [5]. Weighting matrices W and R are important components in the optimizing process of the fuzzy controller since they have great influences on system performance. Sufficient optimality conditions derived by Tanaka [5] for ensuring stability of (5) are given as follows

Theorem 3.1 *[5] The feedback gains to minimize the upper bound of the performance function can be obtained by solving the following LMIs. From the solution of the LMIs, the feedback gains are obtained as*

$$K_i = Y_i Q^{-1}$$

for all i. Then, the performance function satisfies $J < x^T(0)Px(0) < \gamma,$

minimize γ
$Q, Y_1, \ldots Y_r$ *subject to*

$$Q > 0,$$

$$\begin{pmatrix} 1 & x^T(0) \\ x(0) & Q \end{pmatrix} > 0, \tag{7}$$

$$\begin{pmatrix} QA_i^T + A_iQ - Y_i^T B_i^T - B_iY_i & Q\sqrt{W} & (-Y_i^T)\sqrt{R} \\ \sqrt{W}Q & -I & 0 \\ \sqrt{R}(-Y_i) & 0 & -I \end{pmatrix} < 0, \tag{8}$$

$$\begin{pmatrix} T & Q\sqrt{W} & \frac{\sqrt{2}}{2}(-Y_i^T)\sqrt{R} & \frac{\sqrt{2}}{2}(-Y_j^T)\sqrt{R} \\ \sqrt{W}Q & -I & 0 & 0 \\ \sqrt{R}(-Y_i)\frac{\sqrt{2}}{2} & 0 & -I & 0 \\ \sqrt{R}(-Y_j)\frac{\sqrt{2}}{2} & 0 & 0 & -I \end{pmatrix} < 0, \tag{9}$$

where $T = (\frac{QA_i^T + A_iQ}{2}) + \frac{QA_i^T + A_jQ}{2} - \frac{Y_i^T B_j^T + B_jY_i}{2} - \frac{Y_j^T B_i^T + B_iY_j}{2}.$

4   T-S Fuzzy Model of Power System

4.1   Dynamic model of power system

As the global control objective in this paper is to maintain the transient stability and achieve proper post-fault voltage of the multimachine power system, the dynamic model of the i-th generator adopted is given by the following equations:

$$\begin{cases} \Delta\dot{V}_{t_i}(t) = f_{i_1}(t)\Delta\omega_i(t) - \frac{f_{i_2}(t)}{T'_{d0i}}\Delta P_{ei}(t) + \frac{f_{i_2}(t)}{T'_{d0i}}v_{fi}(t), \\ \Delta\dot{\omega}_i(t) = -\frac{D_i}{2H_i}\Delta\omega_i(t) - \frac{\omega_0}{2H_i}\Delta P_{ei}(t), \\ \Delta\dot{P}_{ei}(t) = -\frac{1}{T'_{d0i}}\Delta P_{ei}(t) + \frac{1}{T'_{d0i}}v_{fi}(t). \end{cases} \tag{10}$$

where

$$u_{fi}(t) = \frac{1}{k_{ci}Iqi(t)}(v_{fi}(t) - T'_{d0i}E'_{qi}\dot{I}_{qi}(t) + P_{mi}) + \frac{1}{k_{ci}}((x_{di} - x'_{di})I_{di}(t)), \qquad (11)$$

is the direct feedback linearization (DFL)control law and $v_{fi}(t)$ is the feedback control law

$$v_{fi}(t) = -k_{v_i}\Delta V_i(t) - k_{\omega_i}\Delta\omega_i(t) - k_{p_{ei}}\Delta P_{ei}(t) \qquad (12)$$

and

$$\begin{cases} \Delta V_{t_i}(t) = V_{ti} - V_{ti0}, \\ \Delta\omega_i(t) = \omega_i - \omega_0, \\ \Delta P_{ei}(t) = P_{ei}(t) - P_{mi}, \end{cases} \qquad (13)$$

$$\Delta V_{t_i}(t) = V_{ti} - V_{ti0}, \Delta\omega_i(t) = \omega_i - \omega_0, \Delta P_{ei}(t) = P_{ei}(t) - P_{mi}, \qquad (14)$$

$$f_{i_1} = -\frac{(1 + x'_{di}B_{ii})(-E'^2_{qi}(t)B_{ii} - Q_{ei}(t)V_{ti}(t))}{V_{ti}(t)Ia_{qi}(t)} - \frac{x'_{di}(1 + x'_{di}B_{ii})P_{ei}(t)}{V_{ti}}, \qquad (15)$$

$$f_{i_2} = -\frac{(1 + x'_{di}B_{ii})V_{ti}(t)}{V_{ti}I_{qi}(t)}, \qquad (16)$$

where $\delta_i(t)$ is the angle of the i-th generator, in radian; $\omega_i(t)$ is the relative speed of the i-th generator, in rad/sec; Pmi is the mechanical input power, in p.u.; Pei (t) is the electrical power, in p.u.; ω_0 is the synchronous machine speed, in rad/sec, $\omega_0 = 2\pi f_0$; Di is the per unit damper constant; Hi is the inertia constant, in sec; E'qi(t) is the transient EMF in quadrature axis of the i-th generator, in p.u.; Efi(t) is the equivalent EMF in the excitation coil, in p.u.; Tdoi is the direct axis transient open circuit time constant, in second; Eqi is the EMF in quadrature axis of the i-th generator, in p.u.; Vti is the generator terminal voltage, in p.u.; xdi is the direct axis reactance of the ith generator, in p.u.; $x'di$ is the direct axis transient reactance of the i-th generator, in p.u.; Idi is the direct axis current, in p.u.; Iqi is the quadrature axis current, in p.u.; kci is the gain of the excitation amplifier, in p.u.; ufi(t) is the input of the SCR amplifier of the i-th generator; xadi is the mutual reactance between the excitation coil and the stator coil of the i-th generator; Yij=Gij+jBij is the i-th row and j-th column element of nodal admittance matrix, in p.u.; Qei is the reactive power, in p.u.; Ifi is the excitation current; $f_{i1}(t)$ and $f_{i2}(t)$ are highly nonlinear functions.

The classical third-order single-axis dynamic generator model used in this paper is referred in [14].

4.2   T-S fuzzy model of power system

Bae et al. in [15] presented a method of constructing the T-S fuzzy model using the sum of a product of linearly independent functions. The T-S fuzzy model of the power system adopted is constructed according to the improved Bae method [15]. From (15) and (16), we can find that $f_{i_1}(t)$ and $f_{i_2}(t)$ are dependent on the operating conditions but bounded with a certain operating region. The following bounds of $f_{i_1}(t)$ and $f_{i_2}(t)$ are considered:

$$-3.526 \le f_{1_1} \le -0.259,$$

$$0.266 \leq f_{1_2} \leq 3.794,$$

$$-2.832 \leq f_{2_1} \leq -0.233,$$

$$0.241 \leq f_{2_2} \leq 3.670.$$

According to [14], the nonlinear state equation (10) is expressed by

$$\dot{x}_i(t) = [F_{i_0} + \sum_{j=0}^{2} f_{i_j}(z(t))F_{i_j}]\eta_i(t), \tag{17}$$

where

$$x_i(t) = [\Delta V_{ti}(t), \Delta \omega_i(t), \Delta P_{ei}(t)]^T, \tag{18}$$

$$\eta_i(t) = [\Delta V_{ti}(t), \Delta \omega_i(t), \Delta P_{ei}(t), v_{fi}(t)]^T, \tag{19}$$

$$F_{i_0} = \begin{pmatrix} 0 & 0 & 0 & 0 \\ 0 & -\frac{D_i}{2H_i} & -\frac{\omega_0}{2H_i} & 0 \\ 0 & 0 & -\frac{1}{T'_d oi} & \frac{1}{T'_d oi} \end{pmatrix}, F_{i_1} = \begin{pmatrix} 0 & 1 & 0 & 0 \\ 0 & 0 & 0 & 0 \\ 0 & 0 & 0 & 0 \end{pmatrix}, F_{i_2} = \begin{pmatrix} 0 & 0 & -\frac{1}{T'_{d0i}} & \frac{1}{T'_{d0i}} \\ 0 & 0 & 0 & 0 \\ 0 & 0 & 0 & 0 \end{pmatrix}. \tag{20}$$

As the number of linearly independent functions is 2 and for each function $f_{i_1}(t)$ and $f_{i_2}(t)$ two triangular fuzzy sets are assigned, 4 fuzzy rules are formulated. The T-S fuzzy model of the nonlinear system (10) is such that

$$\dot{x}_i(t) = \sum_{j=1}^{4} h_{i_j}(z(t))(A_{i_j}x(t) + B_{i_j}u(t)), \tag{21}$$

where
$h_{i_1} = M_{i_{10}}M_{i_{20}}, h_{i_2} = M_{i_{10}}M_{i_{21}}, h_{i_3} = M_{i_{11}}M_{i_{20}}, h_{i_4} = M_{i_{11}}M_{i_{21}},$
$M_{i_{j0}}(z(t)) = \frac{(f_{i_{j1}}-f_{i_j}(z(t)))}{(f_{i_{j1}}-f_{i_{j0}})}, M_{i_{j1}}(z(t)) = \frac{(f_{i_j}(z(t))-f_{i_{j0}})}{(f_{i_{j1}}-f_{i_{j0}})},$
$[A_{i_1}, B_{i_1}] = F_{i_0} + f_{i_{10}}F_{i_1} + f_{i_{20}}F_{i_2}, [A_{i_2}, B_{i_2}] = F_{i_0} + f_{i_{10}}F_{i_1} + f_{i_{21}}F_{i_2},$
$[A_{i_3}, B_{i_3}] = F_{i_0} + f_{i_{11}}F_{i_1} + f_{i_{20}}F_{i_2}, [A_{i_2}, B_{i_2}] = F_{i_0} + f_{i_{11}}F_{i_1} + f_{i_{21}}F_{i_2}.$

5   Simulation Results

To evaluate the above control scheme for transient stability enhancement and voltage regulation, the example of two-machine three-bus power system is represented in Figure 2. The generator and the transmission line parameters are listed in Table 1 [14].

The performance of the proposed controller is tested under the following temporary fault sequence:
▷ Stage 1: The system is in a pre-fault steady state.
▷ Stage 2: A fault occurs at t=1s.
▷ Stage 3: The fault is removed by opening the breakers of the faulted line at t=1.15s.
▷ Stage 4: A mechanical input power of the generator1 has a 30% step increase at t = 2s.
▷ Stage 5: The system is in a post-fault state.
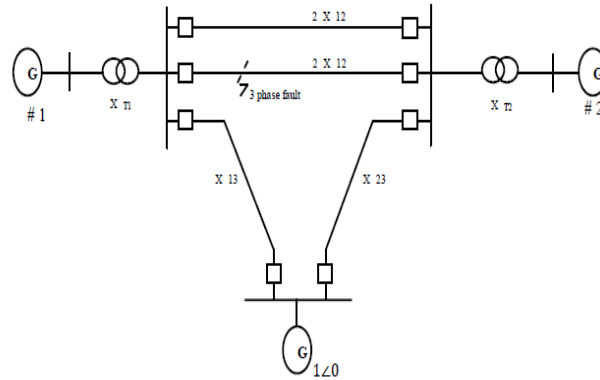
Figure 1: Two-machine infinite bus power system.

Generator	1	2
$x_d(p.u.)$	1.863	2.36
$x'_d(p.u.)$	0.257	0.319
$x_T(p.u.)$	0.129	0.11
$x_{ad}(p.u.)$	1.712	1.7126
$T'_{do}(sec)$	6.9	7.96
$H(s)$	4.0	5.1
$D(p.u.)$	5.0	3
$k_c(p.u.)$	1.0	1.0
$x_{12}(p.u.)$	0.55	
$x_{13}(p.u.)$	0.53	
$x_{23}(p.u.)$	0.6	
$\omega_0(rad/d)$	314.159	

Table 1: System parameters.

The following cases are considered.
• Case 1: Different sets of operating points: Two different operating points are considered:

Operating point 1:

$$\delta_{10} = 46.00°; Pm_{10} = 0.87p.u., V_{t10} = 1.0p.u.$$
$$\delta_{20} = 44.69°; Pm_{20} = 0.86p.u., V_{t20} = 1.0p.u.$$

Operating point 2:

$$\delta_{10} = 34.89°; Pm_{10} = 0.65p.u., V_{t10} = 1.02p.u.$$
$$\delta_{20} = 35.75°; Pm_{20} = 0.61p.u., V_{t20} = 1.09p.u.$$

The fault location is $\lambda = 0.02$. The corresponding closed loop system responses are shown in Figure 2 and Figure 3, respectively.
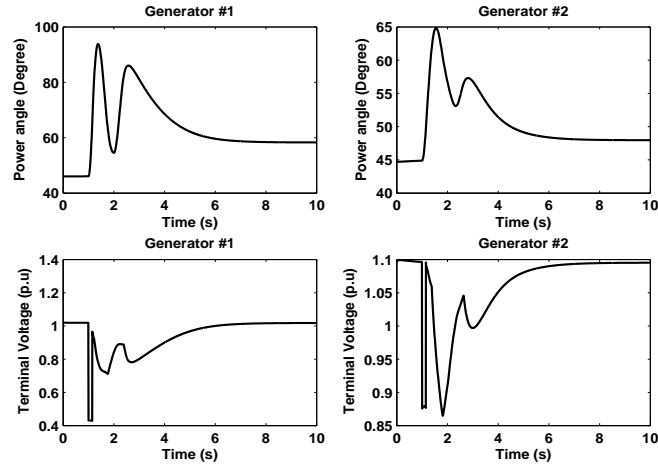
Figure 2: Power system responses for Case 1, operating point 1.
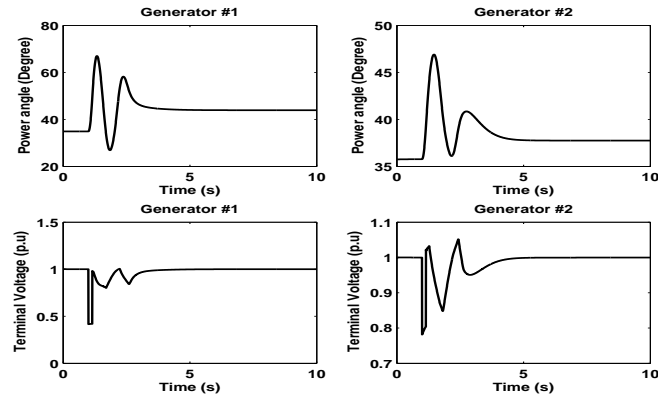
Figure 3: Power system responses for Case 1, operating point 2.

• Case 2: Fault location.

To test the ability of the proposed controller to achieve the proposed control task, two different fault locations are proposed $\lambda = 0.01$ and $\lambda = 0.5$. The operating point considered is

$$\delta_{10} = 18.51°; Pm_{10} = 0.3p.u., V_{t10} = 0.95p.u.$$
$$\delta_{20} = 23.68°; Pm_{20} = 0.4p.u., V_{t20} = 0.95p.u.$$

The corresponding closed loop system responses are shown in Figure 4 and Figure 5, respectively.
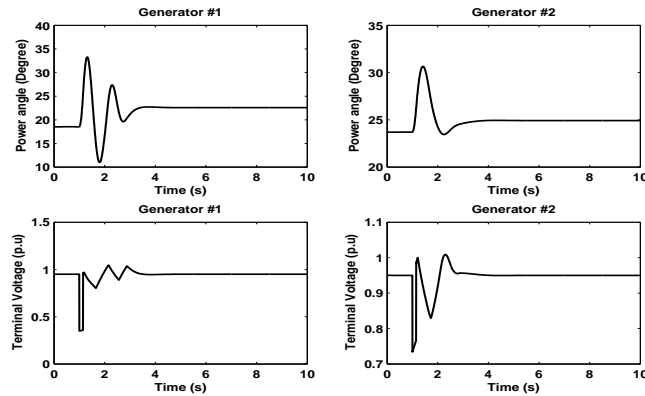
Figure 4: Power system responses for Case 2, fault location $\lambda = 0.01$.
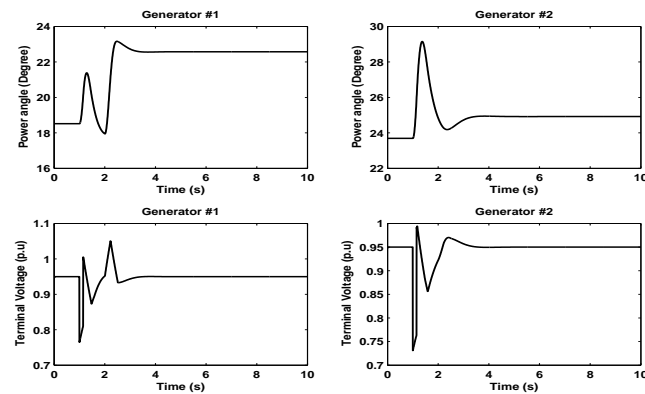
Figure 5: Power system responses for Case 2, fault location $\lambda = 0.5$.

Figures 2-5 show the system performances when subjected to different faults. It can be concluded from the simulation results that the proposed optimal voltage controller exhibits good transient performance: the oscillations are damped out effectively; the terminals voltages of generators are well regulated to their pre-fault values regardless of the operating points, change in the mechanical input power and fault locations.

6   Conclusion

In this paper, the design of optimal nonlinear state feedback voltage regulator for power systems based on the Takagi-Sugeno fuzzy model and parallel distributed compensation (PDC) scheme was presented. The proposed methodology reformulates the stability as

convex optimization problems with linear matrix inequality (LMI). To demonstrate the effectiveness of the proposed controller, a two-machine three-bus power system has been considered. Simulation results show that both transient stability and voltage quality can be improved effectively regardless of the system operating conditions.

References

[1] A. Tlemcani, K. Sebaa and N. Henin. Indirect Adaptive Fuzzy Control of Multivariable Nonlinear Systems Class with Unknown Parameters. *Nonlinear Dynamics and Systems Theory* **14** (2) (2014) 162–174.

[2] G. Hou, F. Zeng and J. Zhang. Improved T-S fuzzy model identification approach and its application in power plants. In: *Proceedings of the 2010 International Conference on Modelling, Identification and Control* (2010) 53–58.

[3] C.Chun and I. Yiao. T-S Fuzzy model identification and the fuzzy model based controller design. In: *IEEE International conference on systems, Man and Cybernetics* (2007) 859–864.

[4] M. Benrejeb, M. Gasmi and P. Borne. New stability conditions for T-S continuous nonlinear models. *Nonlinear Dynamics and Systems Theory* **5** (4) (2005) 369–379.

[5] K. Tanaka and O. Wong. *Fuzzy Control Systems Design and Analysis: A Linear Matrix Inequality Approach.* John Wiley & Sons Inc., 2001.

[6] J. Y. Dieulot and N. Elfelly. Design of Decoupling Nonlinear Controllers for Fuzzy Systems. *Nonlinear Dynamics and Systems Theory* **10** (4) (2010) 363–374.

[7] A. Aydi, M. Djemel and M. Chtourou. Fuzzy Modeling and Robust Pole Assignment Control for Difference Uncertain Systems. *Nonlinear Dynamics and Systems Theory* **15** (4) (2015) 344–359.

[8] E. V. Kumar and J. Jerome. Robust LQR Controller Design for Stabilizing and Trajectory Tracking of Inverted Pendulum. *Procedia Engineering* **64** (2013) 169–178.

[9] D. S.Naidu. *Optimal Control Systems.* CRC press, 2003.

[10] A. Feydi, S. Elloumi and N. Benhadj Braiek. Decentralized stabilization for a class of nonlinear interconnected systems using SDRE optimal control approch. *Nonlinear Dynamics and Systems Theory* **19** (1) (2019) 55–67.

[11] K. Kunisch, S. Volkwein and L. Xie. HJB-POD-Based Feedback Design for the Optimal Control of Evolution Problems. *SIAM J. on Applied Dynamical Systems* **4** (3) (2004) 701–722.

[12] J. Garcke and A. Kroner. Suboptimal feedback control of PDEs by solving HJB equations on adaptive sparse grids. *Journal of Scientific Computing* (2015) 1–28.

[13] M. J. Kharaajoo and M. J. Yazdanpanah. Transient control and voltage regulation of power systems using approximate solution of HJB equation. In: *2003 European Control Conference (ECC)* (2003) 2505–2510.

[14] A. Abbadi, J. Boukhetala, L. Nezli and A. Kouzou. A nonlinear voltage controller using T-S fuzzy model for multimachine power systems. In: *Proceedings of the 9th annual IEEE international multi-conference on systems, signals and devices*, Chemnitz, Germany (2012) 1–8.

[15] H. S. Bae, S. Kwou and E. T. Jeung. Design of stabilizing controller for an inverted pendulum system using the T-S fuzzy model. *J. Control Automat. Syst. Eng.* (2002) 916–921.

Nonlinear Elliptic Equations with Some Measure Data in Musielak-Orlicz Spaces

A. Aberqi [1*], J. Bennouna [2] and M. Elmassoudi [2]

[1] *University sidi Mohamed ben abdellah- ENSA-Fez. Morocco*
[2] *University sidi Mohamed ben abdellah, Faculty of Sciences Dhar El Mahraz, Atlas Fez, Morocco.*

Abstract: Our aim in this paper is to establish an existence result in the framework of Musielak-Orlicz spaces for the following nonlinear Dirichlet problem

$$A(u) + K(x, u, \nabla u) = \mu, \tag{1}$$

where $A(u) = -\text{div}(a(x, u, \nabla u))$ is a Leray-Lions type operator defined on $D(A) \subset W_0^1 L_\varphi(\Omega)$ into its dual and the function K is a lower order term which satisfy some growth condition, and does not satisfy the sign condition. The source data μ is a bounded nonnegative Radon measure on Ω.

Keywords: *Musielak-Orlicz spaces; nonlinear elliptic problems; measure data; weak solution.*

Mathematics Subject Classification (2010): 35J60, 35J66.

1 Introduction

Classical Sobolev spaces do not allow one to solve all problems of the EDP, hence the need to find other spaces, larger and suitable for the recent problems such as the spaces $L^{p(x)}(\Omega)$ or, more generally, the Musielak spaces. These spaces are not always reflexive and separable, adding further difficulties for studying the existence of solutions. Thus all our work will be in these spaces. We consider the following nonlinear Dirichlet problem:

$$A(u) + K(x, u, \nabla u) = f \tag{2}$$

---

* Corresponding author: `mailto:aberqi_ahmed@yahoo.fr`,

on a Lipschitz bounded domain in $\mathbb{R}^N$. $A(u) = -\text{div}(a(x, u, \nabla u))$ is a Leary-Lions opera-tor defined on $D(A) \subset W_0^1 L_\varphi(\Omega) \to W^{-1} L_\psi(\Omega)$, where φ and ψ are two complementary Musielak-Orlicz functions and K is a nonlinear lower term which satisfies the growth condition without the sign condition. In the framework of Sobolev spaces with variable exponents (the φ-function is $\varphi(x, t) = |t|^{p(x)}$), a series of papers on nonlinear elliptic and parabolic equations without sign condition in the nonlinearity studied (see [8], [4]).

On Orlicz spaces, many papers were devoted to the existence of solutions of (2). In fact, Gossez J.P. [17] solved the problem in the variational case, Elmahi A. et al. [14] proved the existence results for the unilateral problem of (2), where K satisfies the growth condition and the right-hand side belongs to $L^1(\Omega)$. Recently, Dong G. et al. in [13] have taken the source term as a bounded nonnegative Radon measure on Ω.

On Musielak-Orlicz spaces, Ait Khellou M. et al. in [7] have shown the existence of solutions for (2) in the case where K satisfies the sign condition and $f \in L^1(\Omega)$. The study of nonlinear partial differential equations is motivated by numerous phenom-ena of physics, namely, the electrorheological fluids, the flow thought the porous media (see the monograph of A. Antsenov [9]).

As an example of operator for which the present result can be applied, we give

$$-\text{div}\Big(\frac{m(x, |\nabla u|).\nabla u}{|\nabla u|}\Big) + u\phi(x, |\nabla u|) = f,$$

where $m(x, s)$ is the derivative of $\phi(x, s)$ with respect to s.

The aim of this paper is the study of the problem (2) in the setting of Musielak-Orlicz spaces overcoming two difficulties. Firstly we do not assume the sign condition on the nonlinearity K, after we prove that there exists at least one solution for approximate equations. Secondly, we show that solutions belong to the Musielak-Sobolev spaces $W_0^1 L_\phi(\Omega)$ where ϕ is in a special class of the Musielak-Orlicz functions of the $\mathcal{A}_\varphi$ (see Definition 3.1).

This paper is organized as follows. Section 2 contains some preliminaries in the Musielak-Sobolev spaces. In Section 3, we give some lemmas and we show that the solution of the problem (2) belongs to the space $W_0^1 L_\phi(\Omega)$. Section 4 is devoted to specifying the assumptions on $A(u)$, K and μ. In Section 5, we give and we prove principal Theorem 5.1.

2   Musielak-Orlicz Spaces – Notations and Properties

2.1   Musielak-Orlicz function

Let Ω be an open subset of $\mathbb{R}^N$ ($N \geq 2$) and let φ be a real-valued function defined in $\Omega \times \mathbb{R}^+$. The function φ is called a Musielak-Orlicz function if

- $\varphi(x, \cdot)$ is an N-function for all $x \in \Omega$ (i.e. convex, non-decreasing, contin-uous, $\varphi(x, 0) = 0$, $\varphi(x, 0) > 0$ for $t > 0$, $\lim_{t \to 0} \sup_{x \in \Omega} \frac{\varphi(x, t)}{t} = 0$ and $\lim_{t \to \infty} \inf_{x \in \Omega} \frac{\varphi(x, t)}{t} = \infty$).

- $\varphi(\cdot, t)$ is a measurable function for all $t \geq 0$.

We put $\varphi_x(t) = \varphi(x, t)$ and we associate its non-negative reciprocal function φ_x^{-1} with respect to t, that is, $\varphi_x^{-1}(\varphi(x, t)) = \varphi(x, \varphi_x^{-1}(t)) = t$.

Let φ and γ be two Musielak-Orlicz functions, we say that φ dominates γ and we write

$\gamma \prec \varphi$ near infinity (respectively, globally) if there exist two positive constants c and t_0 such that for a.e. $x \in \Omega$ $\gamma(x,t) \leq \varphi(x,ct)$ for all $t \geq t_0$ (respectively, for all $t \geq 0$). We say that φ and γ are equivalents, and we write $\varphi \sim \gamma$ if φ dominates γ and γ dominates φ. Finally, we say that γ grows essentially less rapidly than φ at 0 (respectively, near infinity), and we write $\gamma \prec\prec \varphi$, for every positive constant c, we have $\lim_{t\to 0} \sup_{x\in\Omega} \frac{\gamma(x,ct)}{\varphi(x,t)} = 0$ (respectively, $\lim_{t\to\infty} \sup_{x\in\Omega} \frac{\gamma(x,ct)}{\varphi(x,t)}) = 0$).

Remark 2.1   [12] If $\gamma \prec\prec \varphi$ near infinity, then $\forall \epsilon > 0$ there exists $k(\epsilon) > 0$ such that for almost all $x \in \Omega$ we have

$$\gamma(x,t) \leq k(\epsilon)\varphi(x,\epsilon t) \quad \forall t \geq 0.$$

2.2   Musielak-Orlicz space

Let φ be a Musielak-Orlicz function and a measurable function $u : \Omega \to \mathbb{R}$, we define the functional

$$\varrho_{\varphi,\Omega}(u) = \int_\Omega \varphi(x,|u(x)|)dx.$$

The set $K_\varphi(\Omega) = \{u : \Omega \to \mathbb{R} \quad \text{measurable} : \quad \varrho_{\varphi,\Omega}(u) < \infty\}$ is called the Musielak-Orlicz class. The Musielak-Orlicz space $L_\varphi(\Omega)$ is the vector space generated by $K_\varphi(\Omega)$, that is, $L_\varphi(\Omega)$ is the smallest linear space containing the set $K_\varphi(\Omega)$. Equivalently,

$$L_\varphi(\Omega) = \left\{u : \Omega \to \mathbb{R} \quad \text{measurable} : \quad \varrho_{\varphi,\Omega}\left(\frac{u}{\lambda}\right) < \infty, \quad \text{for some} \quad \lambda > 0\right\}.$$

On the other hand, we put $\psi(x,s) = \sup_{t\geq 0}(st - \varphi(x,s))$.

ψ is called the Musielak-Orlicz function complementary to φ (or conjugate of φ) in the sense of Young with respect to s. We say that a sequence of function $u_n \in L_\varphi(\Omega)$ is modular convergent to $u \in L_\varphi(\Omega)$ if there exists a constant $\lambda > 0$ such that $\lim_{n\to\infty} \varrho_{\varphi,\Omega}(\frac{u_n-u}{\lambda}) = 0$. This implies convergence for $\sigma(\prod L_\varphi, \prod L_\psi)$ (see [11]).

In the space $L_\varphi(\Omega)$, we define the following two norms:

$$\|u\|_\varphi = \inf\left\{\lambda > 0 : \int_\Omega \varphi(x, \frac{|u(x)|}{\lambda})dx \leq 1\right\},$$

which is called the Luxemburg norm, and the so-called Orlicz norm

$$|||u|||_{\varphi,\Omega} = \sup_{\|v\|_\psi \leq 1} \int_\Omega |u(x)v(x)|dx,$$

where ψ is the Musielak-Orlicz function complementary to φ. These two norms are equivalent [11]. $K_\varphi(\Omega)$ is a convex subset of $L_\varphi(\Omega)$. We define $E_\varphi(\Omega)$ as the subset of $L_\varphi(\Omega)$ of all measurable functions $u : \Omega \mapsto \mathbb{R}$ such that $\int_\Omega \varphi(x, \frac{|u(x)|}{\lambda})dx < \infty$ for all $\lambda > 0$. It is a separable space and $(E_\varphi(\Omega))^* = L_\varphi(\Omega)$. We have $E_\varphi(\Omega) = K_\varphi(\Omega)$ if and only if φ satisfies the Δ_2-condition for the large values of t or for all values of t, according to whether Ω has finite measure or not. We define

$$W^1 L_\varphi(\Omega) = \{u \in L_\varphi(\Omega) : D^\alpha u \in L_\varphi(\Omega), \quad \forall \alpha \leq 1\},$$
$$W^1 E_\varphi(\Omega) = \{u \in E_\varphi(\Omega) : D^\alpha u \in E_\varphi(\Omega), \quad \forall \alpha \leq 1\},$$

where $\alpha = (\alpha_1, ..., \alpha_N)$, $|\alpha| = |\alpha_1| + ... + |\alpha_N|$ and $D^\alpha u$ denote the distributional derivatives. The space $W^1 L_\varphi(\Omega)$ is called the Musielak-Orlicz-Sobolev space. Let $\overline{\varrho}_{\varphi,\Omega}(u) = \sum_{|\alpha| \leq 1} \varrho_{\varphi,\Omega}(D^\alpha u)$ and $\|u\|^1_{\varphi,\Omega} = \inf\{\lambda > 0 : \overline{\varrho}_{\varphi,\Omega}(\frac{u}{\lambda}) \leq 1\}$ for $u \in W^1 L_\varphi(\Omega)$.

These functionals are convex modular and a norm on $W^1 L_\varphi(\Omega)$, respectively. Then the pair $(W^1 L_\varphi(\Omega), \|u\|^1_{\varphi,\Omega})$ is a Banach space if φ satisfies the following condition (see [19]):

$$\text{There exists a constant} \quad c > 0 \quad \text{such that} \quad \inf_{x \in \Omega} \varphi(x, 1) > c.$$

The space $W^1 L_\varphi(\Omega)$ is identified as a subspace of the product $\prod_{\alpha \leq 1} L_\varphi(\Omega) = \prod L_\varphi$. We denote by $\mathcal{D}(\Omega)$ the Schwartz space of infinitely smooth functions with compact support in Ω and by $\mathcal{D}(\overline{\Omega})$ the restriction of $\mathcal{D}(\mathbb{R})$ on Ω. The space $W^1_0 L_\varphi(\Omega)$ is defined as the $\sigma(\prod L_\varphi, \prod E_\psi)$ closure of $\mathcal{D}(\Omega)$ in $W^1 L_\varphi(\Omega)$ and the space $W^1_0 E_\varphi(\Omega)$ as the(norm) closure of the Schwartz space $\mathcal{D}(\Omega)$ in $W^1 L_\varphi(\Omega)$.

For two complementary Musielak-Orlicz functions φ and ψ, we have (see [11]) the Young inequality, $\quad st \leq \varphi(x, s) + \psi(x, t)$ for all $s, t \geq 0$, $x \in \Omega$,

the Hölder inequality, $\left| \int_\Omega u(x)v(x)dx \right| \leq \|u\|_{\varphi,\Omega}\|v\|_{\psi,\Omega}$; for all $u \in L_\varphi(\Omega), v \in L_\psi(\Omega)$.

We say that a sequence u_n converges to u for the modular convergence in $W^1 L_\varphi(\Omega)$ (respectively, in $W^1_0 L_\varphi(\Omega)$) if, for some $\lambda > 0$,

$$\lim_{n \to \infty} \overline{\varrho}_{\varphi,\Omega}\left(\frac{u_n - u}{\lambda}\right) = 0.$$

Let us define the following spaces of distributions:

$$W^{-1} L_\psi(\Omega) = \left\{ f \in \mathcal{D}'(\Omega) : f = \sum_{\alpha \leq 1} (-1)^\alpha D^\alpha f_\alpha, \text{ where } f_\alpha \in L_\psi(\Omega) \right\},$$

$$W^{-1} E_\psi(\Omega) = \left\{ f \in \mathcal{D}'(\Omega) : f = \sum_{\alpha \leq 1} (-1)^\alpha D^\alpha f_\alpha, \text{ where } f_\alpha \in E_\psi(\Omega) \right\}.$$

Lemma 2.1 *([5]) (Approximation result)   Let Ω be a bounded Lipschitz domain in $\mathbb{R}^N$ and let φ and ψ be two complementary Musielak-Orlicz functions which satisfy the following conditions:*

- *there exists a constant $c > 0$ such that $\inf_{x \in \Omega} \varphi(x, 1) > c$,*

- *there exists a constant $A > 0$ such that for all $x, y \in \Omega$ with $|x - y| \leq \frac{1}{2}$, we have*

$$\frac{\varphi(x, t)}{\varphi(y, t)} \leq |t|^{\left(\frac{A}{\log(\frac{1}{|x-y|})}\right)} \quad \text{for all} \quad t \geq 1,$$

- $\int_K \varphi(x, \lambda)dx < \infty$, *for any constant $\lambda > 0$ and for every compact $K \subset \Omega$.*

- *there exists a constant $\quad C > 0 \quad$ such that $\quad \psi(y, t) \leq C \quad a.e. \quad in \quad \Omega$.*

Under these assumptions $\mathcal{D}(\Omega)$ is dense in $L_\varphi(\Omega)$ with respect to the modular topology, $\mathcal{D}(\Omega)$ is dense in $W^1_0 L_\varphi(\Omega)$ for the modular convergence and $\mathcal{D}(\overline{\Omega})$ is dense in $W^1 L_\varphi(\Omega)$ for the modular convergence. Consequently, the action of a distribution S in $W^{-1} L\psi$ on an element u of $W^1_0 L_\varphi(\Omega)$ is well defined. It will be denoted by $< S, u >$.

Remark 2.2 The second condition in Lemma 2.1 coincides with an alternative log-Hölder continuity condition for the variable exponent p, namely, there exists $A > 0$ such that for x, y close enough and each $t \in \mathbb{R}^N$

$$|p(x) - p(y)| \leq \frac{A}{\log(\frac{1}{|x-y|})}.$$

2.3 Truncation operator

T_k, $k > 0$, denotes the truncation function at level k defined on $\mathbb{R}$ by $T_k(r) = \max(-k, \min(k, r))$. The following abstract lemmas will be applied to the truncation operators.

Lemma 2.2 ([12]) Let $F : \mathbb{R} \to \mathbb{R}$ be uniformly Lipschitzian, with $F(0) = 0$. Let φ be an Musielak-Orlicz function and let $u \in W_0^1 L_\varphi(\Omega)$ (respectively, $u \in W^1 E_\varphi(\Omega)$). Then $F(u) \in W^1 L_\varphi(\Omega)$ (respectively, $u \in W_0^1 E_\varphi(\Omega)$). Moreover, if the set of discontinuity points D of F' is finite, then

$$\frac{\partial}{\partial x_i} F(u) = \begin{cases} F'(x) \frac{\partial u}{\partial x_i}, & \text{a.e. in } \{x \in \Omega; \, u(x) \notin D\}, \\ 0, & \text{a.e. in } \{x \in \Omega; \, u(x) \in D\}. \end{cases}$$

Lemma 2.3 ([12]) Suppose that Ω satisfies the segment property and let $u \in W_0^1 L_\varphi(\Omega)$. Then, there exists a sequence $u_n \in \mathcal{D}(\Omega)$ such that $u_n \to u$ for modular convergence in $W_0^1 L_\varphi(\Omega)$. Furthermore, if $u \in W_0^1 L_\varphi(\Omega) \cap L^\infty(\Omega)$, then $\|u_n\|_\infty \leq (N+1)\|u\|_\infty$.

Let Ω be an open subset of $\mathbb{R}^N$ and let φ be a Musielak-Orlicz function satisfying the condition

$$\int_0^1 \frac{\varphi_x^{-1}(t)}{t^{\frac{N+1}{N}}} dt = \infty \quad \text{a.e.} \quad x \in \Omega,$$

and the conditions of Lemma 2.1. We may assume, without loss of generality, that

$$\int_0^1 \frac{\varphi_x^{-1}(t)}{t^{\frac{N+1}{N}}} dt < \infty \quad \text{a.e.} \quad x \in \Omega.$$

Define a function $\varphi^* : \Omega \times [0, \infty)$ by $\varphi^*(x, s) = \int_0^s \frac{\varphi_x^{-1}(t)}{t^{\frac{N+1}{N}}} dt$ $x \in \Omega$ and $s \in [0, \infty)$. φ^* is called the Sobolev conjugate function of φ (see [1] for the case of the Orlicz function).

Lemma 2.4 ([15]) Let $u_n, u \in L_\varphi(\Omega)$. If $u_n \to u$ with respect to the modular convergence, then $u_n \rightharpoonup u$ for $\sigma(L_\varphi(\Omega), L_\psi(\Omega))$.

3 Technical Lemmas

Throughout this paper, we assume also that every Musielak-Orlicz function $\varphi(.,.)$ is decreasing in x in the following sense. For any $x \in \Omega$, let $\Omega_x = \{s \in \Omega / \|x\| \leq \|s\|\}$,

$$\begin{cases} \varphi(s, t) \leq \varphi(x, t) & \text{if } s \in \Omega_x, \\ \varphi(s, t) \geq \varphi(x, t) & \text{if } s \notin \Omega_x \end{cases} \tag{3}$$

for any $t \in \mathbb{R}$.

Lemma 3.1 *([6]) Under the assumptions of Lemma2.1, and by assuming that $\varphi(x,t)$ depends only on $N-1$ coordinate of x, there exists a constant $C_1 > 0$ which depends only on Ω such that*

$$\int_\Omega \varphi(x,|u|)dx \leq \int_\Omega \varphi(x, C_1|\nabla u|)dx. \tag{4}$$

Definition 3.1 Let φ be a Musielak-Orlicz function. We define the following set:

$$\mathcal{A}_\varphi = \begin{cases} \phi : \Omega \times \mathbb{R}_+ \to \mathbb{R}_+ & \text{is a Musielak-Orlicz function such that} \\ \phi \prec\prec \varphi \quad \text{and} \quad \int_0^1 \phi(x, \beta H^{-1}(x, \frac{1}{r^{1-\frac{1}{N}}}))dr < \infty & \text{a.e. in } \Omega \end{cases}$$

for all constant $\beta \geq 1$, where $H(x,r) = \dfrac{\varphi(x,r)}{r}$.

The following lemma generalizes Lemma 2 in [20].

Lemma 3.2 *Let Ω be an open subset of $\mathbb{R}^N$ with finite measure. Let φ be a Musielak-Orlicz function under assumption (3) and the assumptions of Lemma 2.1.*

For any $u \in W_0^1 L_\varphi(\Omega)$ such that $\displaystyle\int_\Omega \varphi(x,|\nabla u|)dx < \infty$, we have for all $x \in \Omega$,

$$-\mu'(t) \geq NC_N^{\frac{1}{N}}\mu(t)^{1-\frac{1}{N}}C\left(x, \frac{-1}{C_N^{\frac{1}{N}}\mu(t)^{1-\frac{1}{N}}}\frac{d}{dt}\int_{\{|u|>t\}}\varphi(s,|\nabla u|)ds\right) \tag{5}$$

for a.e. $t > 0$. Here μ is the distribution function of u, and the function $C(.,.)$ is defined by $C(x,t) = \frac{1}{H_x^{-1}(x,t)}$ with $H(x,t) = \frac{\varphi(x,t)}{t}$, C_N is the measure of the unit ball of $\mathbb{R}^N$, and $\mu(t) = meas\{|u| > t\}$.

Proof. By definition of the Musielak-Orlicz function, φ is an increasing convex function in t, then H is an increasing convex function in t, and $C(.,.)$ is a decreasing convex function in t.

Fix $x \in \Omega$. Jensen's inequality for a convex function gives

$$C\left(x, \frac{\int_{\{t<|u|\leq t+h\}}\varphi(s,|\nabla u|)\,ds}{\int_{\{t<|u|\leq t+h\}}|\nabla u|\,ds}\right) = C\left(x, \frac{\int_{\{t<|u|\leq t+h\}}H(s,|\nabla u|)|\nabla u|\,ds}{\int_{\{t<|u|\leq t+h\}}|\nabla u|\,ds}\right)$$

$$\leq \frac{\int_{\{t<|u|\leq t+h\}}C\left(x, H(s,|\nabla u|)\right)|\nabla u|ds}{\int_{\{t<|u|\leq t+h\}}|\nabla u|\,ds}$$

$$\leq \frac{\int_{\{t<|u|\leq t+h\}\cap\Omega_x}C\left(x, H(s,|\nabla u|)\right)|\nabla u|ds}{\int_{\{t<|u|\leq t+h\}}|\nabla u|\,ds}$$

$$+\frac{\int_{\{t<|u|\leq t+h\}\cap(\Omega\setminus\Omega_x)}C\left(x, H(s,|\nabla u|)\right)|\nabla u|\,ds}{\int_{\{t<|u|\leq t+h\}}|\nabla u|ds}.$$

By (3) and for all $t > 0$ we have

for $s \in \Omega_x$, $H(s, |\nabla u|) \leq H(x, |\nabla u|)$ and $C(x, H(s, |\nabla u|)) \leq C(x, H(x, |\nabla u|)) = \frac{1}{|\nabla u|}$,

for $s \in \Omega \setminus \Omega_x$, $H(x, |\nabla u|) \leq H(s, |\nabla u|)$ and $|\nabla u| \leq H_x^{-1}(H(s, |\nabla u|))$,

then $C(x, H(s, |\nabla u|)) = \frac{1}{H_x^{-1}(H(s, |\nabla u|))} \leq \frac{1}{|\nabla u|}$. Hence

$$C\left(x, \frac{\displaystyle\int_{\{t < |u| \leq t+h\}} \varphi(s, |\nabla u|)\, ds}{\displaystyle\int_{\{t < |u| \leq t+h\}} |\nabla u|\, ds} \right) \leq \frac{-\mu(t+h) + \mu(t)}{\displaystyle\int_{\{t < |u| \leq t+h\}} |\nabla u|\, ds},$$

letting $h \to 0$, we have

$$C\left(x, \frac{(\frac{d}{dt}) \displaystyle\int_{\{|u| > t\}} \varphi(s, |\nabla u|)\, ds}{(\frac{d}{dt}) \displaystyle\int_{\{|u| > t\}} |\nabla u|\, ds} \right) \leq \frac{\mu'(t)}{(\frac{d}{dt}) \displaystyle\int_{\{|u| > t\}} |\nabla u|\, ds} \tag{6}$$

for all $t > 0$.

On the other hand we can follow [16] to prove that

$$- \frac{d}{dt} \int_{\{|u| > t\}} |\nabla u|\, dx \geq N C_N^{\frac{1}{N}} \mu(t)^{1 - \frac{1}{N}} \tag{7}$$

for a.e. $t > 0$. Finally, combining (6), (7) and the monotony of $C(.,.)$ we get (5).

Lemma 3.3 *Let φ be a Musielak-Orlicz function under assumption (3) and the assumptions of Lemma 2.1 and $\phi \in \mathcal{A}_\varphi$ with $\phi \sim \varphi$, there exists a constant $\beta \geq 1$ such that*

$$\frac{d}{dt} \int_{\{|u| > t\}} \phi(s, |\nabla u|)\, ds \leq -\mu'(t)\phi\left(x, \beta H_x^{-1}\left(\frac{1}{N C_N^{\frac{1}{N}} \mu(t)^{1 - \frac{1}{N}}} \frac{d}{dt} \int_{\{|u| > t\}} \varphi(s, |\nabla u|)\, ds \right) \right)$$

for each $x \in \Omega$ and for any $u \in W_0^1 L_\varphi(\Omega)$ such that $\displaystyle\int_\Omega \varphi(x, |\nabla u|) dx < \infty$.

Proof. For $x \in \Omega$, let $C(x, t) = \dfrac{1}{H_x^{-1}(x, t)}$, then $C(x, t) = \dfrac{t}{\varphi \circ H_x^{-1}(x, t)}$.
By (5), we have

$$-\mu'(t) \geq N C_N^{\frac{1}{N}} \mu(t)^{1 - \frac{1}{N}} C\left(x, \frac{-1}{N C_N^{\frac{1}{N}} \mu(t)^{1 - \frac{1}{N}}} \frac{d}{dt} \int_{\{|u| > t\}} \varphi(s, |\nabla u|)\, ds \right),$$

then

$$-\mu'(t)\varphi \circ H_x^{-1}\left(\frac{-1}{N C_N^{\frac{1}{N}} \mu(t)^{1 - \frac{1}{N}}} \frac{d}{dt} \int_{\{|u| > t\}} \varphi(s, |\nabla u|)\, ds \right)$$

$$\geq N C_N^{\frac{1}{N}} \mu(t)^{1 - \frac{1}{N}} \left(- \frac{1}{N C_N^{\frac{1}{N}} \mu(t)^{1 - \frac{1}{N}}} \frac{d}{dt} \int_{\{|u| > t\}} \varphi(s, |\nabla u|)\, ds \right)$$

$$-\mu^{'}(t)\varphi \circ H_x^{-1}\Big(\frac{-1}{NC_N^{\frac{1}{N}}\mu(t)^{1-\frac{1}{N}}}\frac{d}{dt}\int_{\{|u|>t\}}\varphi(s,|\nabla u|)ds\Big) \geq -\frac{d}{dt}\int_{\{|u|>t\}}\varphi(s,|\nabla u|)\,ds,$$

and also

$$\frac{1}{\mu^{'}(t)}\frac{d}{dt}\int_{\{|u|>t\}}\varphi(s,|\nabla u|)\,ds \leq \varphi \circ H_x^{-1}\left(\frac{-1}{NC_N^{\frac{1}{N}}\mu(t)^{1-\frac{1}{N}}}\frac{d}{dt}\int_{\{|u|>t\}}\varphi(s,|\nabla u|)\,ds\right),$$

using the monotony of the function φ_x^{-1}, we obtain

$$\varphi_x^{-1}\Big(\frac{1}{\mu^{'}(t)}\frac{d}{dt}\int_{\{|u|>t\}}\varphi(s,|\nabla u|)\,ds\Big) \leq H_x^{-1}\Big(\frac{-1}{NC_N^{\frac{1}{N}}\mu(t)^{1-\frac{1}{N}}}\frac{d}{dt}\int_{\{|u|>t\}}\varphi(s,|\nabla u|)\,ds\Big).$$

Let $\phi \in \mathcal{A}_\varphi$ and let $D(x,t) = \varphi(x,\phi_x^{-1}(t))$, then D is convex and by Jensen's inequality we have

$$D\Big(x,\frac{\int_{\{t<|u|<t+h\}}\phi(s,|\nabla u|)\,ds}{-\mu(t+h)+\mu(t)}\Big) \leq \frac{\int_{\{t<|u|<t+h\}}D\Big(x,\phi(s,|\nabla u|)\Big)\,ds}{-\mu(t+h)+\mu(t)}.$$

Since $\phi \sim \varphi$, there exists a constant $\lambda > 0$ such that $\varphi(x,t) \leq \lambda\phi(x,t)$. Then for every $\phi \in \mathcal{A}_\varphi$ with $\lambda \leq 1$ and by the monotony of the functions φ_x and ϕ_x^{-1} for any x and s in Ω, we have

$$D\bigg(x,\phi(s,|\nabla u|)\bigg) = \varphi\Big(x,\phi_x^{-1}(\phi(s,|\nabla u|))\Big) \leq \phi(s,|\nabla u|),$$

and by Remark 2.1, there exists $\beta > 0$ such that $D\Big(x,\phi(s,|\nabla u|)\Big) \leq \beta\varphi(s,|\nabla u|)$, then

$$D\bigg(x,\frac{\int_{\{t<|u|<t+h\}}\phi(s,|\nabla u|)\,ds}{-\mu(t+h)+\mu(t)}\bigg) \leq \frac{\beta\int_{\{t<|u|<t+h\}}\varphi\Big(s,|\nabla u|)\Big)\,ds}{-\mu(t+h)+\mu(t)},$$

using the definition of D(.,.) and the monotony of φ_x^{-1} we have

$$phi_x^{-1}\bigg(x,\frac{1}{\mu^{'}(t)}\frac{d}{dt}\int_{\{|u|>t\}}\phi(s,|\nabla u|)\,ds\bigg) \leq \beta\varphi_x^{-1}\bigg(x,\frac{1}{\mu^{'}(t)}\frac{d}{dt}\int_{\{|u|>t\}}\varphi(s,|\nabla u|)\,ds\bigg),$$

$$\leq \beta H_x^{-1}\Bigg(\frac{-1}{C_N^{\frac{1}{N}}\mu(t)^{1-\frac{1}{N}}}\frac{d}{dt}\int_{\{|u|>t\}}\varphi(s,|\nabla u|)\,ds\Bigg),$$

which gives our result.

4   Essential Assumptions

Let φ and γ be two Musielak-Orlicz functions such that φ and its complementary ψ satisfy the previous conditions and $\gamma \prec\prec \varphi$.

$A : D(A) \subset W_0^1 L_\varphi(\Omega) \to W^{-1}L_\psi(\Omega)$ is defined by $A(u) = -\text{div}(a(x,u,\nabla u))$, where $a : \Omega \times \mathbb{R} \times \mathbb{R}^N \to \mathbb{R}^N$ is a Carathéodory function such that for a.e. $x \in \Omega$ and for all $s \in \mathbb{R}, \xi,\xi^* \in \mathbb{R}^N, \xi \neq \xi^*$.

$$|a(x,s,\xi)| \leq \beta(c(x) + \psi_x^{-1}(\gamma(x,\nu_1|s|)) + \psi_x^{-1}(\varphi(x,\nu_2|\xi|))), \beta > 0, c(x) \in E_\psi(\Omega), \quad (8)$$

$$(a(x,s,\xi) - a(x,s,\xi^*))(\xi - \xi^*) > 0, \quad (9)$$

$$a(x, s, \xi).\xi \geq \alpha\varphi(x, |\xi|), \tag{10}$$

$K : \Omega \times \mathbb{R} \times \mathbb{R}^N \to \mathbb{R}^N$ is a Carathéodory function such that

$$|K(x, s, \xi)| \leq b(x) + \rho(s)\varphi(x, |\xi|), \tag{11}$$

$\rho : \mathbb{R} \to \mathbb{R}^+$ is a continuous positive function which belongs to $L^1(\mathbb{R})$ and b(x) belongs to $L^1(\Omega)$.

$$\mu \in \mathcal{M}_b(\Omega), \tag{12}$$

assume that there exists $\phi \in \mathcal{A}_\varphi$ such that

$$\phi \circ H^{-1} \text{ is a Musielak-Orlicz function.} \tag{13}$$

5 Main Results

Let Ω be an open bounded subset of $\mathbb{R}^N$ ($N \geq 2$), and let φ and ψ be two complementary Musielak-Orlicz functions.
Define the set $\mathcal{T}_0^{1,\varphi}(\Omega) = \{u : \Omega \mapsto \mathbb{R} \text{ is measurable and } T_k(u) \in D(A)\}$.

Theorem 5.1 *Assume that $(8) - (12)$ hold true with $\mathcal{A}_\varphi \neq \emptyset$. Then there exists at least one solution of the following problem:*

$$\begin{cases} u \in \mathcal{T}_0^{1,\varphi}(\Omega) \cap W_0^1 L_\phi(\Omega), \quad \forall \phi \in \mathcal{A}_\varphi, \\ < A(u), v > + \displaystyle\int_\Omega K(x, u, \nabla u)v dx = < \mu, v >, \quad \forall v \in \mathcal{D}(\Omega). \end{cases} \tag{14}$$

Example 5.1 We give an example of equations to which the present result can be applied.

1. We give an example of the Musielak-Orlicz-functions φ for which the set $\mathcal{A}_\varphi$ is not empty. Let $a(.), b(.)$ be two functions in $L^\infty(\Omega)$ such that $a(.), b(.)$ are decreasing strict positive and there exist two constants $\lambda_1 > 0, \lambda_2 > 0$ such that $\lambda_1 \leq \frac{a(x)}{b(x)} \leq \lambda_2$. Take now $\varphi(x, t) = a(x)|t|^p$ and $\phi(x, t) = b(x)|t|^p$ such that $p > N$, then $\phi \in \mathcal{A}_\varphi$.

2. Let us take the functions mentioned above and consider the following problem:

$$\begin{cases} \operatorname{div}(a(x)|\nabla u|^{p-2}\nabla u) + b(x) + \rho(u)\varphi(x, |\nabla u|) = \mu, & \text{in } \Omega, \\ u = 0, & \text{on } \partial\Omega. \end{cases}$$

   Here $a(x, u, \nabla u) = a(x)|\nabla u|^{p-2}\nabla u$ satifies the hypotheses (8)-(10), $K(x, u, \nabla u) = b(x) + \rho(u)\varphi(x, |\nabla u|)$, where $\rho : \mathbb{R} \to \mathbb{R}^+$ is a continuous positive function which belongs to $L^1(\mathbb{R})$ and $\mu \in \mathcal{M}_b(\Omega)$.

Proof of Theorem 5.1.   The proof is divided into four steps.

Step 1: Existence of weak solutions for approximate problems.
We consider the following approximate equation for any $n \in \mathbb{N}$:

$$\int_\Omega [a(x, u, \nabla u) \nabla v + K_n(x, u, \nabla u) v] dx = \int_\Omega \mu_n v \, dx, \quad \forall v \in W_0^1 L_\varphi(\Omega), \qquad (15)$$

where $K_n(x, u, \nabla u) = \dfrac{K(x, u, \nabla u)}{1 + \frac{1}{n}|K(x, u, \nabla u)|}$, and $(\mu_n)_n \in \mathcal{D}(\Omega)$ is a sequence such that

$$\mu_n \to \mu \quad \text{in the sense of the distributions.} \qquad (16)$$

We will prove that, for every n, there exists at least one bounded solution u_n of (15) with $u_n \in W_0^1 E_\varphi(\Omega)$.

Proposition 5.1 *(See [13]) Let φ and ψ be two complementary Musielak-Orlicz functions satisfying the conditions of Lemma 2.1, assume that (8)-(12) hold, then, for any $n \in \mathbb{N}^*$, there exists at least one solution $u_n \in W_0^1 E_\varphi(\Omega)$ of (15).*

Step 2:   Consider the following approximate problems:

$$\begin{cases} u_n \in \mathcal{T}_0^{1,\varphi}(\Omega) \cap W_0^1 E_\varphi(\Omega) \\ < A(u_n), v > + \displaystyle\int_\Omega K_n(x, u_n, \nabla u_n) v dx = < \mu_n, v >, \quad \forall v \in W_0^1 L_\varphi(\Omega). \end{cases} \qquad (17)$$

By proposition, there exists at least one solution u_n of (17).

Lemma 5.1 *Let u_n be a solution of the approximate problem (15), then*

1. *for all $k > 0$, there exists a constant C (which does not depend on n and k) such that*

$$\int_\Omega a(x, T_k(u_n), \nabla T_k(u_n)) \nabla T_k(u_n) dx \le C_2 k, \qquad (18)$$

   and

$$\int_\Omega \varphi(x, |\nabla T_k(u_n)|) dx \le C_3 k. \qquad (19)$$

2. *There exists a measurable function u such that*

$$u_n \to u \quad a.e. \ in \quad \Omega. \qquad (20)$$

3.
$$a(x, T_k(u_n), \nabla T_k(u_n)) \rightharpoonup \varpi_k \ weakly \ in \ \left(L_\psi(\Omega)\right)^N \ for \ \sigma(\Pi L_\psi, \Pi E_\varphi). \qquad (21)$$

Proof of Lemma 5.1.   (1) Let $v_0 \in W_0^1 L_\varphi(\Omega) \cap L^\infty(\Omega)$ with $v_0 \ge 0$.
On the one hand, taking $\exp(G(u_n)) v_0$ as a test function in (15), where $G(s) = \displaystyle\int_0^s \frac{1}{\alpha} \rho(r) dr$, we obtain

$$\int_\Omega a(x, u_n, \nabla u_n) \exp(G(u_n)) \frac{\rho(u_n)}{\alpha} \nabla u_n v_0 \, dx + \int_\Omega a(x, u_n, \nabla u_n) \exp(G(u_n)) \nabla v_0 dx$$

$$+ \int_\Omega K_n(x, u_n, \nabla u_n) \exp(G(u_n)) v_0 dx = \int_\Omega \mu_n \exp(G(u_n)) v_0 dx,$$

by (10) and (11) we simplify by the term $\int_\Omega \rho(u_n)\varphi(x, |\nabla u_n|) v_0 \, dx$ and we have

$$\int_\Omega a(x, u_n, \nabla u_n) \exp(G(u_n)) \nabla v_0 \, dx \le \int_\Omega \mu_n \exp(G(u_n)) v_0 dx + \int_\Omega b(x) \exp(G(u_n)) v_0 \, dx.$$
(22)

On the other hand, taking $\exp(-G(u_n))v_0$ as a test function in (15), we deduce also

$$\int_\Omega a(x, u_n, \nabla u_n) \exp(-G(u_n)) \nabla v_0 dx + \int_\Omega b(x) \exp(-G(u_n)) v_0 \, dx \ge \int_\Omega \mu_n \exp(-G(u_n)) v_0 dx.$$
(23)

By choosing $v_0 = T_k(u_n)^+$ in (22), we otain

$$\int_\Omega a(x, u_n, \nabla u_n) \exp(G(u_n))) \nabla T_k(u_n)^+ dx$$

$$\le \int_\Omega \mu_n \exp(G(u_n))) T_k(u_n)^+ dx + \int_\Omega b(x) \exp(G(u_n))) T_k(u_n)^+ \, dx.$$

Since $\rho \in L^1(\mathbb{R})$, we see that $G(-\infty) \le G(s) \le G(+\infty)$ and $|G(\pm\infty)| \le \frac{1}{\alpha} \|\rho\|_{L^1(\mathbb{R})}$, then we have

$$\int_\Omega a(x, T_k(u_n), \nabla T_k(u_n)) \nabla T_k(u_n)^+ \, dx \le \exp\big(\frac{\|\rho\|_{L^1(\mathbb{R})}}{\alpha}\big) k[\|\mu\|_{\mathcal{M}_b(\Omega)} + \|b\|_{L^1(\Omega)}] = kC_4,$$

and using (10) we get

$$\int_\Omega \varphi(x, |\nabla T_k(u_n)^+|) dx \le kC_5.$$

Choosing again $v_0 = T_k(u_n)^-$ in (23) we get

$$- \int_{\{-k \le u_n \le 0\}} a(x, u_n, \nabla u_n) \exp(-G(u_n))) \nabla u_n \, dx + \int_\Omega b(x) \exp(-G(u_n))) T_k(u_n)^- dx$$

$$\ge \int_\Omega \mu_n \exp(-G(u_n))) T_k(u_n)^- dx.$$

Similarly we obtain

$$\int_{\{-k \le u_n \le 0\}} a(x, T_k(u_n), \nabla T_k(u_n)) \nabla u_n \, dx \le \exp\big(\frac{\|\rho\|_{L^1(\mathbb{R})}}{\alpha}\big) k[\|\mu\|_{\mathcal{M}_b(\Omega)} + \|b\|_{L^1(\Omega)}]$$

$$= kC_4.$$

and by (10) we have

$$\int_\Omega \varphi(x, |\nabla T_k(u_n)^-|) dx \le kC_6.$$

We deduce respectively the results (19) and (18).

(2) Using (4) we have

$$\inf_{x \in \Omega} \varphi(x, \frac{k}{C_1}) \mathrm{meas}\{|u_n| > k\} \le \int_{\{|u_n| > k\}} \varphi(x, \frac{|T_k(u_n)|}{C_1}) \, dx$$

$$\le \int_\Omega \varphi(x, |\nabla T_k(u_n)|) dx \le kC_7.$$

Then

$$\text{meas}\{|u_n| > k\} \leq \frac{kC_7}{\inf_{x \in \Omega} \varphi(x, \frac{k}{C_1})},$$

for all n and for all k.

Assume that there exists a positive function M such that $\lim_{t \to \infty} \frac{M(t)}{t} = +\infty$ and $M(t) \leq ess \inf_{x \in \Omega} \varphi(x, t)$, $\forall t \geq 0$. Thus, we get

$$\lim_{k \to \infty} \text{meas}\{|u_n| > k\} = 0.$$

By the property (1) of Lemma 5.1, we deduce that $T_k(u_n)$ is bounded in $W_0^1 L_\varphi(\Omega)$ and then there exists some $\tau_k \in W_0^1 L_\varphi(\Omega)$ such that

$$T_k(u_n) \rightharpoonup \tau_k \quad \text{weakly in} \quad W_0^1 L_\varphi(\Omega) \quad \text{for} \quad \sigma(\Pi L_\varphi, \Pi E_\psi),$$

$$\text{strongly in} \quad E_\varphi(\Omega) \quad \text{and a.e. in} \quad \Omega,$$

and by (2) of Lemma 5.1, the sequence $(u_n)_n$ converges almost everywhere to some measurable function u. Then we have $T_k(u_n) \rightharpoonup T_k(u)$ weakly in $W_0^1 L_\varphi(\Omega)$ for $\sigma(\Pi L_\varphi, \Pi E_\psi)$, strongly in $E_\varphi(\Omega)$ and a.e. in Ω.

(3) We shall prove that $\{a(x, T_k(u_n), \nabla T_k(u_n))\}_n$ is bounded in $(L_\psi(\Omega))^N$ for all $k > 0$. Let $w \in (E_\varphi(\Omega))^N$ be arbitrary. By (9) we have

$$(a(x, u_n, \nabla u_n) - a(x, u_n, w))(\nabla u_n - w) \geq 0.$$

Then

$$\int_{\{|u_n| \leq k\}} a(x, u_n, \nabla u_n) w \, dx \leq \int_{\{|u_n| \leq k\}} a(x, u_n, \nabla u_n) \nabla u_n \, dx + \int_{\{|u_n| \leq k\}} a(x, u_n, w)(w - \nabla u_n) \, dx.$$

By (8) and according to Remark 2.1 there exists $k' > 0$ such that $\gamma(x, \nu_1 k) \leq k' \varphi(x, 1)$ and for $\lambda > 0$ is large enough

$$\int_{\{|u_n| \leq k\}} \psi\left(\frac{a(x, u_n, \frac{w}{\nu_2})}{3\beta}\right) dx \leq \frac{1}{3}\left[\int_\Omega \psi(c(x)) dx + \int_\Omega k' \varphi(x, 1) dx + \int_\Omega \varphi(x, w) dx\right] \leq C_7.$$
(24)

Thus $\{a(x, T_k(u_n), \frac{w}{\nu_2})\}$ is bounded in $(L_\psi(\Omega))^N$, by (24),(18) and in view of the Banach-Steinhaus theorem, the sequence $\{a(x, T_k(u_n), \nabla T_k(u_n))\}$ remains bounded in $(L_\psi(\Omega))^N$ and for a subsequence

$$a(x, T_k(u_n), \nabla T_k(u_n)) \rightharpoonup \varpi_k \quad \text{weakly in} \quad (L_\psi(\Omega))^N \quad \text{for} \quad \sigma(\Pi L_\psi, \Pi E_\varphi).$$

Step 3: Almost everywhere convergence of the gradients.
To have that the gradient converges almost everywhere, we need to prove the following proposition.

Proposition 5.2 *Let $\{u_n\}_n$ be a solution of the approximate problem(15), then*

1.

$$\lim_{m \to \infty} \limsup_{n \to \infty} \int_{\{-(m+1) \leq u_n \leq -m\}} a(x, u_n, \nabla u_n) \nabla u_n \, dx = 0; \qquad (25)$$

2. for a subsequence as $n \to \infty$

$$\nabla u_n \to \nabla u \quad a.e. \ in \quad \Omega. \tag{26}$$

Proof. (1) Take the function $v_0 = T_1(u_n - T_m(u_n))^-$ in (23), this function is admissible since $v_0 \in W_0^1 L_\varphi(\Omega) \cap L^\infty(\Omega)$, and $v_0 \geq 0$, then we have

$$- \int_\Omega a(x, u_n, \nabla u_n) \exp(-G(u_n)) \nabla T_1(u_n - T_m(u_n))^- \, dx$$

$$\leq \int_\Omega b(x) \exp(-G(u_n)) T_1(u_n - T_m(u_n))^- dx.$$

Since μ is nonnegative, we get

$$\int_{\{-(m+1) \leq u_n \leq -m\}} a(x, u_n, \nabla u_n) \exp(-G(u_n))) \nabla u_n \, dx$$

$$\leq \int_\Omega b(x) \exp(-G(u_n))) T_1(u_n - T_m(u_n))^- dx$$

$$\leq \exp\left(\frac{\|\rho\|_{L^1_{\mathbb{R}}}}{\alpha}\right) \int_\Omega |b(x)| T_1(u_n - T_m(u_n))^- \, dx.$$

By Lebesgue's theorem, we conclude the result (25).

(2) To show that $\nabla u_n \to \nabla u$ a.e. in Ω is true, simply adapt the proof from [3] and follow the same steps by taking $\Phi = 0$.

Step 4: Equi-integrability of the nonlinearity sequence.
We shall prove that

$$K_n(x, u_n, \nabla u_n) \to K(x, u, \nabla u) \quad \text{strongly in} \quad L^1(\Omega). \tag{27}$$

Consider $v_0 = \int_0^{u_n} \rho(s) \chi_{\{s>h\}} dx$ in (22), we get

$$\int_\Omega a(x, u_n, \nabla u_n) \exp(G(u_n)) \nabla v_0 dx \leq \int_\Omega \mu_n \exp(G(u_n)) v_0 dx + \int_\Omega b(x) \exp(G(u_n)) v_0 dx.$$

Then using (10) and (11) we have

$$\alpha \int_{\{u_n>h\}} \rho(u_n)\varphi(x, \nabla u_n) dx \leq \left(\int_h^{+\infty} \rho(s) dx\right) \exp\left(\frac{\|\rho\|_{L^1(\mathbb{R})}}{\alpha}\right) [\|\mu\|_{\mathcal{M}_b(\Omega)} + \|b\|_{L^1(\Omega)}]$$

$$\int_{\{u_n>h\}} \rho(u_n)\varphi(x, \nabla u_n) dx \leq \frac{C_4}{\alpha}\left(\int_h^{+\infty} \rho(s) dx\right).$$

Since $\rho \in L^1(\mathbb{R})$, we get

$$\lim_{h \to +\infty} \sup_{n \in \mathbb{N}} \int_{\{u_n>h\}} \rho(u_n)\varphi(x, \nabla u_n) dx = 0.$$

Similarly, let $v_0 = \int_{u_n}^0 \rho(s) \chi_{\{s<-h\}} dx$ in (23), we have also

$$\lim_{h \to +\infty} \sup_{n \in \mathbb{N}} \int_{\{u_n<-h\}} \rho(u_n)\varphi(x, \nabla u_n) dx = 0.$$

We conclude that

$$\lim_{h\to+\infty}\sup_{n\in\mathbb{N}}\int_{\{|u_n|>h\}}\rho(u_n)\varphi(x,\nabla u_n)dx = 0. \tag{28}$$

Let $D \subset \Omega$, then

$$\int_D \rho(u_n)\varphi(x,\nabla u_n)dx \leq \max_{\{|u_n|\leq h\}}(\rho(x))\int_{D\cap\{|u_n|\leq h\}}\varphi(x,\nabla u_n)dx$$

$$+\int_{D\cap\{|u_n|>h\}}\rho(u_n)\varphi(x,\nabla u_n)dx.$$

Consequently, $\rho(u_n)\varphi(x,\nabla u_n)$ is equi-integrable, and since $\rho(u_n)\varphi(x,\nabla u_n)$ converges to $\rho(u)\varphi(x,\nabla u)$ strongly in $L^1(\mathbb{R})$, we get our result.

Step 5: We show that u satisfies (14).

 • $\{u_n\}$ is bounded $W_0^1 L_\phi(\Omega)$ and converges to u strongly in $L_\phi(\Omega)$, where $\phi \in \mathcal{A}_\varphi$.

Firstly, we can take $T_\epsilon(u_n - T_t(u_n)), \epsilon > 0, t > 0$ as a test function in (17), from (11) and (28) we have

$$\int_{\{t\leq|u_n|\leq t+\epsilon\}} a(x,u_n,\nabla u_n)\nabla u_n dx \leq \epsilon C_{10}.$$

The constant C_{10} is independent of n, ϵ and t, then

$$\frac{1}{\epsilon}\int_{\{t\leq|u_n|\leq t+\epsilon\}}\varphi(x,\nabla u_n)dx \leq \frac{C_{10}}{\alpha}.$$

Let now $\epsilon \to 0$, we have

$$-\frac{d}{dt}\int_{\{t\leq|u_n|\}}\varphi(x,\nabla u_n)dx \leq \frac{C_{10}}{\alpha}. \tag{29}$$

Secondly, let $\phi \in \mathcal{A}_\varphi$ and $\phi \sim \varphi$. Using Lemma 3.2, Lemma 3.3, the equation (29) and the same techniques as in [10], we deduce that ∇u_n is bounded in $L_\phi(\Omega)$ for each $\phi \in \mathcal{A}_\varphi$, then u_n is bounded in $W_0^1 L_\phi(\Omega)$ for each $\phi \in \mathcal{A}_\varphi$.

 • $a(x,u_n,\nabla u_n) \rightharpoonup a(x,u,\nabla u)$ weakly for $\sigma(\Pi L_{\phi\circ H^{-1}},\Pi E_\varpi)$,
   where ϖ and $\phi \circ H^{-1}$ are two complementary Musielak-Orlicz functions.
   The first time, using (8) and Remark 2.1, we have

$$\int_\Omega \phi\circ H_x^{-1}\Big(\frac{|a(x,u_n,\nabla u_n)|}{6\beta}\Big)dx \leq \int_\Omega \phi\circ H_x^{-1}\Big(\frac{1}{6}[c(x)+k(\nu_1)\psi_x^{-1}(\varphi(x,|u_n|))$$

$$+\psi_x^{-1}(\varphi(x,\nu_2|\nabla u_n|))])dx.$$

Since $\phi \circ H_x^{-1}$ is a Musielak-Orlicz function, we get

$$\int_\Omega \phi\circ H_x^{-1}\Big(\frac{|a(x,u_n,\nabla u_n)|}{6\beta}\Big)dx \leq \frac{1}{3}\int_\Omega[\phi\circ H_x^{-1}\Big(\frac{1}{2}(c(x))$$

$$+\phi\circ H_x^{-1}\Big(\frac{1}{2}(k(\nu_1)\psi_x^{-1}(\varphi(x,|u_n|)))\Big)+\phi\circ H_x^{-1}\Big(\frac{1}{2}\psi_x^{-1}(\varphi(x,\nu_2|\nabla u_n|)))\Big)]dx. \tag{30}$$

On the other hand, due to the definition of Musielak-Orlicz function, we can easily deduce

$$\frac{1}{2}\psi_x^{-1}(\varphi(x,t)) \le \frac{\varphi(x,t)}{t},$$

by definition of H we have

$$\varphi(x, H_x^{-1}(\frac{t}{2})) \le \psi(x,t),$$

and hence, by Remark 2.1,

$$\phi \circ H_x^{-1}\big(\frac{1}{2}c(x)\big) \le k_1 \varphi(x, H_x^{-1}(\frac{c(x)}{2})) \le k_1 \psi(x, c(x)), \tag{31}$$

also we have

$$\phi \circ H^{-1}\big(\frac{1}{2}\psi_x^{-1}(k(\nu_1)\varphi(x,|u_n|))\big) \le \phi \circ H_x^{-1}\big(\frac{1}{2}\psi_x^{-1}\varphi(x, k_2|u_n|)\big)$$

$$\le \phi \circ H_x^{-1}\big(\frac{\varphi(x, k_2|\nabla u_n|)}{k_2|\nabla u_n|}\big),$$

where $k_2 = \max(1, k(\nu_1))$, then

$$\phi \circ H^{-1}\big(\frac{1}{2}\psi_x^{-1}(k(\nu_1)\varphi(x,|u_n|))\big) \le k_3 \varphi(x, |u_n|), \tag{32}$$

and

$$\phi \circ H_x^{-1}\big(\psi_x^{-1}(\frac{1}{2}\varphi(x, \nu_2|\nabla u_n|))\big) \le \phi \circ H_x^{-1}\big(\frac{\varphi(x, \nu_2|\nabla u_n|)}{\nu_2|\nabla u_n|}\big).$$

$$= \phi(x, \nu_2|\nabla u_n|).$$

Using Remark 2.1 we get

$$\phi \circ H_x^{-1}\big(\psi_x^{-1}(\frac{1}{2}\varphi(x, \nu_2|\nabla u_n|))\big) \le k_4 \varphi(x, |\nabla u_n|), \tag{33}$$

applying (31), (32) and (33) in (30) we obtain

$$\int_\Omega \frac{1}{3}\phi \circ H_x^{-1}\big(\frac{|a(x, u_n, \nabla u_n)|}{6\beta}\big)dx$$

$$\le \int_\Omega [k_1\psi(x, c(x))dx + k_3\varphi(x, |u_n|) + k_4\varphi(x, |\nabla u_n|)]dx < C_{11}.$$

Consequently, $a(x, u_n, \nabla u_n) \rightharpoonup a(x, u, \nabla u)$ weakly for $\sigma(\Pi L_{\phi \circ H^{-1}}, \Pi E_\varpi)$.

• Take now $v \in \mathcal{D}(\Omega)$ as a test function in approximate equation (15), one has

$$\int_\Omega a(x, u_n, \nabla u_n)vdx + \int_\Omega K(x, u_n, \nabla u_n)vdx = \int_\Omega \mu_n vdx,$$

since we have $u_n \to u$ strongly in $(E_\kappa(\Omega))^N$, for every $\kappa \prec\prec \phi$, $\forall \phi \in \mathcal{A}_\varphi$.

Using (27) and (16) we can pass to the limit as $n \to +\infty$ to end the proof of Theorem 5.1.

References

[1] R.A. Adams. *Sobolev Spaces.* New York, Academic Press, 1975.

[2] A. Aberqi, J. Bennouna and M. Hammoumi. Existence Result for Nonlinear Degenerated Parabolic Systems. *Nonlinear Dynamics and Systems Theory.* **17**(3) (2017) 217–229.

[3] A. Aberqi, J. Bennouna and M. Elmassoudi. Nonlinear elliptic equations with measure data in Musielak-Orlicz spaces. *Gulf Journal of Mathematics.* **6** (4) (2018) 79–100.

[4] T. Ahmedatt, A. Aberqi, A. Touzani and C. Yazough. On some nonlinear hyperbolic $p(x,t)$-Laplacian equations. *J. Appl. Anal.* **24**(1) (2018) 55–69.

[5] M. Ait Khellou and A. Benkirane. Elliptic inequalities with L^1 data in Musielak-Orlicz spaces. *Monatsh Math.* **183** (1) (2017) 1–33.

[6] M. Ait Khellou, A. Benkirane and S. M. Douiri. Strongly non-linear elliptic problems in Musielak spaces with L^1 data. *Nonlinear Studies.* **23** (3) (2016) 491–510.

[7] M. Ait Kellou, A. Benkirane and S. M. Douiri. An inequality of type Poincaré in Musielak spaces and applications to some nonlinear elliptic problems with L^1-data. *Complex Variables and Elliptic Equations.* **60** (2015) 1217–1242.

[8] Y. Akdim, N. El gorch and M. Mekkour. Existence of renormalized solutions for $p(x)$-parabolic equations with three unbounded non-linearities. *Bol. Soc. Parana. Mat.* **34** (1) (2016) 225–252.

[9] S. Antontsev and S. Shmarev. *Evolution PDEs with Nonstandard Growth Conditions, Existence, Uniqueness, Localization, Blow-up.* Atlantis Studies in Differential Equations, v. 4. Series editor Michel Chipot. Zürich, Switzerland, 2015.

[10] A. Benkirane and J. Bennouna. Existence of entropy solutions for some nonlinear problems in Orlicz spaces. *Abstract and Applied Analysis.* **7** (2) (2002) 85–102.

[11] A. Benkirane and M. Sidi El Vally. Some approximation properties in Musielak-Orlicz-Sobolev spaces. *Thai. J. Math.* (2012) 371-381.

[12] A. Benkirane and M. Sidi El Vally. Variational inequalities in Musielak-Orlicz-Sobolev spaces. *Bull. Belg. Math. Soc.* Simon Stevin, (2014) 787–811.

[13] G. Dong and X. Fang. Existence results for some nonlinear elliptic equations with measure data in Orlicz-Sobolev spaces. *Boundary Value Problems.* **2015** (2015) 18.

[14] A. Elmahi and D. Meskine. Existence of solutions for elliptic equations having natural growth terms in Orlicz spaces. *Abstr. Appl. Anal.* **12** (2004) 1031–1045.

[15] M. Elmassoudi, A. Aberqi and J. Bennouna. Existence of Entropy Solutions in Musielak-Orlicz Spaces Via a Sequence of Penalized Equations. *Bol. Soc. Paran. Mat.* **38** (6) (2020) 203–238.

[16] W. Fleming and R. Rishel. An integral formula for total gradient variation. *Arch. Math.* **11** (1960).

[17] J.P. Gossez. A strongly nonlinear elliptic problem in Orlicz Sobolev spaces. *Proc. Am. Math. Soc. Symp. Pure Math.* **45** (1986) 455–462.

[18] M. C. Hassib, Y. Akdim, A. Benkirane and N. Aissaoui. Capacity, Theorem of H. Brezis and F.E. Browder Type in Musielak Orlicz Sobolev Spaces and Application. *Nonlinear Dynamics and Systems Theory.* **17** (2) (2017) 175–192.

[19] J. Musielak. *Modular Spaces and Orlicz Spaces. Lecture Notes in Math.* 1983.

[20] G. Talenti. Nonlinear elliptic equations, Rearrangements of functions and Orlicz Spaces. *Annali di Matematica.* (1976) 159–184.

A New Integral Transform for Solving Higher Order Ordinary Differential Equations

S.A. Pourreza Ahmadi *, H. Hosseinzadeh and A. Yazdani Cherati

Department of Mathematics, University of Mazandaran, Babolsar, Iran

Abstract: In this work a new integral transform is introduced and applied to solve higher order linear ordinary differential equations with constants coefficients and variable coefficients as well as. We compare the present transform with other existing transforms such as the Laplace, Elzaki, Sumudu and other ones.

Keywords: *integral transform; ordinary differential equations; Laplace transform; Sumudu transform; Elzaki transform.*

Mathematics Subject Classification (2010): 34A37, 44A05, 45E10.

1 Introduction

The differential equations have played a fundamental role in every aspect of applied mathematics for a very long time [1, 5–8, 10, 15, 19, 20]. Integral transform methods have been modified to solve several dynamic equations with initial or boundary conditions in many ways the Laplace, Sumudu and Elzaki transforms are such typical tools [4, 5, 9, 11–15]. In this paper we introduce a new integral transform and then some relationship between this transform and the Laplace, Sumudu, Elzaki and natural transforms; further, for the comparison purpose, we apply all transforms to solve differential equations to see the differences and similarities. Finally, we provide some examples relating to the second order differential equations with non-constant coefficients as a special case. For the function $f(t)$ that is piecewise continuously differentiable in every finite interval and is absolutely integrable on the whole real line the following integral equations hold true in the domain $-\infty < t < +\infty :$

$$\mathcal{F}\{f(t)\} = F(k) = \frac{1}{\sqrt{2}} \int_{-\infty}^{+\infty} e^{-ikt} f(t)\, dt,\ \ t \neq 0. \tag{1}$$

---

* Corresponding author: mailto:s.a.pourreza@stu.umz.ac.ir

This transform is called the Fourier transform of f(t). The natural transform of f(t) for t$\in (0, +\infty)$, obtained from the Fourier transform, is defined as.

$$\mathcal{N}\{f(t)\} = \int_0^{+\infty} e^{-st} f(ut) dt; \quad s > 0, u > 0. \tag{2}$$

If we assign $u = 1$ in (2), then it is called the Laplace transform and written as

$$\mathcal{L}\{f(t)\} = \int_0^{+\infty} e^{-st} f(t) dt; \quad s > 0. \tag{3}$$

If we assign $s = 1$ in (2), then it is called Sumudu transform and written as

$$\mathcal{G}\{f(t)\} = \int_0^{+\infty} e^{-t} f(ut) dt; \quad u > 0. \tag{4}$$

Finally, we assign $u = 1$ and $s = \frac{1}{\lambda}$ in (2) and multiply it by λ, then it is called the Elzaki transform and written as

$$\mathcal{T}\{f(t)\} = \lambda \int_0^{+\infty} e^{-\frac{1}{\lambda}t} f(t) dt. \tag{5}$$

The above mentioned integral transforms has been applied to solve higher order linear ordinary differential equation (ODEs), partial differential equations (PDEs), a system of ordinary and partial differential equations and integral equations.

In this paper, we introduced a new integral transform. We have compared the new transform with other exiting transforms. We solve ODEs with variable and constant coefficients using the new transform. Moreover, we obtain the solution of integral equations using this transform. The new transform is very effective for the solution of the response of linear and nonlinear differential equations.

2   A New Integral Transform and Its Properties

Definition 2.1 The HY integral transform is defined by

$$\mathbf{P}(\nu) = HY\{f(t)\} = \nu \int_0^{+\infty} e^{-\nu^2 t} f(t) dt. \tag{6}$$

The HY integral transform states that, if $f(t)$ is piecewise continuous on every finite interval in $t \in [0, +\infty)$ satisfying

$$|f(t)| \leq M e^{at}, \ \exists M > 0 \tag{7}$$

for all $t \in [0, \infty)$, then $HY\{f(t)\}(\nu)$ exists for all $\nu > a$.

If we assign $u = 1$ and $s = v^2$ in (2) and multiply it by v, then we obtain our defined new integral transform which is (6).

Theorem 2.1 *(Criteria for convergence)*
The HY integral transform of f(t) exists, if it has exponential order and the integral

$$\int_0^b |f(t)| dt$$

exists for any b>0.

Proof: Since we only need to show convergence for sufficiently large ν, assume $\boldsymbol{\nu} > \sqrt{c}$ and $\boldsymbol{\nu} > 0$.

$$
\begin{aligned}
\boldsymbol{\nu} \int_0^\infty \left| f(t) e^{-\boldsymbol{\nu}^2 t} \right| dt &= \boldsymbol{\nu} \int_0^n \left| f(t) e^{-\boldsymbol{\nu}^2 t} \right| dt + \boldsymbol{\nu} \int_n^\infty \left| f(t) e^{-\boldsymbol{\nu}^2 t} \right| dt \\
&\leq \boldsymbol{\nu} \int_0^n |f(t)| \, dt + \boldsymbol{\nu} \int_n^\infty e^{-\boldsymbol{\nu}^2 t} |f(t)| \, dt, \qquad 0 \leq e^{-\boldsymbol{\nu}^2 t} \leq 1 \\
&\leq \boldsymbol{\nu} \int_0^n |f(t)| \, dt + \boldsymbol{\nu} \int_n^\infty e^{-\boldsymbol{\nu}^2 t} M e^{ct} \, dt \\
&\leq \boldsymbol{\nu} \int_0^n |f(t)| \, dt + \boldsymbol{\nu} M \left[\frac{e^{(c-\boldsymbol{\nu}^2)t}}{c - \boldsymbol{\nu}^2} \right]_n^\infty, \qquad \boldsymbol{\nu} > \sqrt{c} \\
&\leq \boldsymbol{\nu} \int_0^n |f(t)| \, dt + \boldsymbol{\nu} M \left[\frac{e^{(c-\boldsymbol{\nu}^2)n}}{c - \boldsymbol{\nu}^2} \right], \qquad \boldsymbol{\nu} > \sqrt{c}.
\end{aligned}
$$

The first integral exists by assumption, and the second term is finite for $\boldsymbol{\nu}^2 > c$, so the integral $\nu \int_0^{+\infty} e^{-\nu^2 t} f(t) \, dt$ is convergent absolutely and the HY transform of $f(t)$ exist.
□

Theorem 2.2 (*Linear property of HY transform*)
Let $P(v)$ and $Q(v)$ be HY transforms of $f(t)$ and $g(t)$, respectivly, for each constants of c_1 and c_2, Then

$$
HY\{c_1 f(t) + c_2 g(t)\} = c_1 HY\{f(t)\} + c_2 HY\{g(t)\} = c_1 P(v) + c_2 Q(v).
$$

Proof: Beacuase of the linear property of the Integrals, the proof is obvious. □

Theorem 2.3 *Let $P(v)$ be the HY transform of $f(t)$. Then*

$$
\begin{aligned}
HY\left\{ f'(t) \right\} &= \boldsymbol{\nu}^2 P(\boldsymbol{\nu}) - \boldsymbol{\nu} f(0), & (8) \\
HY\left\{ f''(t) \right\} &= \boldsymbol{\nu}^4 P(\boldsymbol{\nu}) - \boldsymbol{\nu}^3 f(0) - \boldsymbol{\nu} f'(0), & (9) \\
HY\left\{ f^{(n)}(t) \right\} &= \boldsymbol{\nu}^{2n} P(\boldsymbol{\nu}) - \sum_{k=0}^{n-1} \boldsymbol{\nu}^{2(n-k)-1} f^{(k)}(0), & n \geq 1. & (10)
\end{aligned}
$$

Proof: Replacing $f(t)$ with $f'(t)$ in (6) gives $HY\left\{ f'(t) \right\} = \boldsymbol{\nu} \int_0^\infty e^{-\boldsymbol{\nu}^2 t} f'(t) dt$. Integrate by parts to find that $HY\left\{ f'(t) \right\} = \boldsymbol{\nu}^2 \mathrm{P}(\boldsymbol{\nu}) - \boldsymbol{\nu} f(0)$.

Let g(t)= $f'(t)$, then $g'(t) = f''(t)$, thus by using (9), we get $HY\left\{ f''(t) \right\} = \boldsymbol{\nu}^4 \mathrm{P}(\boldsymbol{\nu}) - \boldsymbol{\nu}^3 f(0) - \boldsymbol{\nu} f'(0)$. (10) can be provided by mathematical induction. □

In the following table, we showed the HY transform of some important functions, where $\delta(t)$ is the unit impulse function.

Function (f(t))	HY Transform	HY^{-1} Transform
$\delta\left(t\right)$	$\boldsymbol{\nu}$	$\delta\left(t\right)$
1	$\frac{1}{\boldsymbol{\nu}}$	1
at^n	$\frac{a.n!}{\boldsymbol{\nu}^{2n+1}}, \quad$ a constant	at^n
t^a	$\frac{\Gamma(a+1)}{\boldsymbol{\nu}^{2n+1}}, \quad$ a>-1	t^a
$e^{\pm\alpha t}$	$\frac{\boldsymbol{\nu}}{\boldsymbol{\nu}^2 \pm\alpha}$	$e^{\pm\alpha t}$
$\sin at$	$\frac{\alpha\boldsymbol{\nu}}{\boldsymbol{\nu}^4 +a^2}$	$\sin at$
$\cos at$	$\frac{\boldsymbol{\nu}^3}{\boldsymbol{\nu}^4 +a^2}$	$\cos at$
$\sinh at$	$\frac{\alpha\boldsymbol{\nu}}{\boldsymbol{\nu}^4 -a^2}$	$\sinh at$
$\cosh at$	$\frac{\boldsymbol{\nu}^3}{\boldsymbol{\nu}^4 -a^2}$	$\cosh at$

Table 1: HY transforms for some basic functions.

3   Application

3.1   Solving higher order ODEs with constant coefficient using new integral transform

In this section we use new the integral transform for solving higher order ODEs with constant and variable coefficients and integral equations. At first, we solve the linear equation of order n with constant coefficients as

$$L\left(D\right)\left[y\left(t\right)\right] = D^n y(t) + a_1 D^{n-1} y\left(t\right) + a_2 D^{n-2} y\left(t\right) + \cdots + a_n y\left(t\right) = \phi\left(t\right) \quad (11)$$

with the initial conditions

$$y\left(t_0\right) = y_0, Dy\left(t_1\right) = y_1, D^2 y\left(t_2\right) = y_2, \cdots, D^{n-1} y\left(t_{n-1}\right) = y_{n-1},$$

where $D = \frac{d}{dt}$ is a differential operator. $y_0, \; y_1, \; \cdots, \; y_{n-1}$ and $a_1, \; a_2, \cdots, \; a_n$ are constants. We apply the new integral transform on both side of (11)

$$HY(D^n y\left(t\right) + a_1 D^{n-1} y\left(t\right) + a_2 D^{n-2} y\left(t\right) + \cdots + a_n y\left(t\right)) = HY(\phi\left(t\right)).$$

By using the linear property of this transform we have

$$HY(D^n y\left(t\right)) + a_1 HY\left(D^{n-1} y\left(t\right)\right) + a_2 HY\left(D^{n-2} y\left(t\right)\right) + \cdots + a_n HY(y\left(t\right))$$

$$= HY(\phi\left(t\right)) = \phi(\boldsymbol{\nu})$$

$$\left\{\boldsymbol{\nu}^{2n}\mathrm{P}(\boldsymbol{\nu}) - \sum_{k=0}^{n-1} \boldsymbol{\nu}^{2(n-k)-1} f^{(k)}(0)\right\} + a_1 \left\{\boldsymbol{\nu}^{2(n-1)}\mathrm{P}(\boldsymbol{\nu}) - \sum_{k=0}^{n-2} \boldsymbol{\nu}^{2(n-k)-2} f^{(k)}(0)\right\}$$

$$+ \cdots + a_n \mathrm{P}\left(\boldsymbol{\nu}\right) = \phi\left(\boldsymbol{\nu}\right), \quad\quad\quad (12)$$

where $\phi\left(\boldsymbol{\nu}\right)$ is the HY transform of $\phi\left(t\right)$. (10) can be writen in the following form:

$$\underbrace{\left[\boldsymbol{\nu}^{2n} + a_1 \boldsymbol{\nu}^{2(n-1)} + \cdots + a_n\right]}_{f(\boldsymbol{\nu})} \mathrm{P}\left(\boldsymbol{\nu}\right) = \phi\left(\boldsymbol{\nu}\right) + \psi\left(\boldsymbol{\nu}\right),$$

$$\mathrm{P}\left(\boldsymbol{\nu}\right) = \frac{\phi(\boldsymbol{\nu}) + \psi(\boldsymbol{\nu})}{f(v)}, \quad\quad \mathrm{P}\left(\boldsymbol{\nu}\right) = HY\left(y\left(t\right)\right) = \frac{\phi(\boldsymbol{\nu})}{f(v)} + \frac{\psi(\boldsymbol{\nu})}{f(\boldsymbol{\nu})}.$$

Inversion yields:

$$y\left(t\right) = HY^{-1}\left(\frac{\phi\left(\boldsymbol{\nu}\right)}{f\left(\boldsymbol{\nu}\right)}\right) + HY^{-1}\left(\frac{\psi\left(\boldsymbol{\nu}\right)}{f\left(\boldsymbol{\nu}\right)}\right). \tag{13}$$

The inverse operation on the right hand can be carried out by a partial fraction or any method.

Example 3.1 Solve the following initial value problem:

$$y^{'''}\left(t\right) + 2y^{''}\left(t\right) + 2\ y^{'}\left(t\right) + 3y\left(t\right) = \sin t + \cos t, \tag{14}$$
$$\text{y}\left(0\right) = \text{y}^{'}\left(0\right) = \text{y}^{''}\left(0\right) = 0.$$

Taking the HY transform on both sides (14) , we get

$$HY\left\{y^{'''}\left(t\right)\right\} + 2HY\left\{y^{''}\left(t\right)\right\} + 2HY\left\{y^{'}\left(t\right)\right\} + 3\ HY\left\{y\left(t\right)\right\} = HY\left\{\sin\left(t\right)\right\} + HY\left\{\cos\left(t\right)\right\},$$

$\boldsymbol{\nu}^6\mathrm{P}\left(\boldsymbol{\nu}\right) + 2\boldsymbol{\nu}^4\mathrm{P}\left(\boldsymbol{\nu}\right) + 2\boldsymbol{\nu}^2\mathrm{P}\left(\boldsymbol{\nu}\right) + 3P\left(v\right) = \frac{\boldsymbol{\nu}}{\boldsymbol{\nu}^4+1} + \frac{\boldsymbol{\nu}^3}{\boldsymbol{\nu}^4+1} + v^3 + 2v,$
$\mathrm{P}\left(\boldsymbol{\nu}\right) = \frac{\boldsymbol{\nu}}{\boldsymbol{\nu}^4+1}$. Take the inverse HY transform $y\left(t\right) = \sin\left(t\right)$, which is an exact solution of (14).

3.2 Solving higher order ODEs with variable coefficient using new integral transform

Now we want to apply the new integral transform to solve ODE with variable coefficient. Before doing this, process we present few theorems which are useful in our work.

Theorem 3.1 Let $P(v)$ be the HY of function $f\left(t\right)$, then

$$HY\{tf\left(t\right)\} = \left(\frac{-1}{2}\right)\frac{d}{d\boldsymbol{\nu}}\left(\frac{p\left(\boldsymbol{\nu}\right)}{\boldsymbol{\nu}}\right), \tag{15}$$

$$HY\{t^2 f\left(t\right)\} = \left(\frac{-1}{2}\right)^2\frac{d}{d\boldsymbol{\nu}}\left(\frac{1}{\boldsymbol{\nu}}\frac{d}{d\boldsymbol{\nu}}\left(\frac{p\left(\boldsymbol{\nu}\right)}{\boldsymbol{\nu}}\right)\right), \tag{16}$$

$$HY\{t^n f\left(t\right)\} = \left(\frac{-1}{2}\right)^n\frac{d}{d\boldsymbol{\nu}}\left(\underbrace{\frac{1}{\boldsymbol{\nu}}\cdots\frac{d}{d\boldsymbol{\nu}}}_{n\ times}\left(\frac{p\left(\boldsymbol{\nu}\right)}{\boldsymbol{\nu}}\right)\cdots\right), \quad n \geq 1. \tag{17}$$

Proof: Since $p\left(\boldsymbol{\nu}\right) = HY\{\text{f(t)}\} = \boldsymbol{\nu}\int\limits_0^\infty e^{-\boldsymbol{\nu}^2 t}f\left(t\right)dt,$

$\frac{\mathrm{d}}{\mathrm{d}\boldsymbol{\nu}}\left(\frac{p(\boldsymbol{\nu})}{\boldsymbol{\nu}}\right) = -2\boldsymbol{\nu}\underbrace{\int_0^\infty e^{-\boldsymbol{\nu}^2 t}tf\left(t\right)dt}_{HY\{tf(t)\}}$. First, divide both sides of the above equation by $\boldsymbol{\nu}$ and take the derivative with respect to $\boldsymbol{\nu}$, we get

$$HY\{tf\left(t\right)\} = \left(\frac{-1}{2}\right)^1\frac{\mathrm{d}}{\mathrm{d}\boldsymbol{\nu}}\left(\frac{p\left(\boldsymbol{\nu}\right)}{\boldsymbol{\nu}}\right).$$

From (15). we have $HY\{tf(t)\} = \left(\frac{-1}{2}\right)^1 \frac{d}{d\nu}\left(\frac{p(\nu)}{\nu}\right)$,

$\nu \int_0^\infty e^{-\nu^2 t} tf(t)\, dt = \left(\frac{-1}{2}\right)^1 \frac{d}{d\nu}\left(\frac{p(\nu)}{\nu}\right)$ divide both sides of this equation by ν and taking derivative with respect to ν again, result in

$$HY\{t^2 f(t)\} = \left(\frac{-1}{2}\right)^2 \frac{d}{d\nu}\left(\frac{1}{\nu}\frac{d}{d\nu}\left(\frac{p(\nu)}{\nu}\right)\right).$$

(17) can be provided by mathematical induction. □

Theorem 3.2 *Let $P(v)$ be the HY of function $f(t)$, then*

$$HY\left\{tf'(t)\right\} = \left(\frac{-1}{2}\right)^1\left[\frac{d}{d\nu}\left[\frac{1}{\nu}\left[HY\left\{f'(t)\right\}\right]\right]\right], \tag{18}$$

$$HY\left\{tf''(t)\right\} = \left(\frac{-1}{2}\right)^1\left[\frac{d}{d\nu}\left[\frac{1}{\nu}\left[HY\left\{f''(t)\right\}\right]\right]\right], \tag{19}$$

$$HY\left\{t^2 f'(t)\right\} = \left(\frac{-1}{2}\right)^2\frac{d}{d\nu}\left[\frac{1}{\nu}\frac{d}{d\nu}\left[\frac{1}{\nu}\left[HY\left\{f'(t)\right\}\right]\right]\right], \tag{20}$$

$$HY\left\{t^2 f''(t)\right\} = \left(\frac{-1}{2}\right)^2\frac{d}{d\nu}\left[\frac{1}{\nu}\frac{d}{d\nu}\left[\frac{1}{\nu}\left[HY\left\{f''(t)\right\}\right]\right]\right], \tag{21}$$

$$HY\left\{t^n f^{(m)}(t)\right\} = \left(\frac{-1}{2}\right)^n\frac{d}{d\nu}\left[\frac{1}{\nu}\frac{d}{d\nu}\left[\cdots\left[\frac{1}{\nu}\frac{d}{d\nu}\left[\frac{1}{\nu}\left[HY\left\{f^{(m)}(t)\right\}\right]\right]\right]\cdots\right]\right], \tag{22}$$

where $n, m \geq 1$.

Proof: As we know $HY\left\{f'(t)\right\} = \nu \int_0^\infty e^{-\nu^2 t} f'(t)\, dt$, $\frac{1}{\nu}HY\left\{f'(t)\right\} = \int_0^\infty e^{-\nu^2 t} f'(t)\, dt$. First, divide both sides of this equation by ν and take the derivative with respect to ν, we get

$HY\left\{tf'(t)\right\} = \left(\frac{-1}{2}\right)^1\left[\frac{d}{d\nu}\left[\frac{1}{\nu}\left[HY\left\{f'(t)\right\}\right]\right]\right]$ is (18),

replacing $f''(t)$ with $f'(t)$ in (18) results in

$HY\left\{tf''(t)\right\} = \left(\frac{-1}{2}\right)^1\left[\frac{d}{d\nu}\left[\frac{1}{\nu}\left[HY\left\{f''(t)\right\}\right]\right]\right]$ is (19).

Rewrite formula (18) and divide both sides of this equation by ν and take the derivative with respect to ν again, we get

$HY\left\{t^2 f'(t)\right\} = \left(\frac{-1}{2}\right)^2\frac{d}{d\nu}\left[\frac{1}{\nu}\frac{d}{d\nu}\left[\frac{1}{\nu}\left[HY\left\{f'(t)\right\}\right]\right]\right]$ is (20),

replacing $f''(t)$ with $f'(t)$ in (20) results in

$HY\left\{t^2 f''(t)\right\} = \left(\frac{-1}{2}\right)^2\frac{d}{d\nu}\left[\frac{1}{\nu}\frac{d}{d\nu}\left[\frac{1}{\nu}\left[HY\left\{f''(t)\right\}\right]\right]\right]$ is (21).

(22) can be provided by mathematical induction. □

Example 3.2 Solve the following equation with initial values:

$$y''(t) + 3ty'(t) - 6y(t) = 2, \qquad y(0) = y'(0) = 0. \tag{23}$$

Taking the HY transform on both sides of (23), we get

$HY\left\{y^{''}(t)\right\} + 3tHY\left\{y^{'}(t)\right\} - 6\ HY\{y(t)\} = HY\{2\}$,

$\nu^4 P(\nu) - \nu^3 y^{'}(0) - \nu y(0) + 3\left(\left(\frac{-1}{2}\right)\left[\frac{d}{d\nu}\left[\frac{1}{\nu}\left[\nu^2 P(\nu) - \nu y(0)\right]\right]\right]\right) - 6P(\nu) = \frac{2}{\nu}$,

$-\frac{3}{2}\nu\ P^{'}(\nu) - \frac{15}{2}P(\nu)\ +\ \nu^4 P(\nu)\ = \frac{2}{v}$.

This equation is written as follows:

$$P^{'}(\nu) + \frac{(15\nu - 2\nu^5)}{3\nu^2}\ P(\nu)\ = \frac{4}{-3\nu^2}.$$

Thus, we get a linear first order differential equation that must be solved in order to get transform for the solution. In this equation $f(\nu) = \frac{15\nu - 2\nu^5}{3\nu^2}$ and $g(\nu) = \frac{4}{-3\nu^2}$.

Thus the general solution of this equation is

$$P(\nu) = e^{-\int f(\nu)d\nu}\left(\int g(\nu)e^{\int f(\nu)d\nu}d\nu\right)$$

$$= e^{-\int \frac{(15\nu - 2\nu^5)}{3\nu^2}d\nu}\left(\int \frac{4}{-3\nu^2}e^{\int \frac{(15\nu - 2\nu^5)}{3\nu^2}d\nu}d\nu\right) = 2\nu^{-5}e^{\frac{1}{6}\nu^4}e^{-\frac{1}{6}\nu^4} = 2\nu^{-5},$$

$$HY\{y(t)\} = 2\nu^{-5}.$$

Take the inverse HY transform $y(t) = t^2$, which is an exact solution of (23).

Example 3.3 Solve the following initial value problem:

$$2t^2 y^{'''}(t) + 9ty^{''}(t) + 9y^{'}(t) = 60t^2, \qquad y(0) = y^{'}(0) = y^{''}(0) = 0. \qquad (24)$$

Apply the HY transform to equation (24), and make use of the initial conditions and the above mentioned theorems, then we get

$2HY\left\{t^2 y^{'''}(t)\right\} + 9HY\left\{ty^{''}(t)\right\} + 9HY\left\{y^{'}(t)\right\} = HY\{60u^2\}$,

$\frac{15}{2}\nu^2\ P(\nu) + \frac{9}{2}\nu^3 P^{'}(\nu) + \frac{1}{2}\nu^4 P^{''}(\nu) - \frac{27}{2}\nu^2 P(\nu) - \frac{9}{2}\nu^3 P^{'}(\nu) + 6\nu^2 P(\nu) = \frac{60 \times 2!}{\nu^5}$,

$P^{''}(\nu) = \frac{240}{\nu^7}$, $P(\nu) = \frac{30}{7}\frac{1}{\nu^7}$, $y(t) = \frac{5}{7}t^3$, which is an exact solution of (24).

Theorem 3.3 *Let $P(v)$ be the HY of function $f(t)$, then the solution of the Euler-Cauchy equation*

$$t^2 y^{''}(t) + aty^{'}(t) + by(t) = 0 \qquad (25)$$

can be represented by $y = HY^{-1}(\nu^m)$, *where* $m = (a-2) \pm \sqrt{(a-1)^2 - 4b}$ *for* $y(t) = \nu^m$.

Proof: Taking the HY transform on both sides, we have

$HY\left\{t^2 y^{''}(t)\right\} + aHY\left\{ty^{'}(t)\right\} + bHY\{y(t)\} = 0$,

$\left(\frac{-1}{2}\right)^2 \frac{d}{d\nu}\left[\frac{1}{\nu}\frac{d}{d\nu}\left[\frac{1}{\nu}\left[\nu^4 P(\nu) - \nu^3 f(0) - \nu f^{'}(0)\right]\right]\right] + a\left(\frac{-1}{2}\right)\left[\frac{d}{d\nu}\left[\frac{1}{\nu}\left[\nu^2 P(\nu) - \nu f(0)\right]\right]\right] + bP(\nu) = 0$,

$\nu^2 P^{''}(\nu) + (5 - 2a)\nu P^{'}(\nu) + (3 - 2a + 4b) = 0$.

For $Y = HY\{f(t)\} = P(\nu)$. Since Y is a function of ν, let us put $Y = P(\nu) = \nu^m$ as m is constant. Then we have $P^{'}(\nu) = m\nu^{m-1}$ and $P^{''}(\nu) = m(m-1)\nu^{m-2}$, and the given equation becomes

$m(m-1)\boldsymbol{\nu}^m + (5-2a)m\boldsymbol{\nu}^m + (3-2a+4b)\boldsymbol{\nu}^m = 0.$
As we know $\boldsymbol{\nu}^m \neq 0$, then $m(m-1) + (5-2a)m + (3-2a+4b) = 0.$

Organizing this equality, we have $m^2 + (4-2a)m + (3-2a+4b) = 0.$

Hence, $m = log_{\boldsymbol{\nu}} Y = (a-2)\pm\sqrt{(a-1)^2 - 4b}$ and the solution is $y(t) = HY^{-1}(Y) = HY^{-1}\left(\boldsymbol{\nu}^{(a-2)\pm\sqrt{(a-1)^2-4b}}\right).$

Example 3.4 Solve the following Euler-Cauchy equation:

$$t^2 y''(t) - 3ty'(t) + 3y(t) = 0. \tag{26}$$

According to (25), we have $a = -3, \quad b = 3$ and $m = (a-2) \pm \sqrt{(a-1)^2 - 4b}, \quad$ so

$m = (-3-2) \pm \sqrt{(-3-1)^2 - 4(3)}, \quad$ then first, $m = -3$ and second, $m = -7,$
$y_1 = HY^{-1}\left(v^{-3}\right) = t, \quad y_2 = HY^{-1}\left(v^{-7}\right) = t^3.$ Then
the solution is $y = c_1 t + c_2 t^3$, Which is an exact solution of (26).

Example 3.5 Solve the following Euler-Cauchy equation:

$$t^2 y''(t) + \frac{3}{2}ty'(t) - \frac{1}{2}y(t) = 0. \tag{27}$$

According to (25), we have $a = \frac{3}{2}, \quad b = -\frac{1}{2}, \quad m = (a-2) \pm \sqrt{(a-1)^2 - 4b}, \quad$ so

$m = \left(\frac{3}{2} - 2\right) \pm \sqrt{\left(\frac{3}{2} - 1\right)^2 - 4(-\frac{1}{2})}, \quad$ then first, $m = 1$ and second, $m = -2,$
$y_1 = HY^{-1}\left(v^{+1}\right) = \frac{1}{t}, \quad y_2 = HY^{-1}\left(v^{-2}\right) = \sqrt{\frac{t}{\pi}}.$ Then

the solution is $\quad y = c_1 \frac{1}{t} + c_2 \sqrt{\frac{t}{\pi}}$ which is an exact solution of (27).

3.3 Application of new integral transform for integral equations

The integral equations can be solved by our new transform. Before the application of convolution of two functions f(x) and g(x), a theorem should be proved.

Theorem 3.4 *Let $P(\nu)$ and $Q(\nu)$ be the $HY\{f(x)\}$ and $HY\{g(x)\}$ transforms of function $f(x)$ and $g(x)$. Then the HY transform of the convolution of $f(x)$ and $g(x)$, $(f * g)(t) = \int_0^\infty f(t)g(t-\tau)d\tau$ is given by*

$$HY\{(f * g)(t)\} = \frac{1}{\nu}P(\nu)Q(\nu). \tag{28}$$

Proof: The HY transform of $(f * g)(t)$ is defined by

$$HY\{(f * g)(t)\}$$

$$= \nu \int_0^\infty e^{-\nu^2 t} \int_0^\infty f(t).g(t-\tau)d\tau\, dt = \nu \int_0^\infty f(\tau)d\tau \int_0^\infty e^{-\nu^2 t}.g(t-\tau)dt.$$

Now setting $t - \tau = u \quad$ results in:
$$\nu 0\int\limits^\infty e^{-\nu^2 \tau} f(\tau)d\tau.\int\limits_0^\infty e^{-\nu^2 t}.g(t)\ dt = \nu[\frac{1}{\nu}\underbrace{\nu\int_0^\infty e^{-\nu^2\tau}f(\tau)d\tau}_{P(\nu)}\frac{1}{\nu}\underbrace{\nu\int_0^\infty e^{-\nu^2\tau}g(t)\ dt}_{Q(\nu)}].$$

then $HY\{(f * g)(t)\} = \frac{1}{\nu}P(\nu)Q(\nu).$ $\square$

Transform	Natural	Laplace	Sumudu	Elzaki	*HY*
Natural	$R(s,u)$	$R(1,u)$	$R(s,1)$	$vR(\frac{1}{v},1)$	$vR(v^2,1)$
Laplace	$\frac{1}{u}F(\frac{s}{u})$	$F(s)$	$\frac{1}{u}F(\frac{1}{u})$	$vF(\frac{1}{v})$	$vF(v^2)$
Sumudu	$\frac{1}{s}G(\frac{u}{s})$	$\frac{1}{s}G(\frac{1}{s})$	$G(u)$	$v^2G(v)$	$\frac{1}{v}G(\frac{1}{v^2})$
Elzaki	$\frac{s}{v^2}T(\frac{v}{s})$	$sT(\frac{1}{s})$	$\frac{1}{v}T(v)$	$T(v)$	$\frac{1}{\sqrt{V}}T(v)$
HY	$\frac{1}{\sqrt{sv}}P(\sqrt{\frac{s}{v}})$	$\frac{1}{\sqrt{s}}P(\sqrt{s})$	$\sqrt{\frac{1}{v}}P(\sqrt{\frac{1}{v}})$	$\frac{1}{v^3}P(\frac{v}{s})$	$P(v)$

Table 2: Relation between mentioned transforms.

Example 3.6 Solve the following Volterra integral equation:

$$u(x) = 1 - sinhx + \int_0^x (x - t + 2)u(t) \ dt. \tag{29}$$

Upon taking the *HY* transforms of (29) we get

$$HY\{u(x)\} = HY\{1\} - HY\{sinhx\} + HY\left\{\int_0^x (x - t + 2)u(t) \ dt\right\}.$$

Let $HY\{u(x)\} = P(u)$, $P(u) = \frac{1}{\nu} - \frac{\nu}{\nu^4 - 1} + \frac{1}{\nu}\left(\frac{1}{\nu^3} + \frac{2}{\nu}\right)P(u)$, $HY\{u(x)\} = P(u) = \frac{\nu^3}{\nu^4 - 1}$. Then $u(x) = cosh(x)$, which is an exact solution of (29).

In Table 2, we adjust the relationship between the mentioned transform with the Laplace, Elzaki, Sumudu and natural transforms.

4 Conclusion

In this paper, we have introduced a new integral transform. Namely, an *HY* transform for solving some of differential and integral equations with constant and non-constant coefficients which were not solved by other transforms like the Sumudu and Laplace once. Some of differential equations like the Euler-Cauchy equations that were solved by the power series only, are solved by this new transform. In a large domain we will discuss the *HY* transform for solving some of well known differential equations like the Legendre and Bessel equations.

References

[1] H.D. Alimorad, E. Hesameddini and A.J. FakharZadeh. Using Elzaki Transform Solving The Klein-Gordon Equation. *Twms Junal of Pure and Applied Mathematics* **7**(2) (2016) 177–184.

[2] F.B.M. Belgacem and R. Silambarasan. Theory of Natural transform. *Mathematics in Engineering, Science and Aerospace Mesa* **3**(1) (2012) 105–135.

[3] I. Cho and K. Hwajoon. The solution of Bessels equation by using Integral Transform. *Applied mathematical Sciense* **7** (122) (2014) 6069–6075.

[4] T.M. Elzaki. The new integral transform "Elzaki Transform". *Global Journal of Pure and Applied Mathematics* **7**(1) (2011) 57–64.

[5] T.M. Elzaki. On the Connections between Laplace and Elzaki transforms. *Advances in Theoretical and Applied Mathematics* **6**(1) (2011) 1–11.

[6] T.M. Elzaki and S.M. Elzaki. Solution of IntegroDifferential Equations by Using ELzaki Transform. *Global J. of Mat. and Sci.: Theory and Practical* **3**(1) (2011) 1–11.

[7] T.M. Elzaki and S.M. Elzaki. On the Elzaki transform and ordinary differential equation with variable coefficients. *Advances in Theoretical and Applied Mathematics* **6**(1) (2011) 13–18.

[8] T.M. Elzaki and S.M. Elzaki. New Integral Transform "Tarig Transform" ans system of Integro-Differential Equations. *Applied Mathematics, Elixir Appl. Math.* **57** (2013) 13982–13985.

[9] T.M. Elzaki and E.M. Hilal. Homotopy perturbation and Elzaki transform for solving nonlinear partial differential equations. *Mathematical Theory and Modeling* **2**(3) (2012) 33–42.

[10] K. Hwajoon. A Note on the shifting theorems for the Elzaki transform. *Int. Journal of Math. Analysis* **8** (10) (2012) 481–488.

[11] A.P. Hiwarekar. Application of LAPLACE Transform for Cryptography. *Internation Journal of engineering Science Research* **5**(4) (2015) 129–135.

[12] A. Kilicman and H. Eltayeb. A note on integral transforms and partial differential equations. *Applied Mathematical Sciences* **4**(3) 109–118. *Mathematics in Engineering Science and Aerospace* **3**(1) (2010) 99–124.

[13] A. Kilicman and H.E. Gadain. An application of double Laplace transform and double Sumudu transform. *Lobachevskii Journal of Mathematics* **30**(3) (2009) 214–223.

[14] K. Maleknejad and M. Hadizadeh. A new computational method for Volterra-Fredholm integral equations. *Computers & Mathematics with Applications* **37**(9) (1999) 1–8.

[15] P. D. Panasare, S.P. Chalke and A.G. Choure. Application of Laplace transformation in cryptography. *Internation Journal of Mathematical Archive* **3**(7) (2012) 2470–2473.

[16] K. Shah and M. Junaid and N. Ali. Extraction of Laplace, Sumudu, Fourier and Mellin transform from the Natural transform. *J. Appl. Envron. Biol. Sci.* **5**(9) (2015) 1–10.

[17] J.M. Yoon, S. Xie and V. Hrynkiv. Two numerical algorithms for solving a partial Integro-Differential equation with a weakly singular kernel. *Applications and Applied Mathematics* **7**(1) (2012).

[18] J. Zhang. A Sumudu based algorithm for solving differential equations. *Computer Science Journal of Moldova* **15**(3) (2007) 45.

[19] Asgari, R. Ezzati and H. Jafari. Solution of 2D Fractional Order Integral Equations by Bernstein Polynomials Operational Matrices. *Nonlinear Dynamics and Systems Theory* **19** (1) (2019) 10–20.

[20] B.S. Desale and K.D. Patil. Singular Analysis of Reduced ODEs of Rotating Stratied Boussinesq Equations Through the Mirror Transformations. *Nonlinear Dynamics and Systems Theory* **19** (1) (2019) 21–35.

Degenerate Bogdanov-Takens Bifurcations in the Gray-Scott Model

B. Al-Hdaibat [1*], M.F.M. Naser [2] and M.A. Safi [1]

[1] *Department of Mathematics, Hashemite University, P.O. Box 330127, Zarqa 13133, Jordan*

[2] *Faculty of Engineering Technology, Al-Balqa Applied University, Amman 11134, Jordan*

Abstract: In this paper, we show that for a wide range of parameter values, the Gray-Scott model of families of traveling wave solutions posses two degenerate Bogdanov-Takens points. Furthermore, we explicitly define a unique compact form for the critical normal form coefficients of order 3 and 4. This is guaranteed by applying suitable solvability conditions to singular linear systems coming from the center manifold reduction combined with a normalization technique.

Keywords: *Gray-Scott model; travelling waves; degenerate Bogdanov-Takens bifurcation.*

Mathematics Subject Classification (2010): 34C23, 37L10, 97N80.

1 Introduction

One of the most important contributions to the bifurcation theory has been developed independently and simultaneously by Bogdanov [3,4] and Takens [19], where the topological normal form of the so-called "Bogdanov-Takens (BT) bifurcation" is derived. This bifurcation plays an important role in the analysis of dynamical systems because it gives the appearance of local bifurcations (Saddle-node bifurcation and Hopf bifurcation) and global bifurcations (homoclinic orbits to saddle equilibria) near the critical parameter values [12].

The exact bifurcation scenario near a BT point is determined by an unfolding of the critical ODE on the 2D center manifold, with as many unfolding parameters as the codimension of the bifurcation. More precisely, the bifurcation diagram of the unfolding depends on the coefficients of the critical normal form on the center manifold. The

---

* Corresponding author: `mailto:b.alhdaibat@hu.edu.jo`

restriction of a system of ODEs to any center manifold at the critical parameter values can be transformed by formal smooth coordinate changes to the form [2, 13]

$$
\begin{cases}
\dot{w}_0 & = \ w_1, \\
\dot{w}_1 & = \ \displaystyle\sum_{k \geq 2} a_k w_0^k + b_k w_0^{k-1} w_1^k,
\end{cases}
\tag{1}
$$

where $w = (w_0, w_1) \in \mathbb{R}^2$ are the center manifold coordinates and a_k, b_k are the critical normal form coefficients.

The Gray-Scott model consists of the following coupled pair of reaction-diffusion equations:

$$
\begin{cases}
\dfrac{\partial U}{\partial t} & = \ D_u \nabla^2 U - UV^2 + \alpha_1(1 - U), \\[2mm]
\dfrac{\partial V}{\partial t} & = \ D_v \nabla^2 V + UV^2 - \alpha_2 V,
\end{cases}
\tag{2}
$$

where α_1 and α_2 are the rate constants, D_u and D_v are the diffusivities, $U = U(x, t)$ and $V = V(x, t)$ are the concentration of the chemical species U (the inhibitor of the reaction) and V (the catalyst or the activator). A standard notation, ∇^2 is the Laplacian operator. Equation (1) was proposed by P. Gray and S. K. Scott in 1983 [8]; that's why it's called the Gray-Scott model. We refer the interested reader to [9, 10] more physical and chemical backgrounds of the model. Motivated by the experiments and simulations of Pearson [17] (see also [16, 21]), attention is primarily focused on the case in which the diffusivity of the inhibitor U is greater than that of the activator V. In this case, U is able to rapidly reach the localized regions of high V concentration and hence sustain the reaction, while the relatively slow diffusion of V makes it possible for these localized regions to persist. We thus set $D_u = 1$ and introduce the small parameter ε by setting $D_v = \varepsilon$, with $0 < \varepsilon << 1$. This choice of the diffusion coefficient D_v will enable us to explore a wide region of the parameter space. The existence of the saddle-node, Hopf, and nondegenrate BT bifurcations in (1) was studied by many authors, see [6, 14–16, 18, 20]. They pointed out that the homoclinic bifurcation occurs.

The purpose of this study is to derive conditions for the appearance of degenerate BT bifurcation (where the nondegeneracy condition $a_2 b_2 \neq 0$ is no longer satisfied). For a range of parameter values, we show that the Gray-Scott model of families of traveling wave solutions posses two degenerate BT points. Under certain conditions, we explicitly define a unique formula from the critical normal form coefficients, namely $\{a_k, b_k\}$ for $k = 3, 4$. This is guaranteed by defining a unique compact form explicitly for the Taylor expansion of the center manifold near the critical parameter values under reasonable conditions. To this end, we apply suitable solvability conditions to singular linear systems coming from the center manifold reduction combined with the normalization technique.

The paper is organized as follows. In Section 2, we describe the model to be studied in the paper and its equilibria. A traveling wave ansatz will be introduced, such that one variable will describe both the spatial and the temporal behavior. This reduces the system of PDEs to a system of ODEs. Also, we provide explicit formulas for the equilibrium points. In Section 3, a unique explicit formula for the Taylor expansion of the 2D center manifold up to order 4 and the critical normal form coefficients of order 3 and 4 will then be derived for not only the Gray-Scott model, but also for any n-dimensional ODEs using the combined reduction-normalization technique. Numerical

examples and discussions are given in Section 4. All the computations shown in this paper have been performed using the symbolic algebra system MAPLE.

2 The Model under Study

Consider the traveling wave ansatz $U = u(x - ct)$, $V = v(x - ct)$ [6],

$$\frac{\partial U}{\partial t} = -cu', \quad \nabla^2 U = \frac{\partial^2}{\partial x^2}(u(x - ct)) = u'',$$

$$\frac{\partial V}{\partial t} = -cv', \quad \nabla^2 V = \frac{\partial^2}{\partial x^2}(v(x - ct)) = v'',$$

where $c \in \mathbb{R}$ is the wave speed and $c = 0$ corresponds to stationary states, $'$ is the derivative with respect to the independent variable $x - ct$. Substituting this traveling wave ansatz in (2) and by assuming that $u' = p$ and $\varepsilon v' = q$, we obtain the following wave system:

$$\begin{cases} u' &= p, \\ p' &= -cp + uv^2 - \alpha_1(1 - u), \\ \varepsilon v' &= q, \\ \varepsilon q' &= \frac{-c}{\varepsilon}p - uv^2 + \alpha_2 v. \end{cases} \tag{3}$$

This system possesses fast-slow time scales. As $\varepsilon \to 0$, the system (3) reduces into a fast subsystem

$$\begin{cases} u' &= p, \\ p' &= -cp + uv^2 - \alpha_1(1 - u). \end{cases}$$

On the other hand, introducing γ by $\gamma = \frac{c}{\varepsilon}$ and rescaling the independent variable $x - ct = \varepsilon\eta$ yield

$$\begin{cases} \dot{u} &= \varepsilon p, \\ \dot{p} &= \varepsilon\left(-\varepsilon\gamma p + uv^2 - \alpha_1(1 - u)\right), \\ \dot{v} &= q, \\ \dot{q} &= -\gamma q - uv^2 + \alpha_2 v, \end{cases} \tag{4}$$

where $\dot{}$ denotes the derivative with respect to the new independent variable η. Hence, as $\varepsilon \to 0$, the systems (4) reduces into a slow subsystem

$$\begin{cases} \dot{v} &= q, \\ \dot{q} &= -\gamma q - uv^2 + \alpha_2 v. \end{cases}$$

Any bounded orbit of (3) corresponds to a traveling wave solution of the model (2) at the parameter value $(\alpha_1, \alpha_2, \varepsilon)$ propagating with wave velocity c. For $c \geq 0$, the system (3) has equilibrium points $(u_e, 0, v_e, 0)$ with the solution sets of

$$u_e v_e^2 - \alpha_1(1 - u_e) = 0, \quad -u_e v_e^2 + \alpha_2 v_e = 0.$$

Therefore, the system (3) has the following equilibria $E_1 = (1, 0, 0, 0)$ for all $(\alpha_1, \alpha_2, \varepsilon, c)$, and

$$E_2 = \left(\frac{\alpha_1 \pm \tau}{2\alpha_1}, 0, \frac{\alpha_1}{\alpha_2}\left(1 - \frac{\alpha_1 \pm \tau}{2\alpha_1}\right), 0\right), \quad \tau = \sqrt{\alpha_1^2 - 4\alpha_1\alpha_2^2},$$

for all $\alpha_1 \geq 4\alpha_2^2$. The Jacobian matrix of the system (3) is given by

$$
A = \begin{pmatrix}
0 & 1 & 0 & 0 \\
v_e^2 + \alpha_1 & -c & 2u_e v_e & 0 \\
0 & 0 & 0 & \frac{1}{\varepsilon} \\
\frac{1}{\varepsilon}(-v_e^2) & \frac{-c}{\varepsilon^2} & \frac{1}{\varepsilon}(-2u_e v_e + \alpha_2) & 0
\end{pmatrix}. \tag{5}
$$

The eigenvalues of the Jacobian matrix corresponding to the equilibrium E_1 are given by $\lambda = \left\{ \pm \frac{\sqrt{\alpha_2}}{\varepsilon}, \ \frac{1}{2}\left(-1 \pm \sqrt{c^2 + 4\alpha_1}\right) \right\}$. It is clear that for the case $\alpha_2 = 0$, the Jacobian matrix (5) has a double zero eigenvalue. On the other hand, at the equilibrium point E_2, the characteristic polynomial is

$$
P(\lambda) \quad := \lambda^4 + c\lambda^3 - \left(\frac{\alpha_1(\alpha_1 \mp k)}{2\alpha_2^2} - \frac{\alpha_2}{\varepsilon^2} \right) \lambda^2 + \frac{c\alpha_2(\varepsilon + 2)}{\varepsilon^3}\lambda - \frac{(\alpha_1 \mp k)k}{2\varepsilon^2 \alpha_2},
$$

where $k = \sqrt{\alpha_1^2 - 4\alpha_1 \alpha_2^2}$. If we consider the case when $\alpha_1 = 4\alpha_2^2$ and $c = 0$, then

$$
P(\lambda) = \lambda^4 - \frac{\alpha_2 \left(8\alpha_2 \varepsilon^2 - 1\right)}{\varepsilon^2}\lambda^2,
$$

which has a double-zero root given by $\lambda = 0, \ 0, \ \frac{\sqrt{8\alpha_2^2 \varepsilon^2 - \alpha_2}}{\varepsilon}, \ -\frac{\sqrt{8\alpha_2^2 \varepsilon^2 - \alpha_2}}{\varepsilon}$.

3   Center Manifold Reduction Combined with Normalization

In this section, we discuss the computation of normal form coefficients a_k and b_k of the critical normal form (1). First, suppose that at $x_0 = 0$, the Jacobian matrix $A = f_x(x_0)$ of a generic smooth family of autonomous ODEs

$$
\dot{x} = f(x), \quad f : \mathbb{R}^n \to \mathbb{R}^n, \tag{6}
$$

has a double (and not semi-simple) zero eigenvalue, i.e. x_0 is a BT point. Then, there exist two real linearly independent (generalized) eigenvectors $q_{0,1} \in \mathbb{R}^n$, of A, and two adjoint eigenvectors $p_{0,1} \in \mathbb{R}^n$, of A^T, such that

$$
\begin{pmatrix} A & 0 \\ -I_n & A \end{pmatrix} \begin{pmatrix} q_0 \\ q_1 \end{pmatrix} = 0, \quad \begin{pmatrix} A^\mathrm{T} & 0 \\ -I_n & A^\mathrm{T} \end{pmatrix} \begin{pmatrix} p_1 \\ p_0 \end{pmatrix} = 0. \tag{7}
$$

Assume that the vectors $\{q_0, q_1, p_0, p_1\}$ satisfy

$$
p_0^\mathrm{T} q_0 = p_1^\mathrm{T} q_1 = 1, \quad p_0^\mathrm{T} q_1 = p_1^\mathrm{T} q_0 = 0. \tag{8}
$$

If we impose the conditions (see [13])

$$
q_0^\mathrm{T} q_0 = 1, \quad q_1^\mathrm{T} q_0 = 0, \tag{9}
$$

then the vectors $\{q_0, q_1, p_0, p_1\}$ are uniquely defined up to a $\pm$ sign. We can parametrize the critical center manifold for (6) with respect to $w = (w_0, w_1) \in \mathbb{R}^2$ as

$$
x = H(w), \quad H : \mathbb{R}^2 \to \mathbb{R}^n. \tag{10}
$$

The invariance of the center manifold implies the *homological equation* [5, 7, 11]

$$\frac{\partial H}{\partial w_0}\dot{w}_0 + \frac{\partial H}{\partial w_1}\dot{w}_1 = f(H(w)). \tag{11}$$

We write the Taylor expansions of H and f as

$$f(x) = Ax + \frac{1}{2}B(x,x) + \frac{1}{6}C(x,x,x) + \frac{1}{24}D(x,x,x,x) + \mathcal{O}\left(||x||^5\right), \tag{12a}$$

$$H(w) = q_0 w_0 + q_1 w_1 + \sum_{2 \le j+k \le 4} \frac{1}{j!k!}H_{jk}w_0^j w_1^k + \mathcal{O}(||w||^5), \tag{12b}$$

where B, C, D, and E are vector-valued functions with n-components. The ith component of these functions are defined by

$$B_i(x,y) = \sum_{j,k=1}^{n} \frac{\partial^2 f_i(\xi)}{\partial \xi_j \partial \xi_k}\Big|_{\xi=0}x_j y_k, \quad C_i(x,y,z) = \sum_{j,k,l=1}^{n} \frac{\partial^3 f_i(\xi)}{\partial \xi_j \partial \xi_k \partial \xi_l}\Big|_{\xi=0}x_j y_k z_l,$$

$$D_i(x,y,z,w) = \sum_{j,k,l,m=1}^{n} \frac{\partial^4 f_i(\xi)}{\partial \xi_j \partial \xi_k \partial \xi_l \partial \xi_m}\Big|_{\xi=0}x_j y_k z_l w_m.$$

We insert the expansions (12a) and (12a) into (11) together with $(\dot{w}_0, \dot{w}_1)$ as we defined in (1). Then, collecting the terms with equal components in w^{j+k} at the homological equation gives a linear systems that can be solved for the coefficients $H_{jk} \in \mathbb{R}^n$ by a recursive procedure based on Fredholm's solvability condition.

The quadratic w-terms in the homological equation (11) lead to (see [1, 11, 13]):

$$a_2 = \frac{1}{2}p_1^{\text{T}}B(q_0,q_0), \tag{13}$$

$$b_2 = p_0^{\text{T}}B(q_0,q_0) + p_1^{\text{T}}B(q_0,q_1), \tag{14}$$

$$H_{20} = -A^{\text{INV}}\left(B(q_0,q_0) - 2a_2q_1\right) + \gamma_0 q_0, \tag{15}$$

$$H_{11} = -A^{\text{INV}}\left(B(q_0,q_1) - H_{20} - b_2q_1\right), \tag{16}$$

$$H_{02} = -A^{\text{INV}}\left(B(q_1,q_1) - 2H_{11}\right), \tag{17}$$

where $\gamma_0 := \frac{1}{2}p_1^{\text{T}}B(q_1,q_1) + p_0^{\text{T}}\left(B(q_0,q_1) - H_{20}\right)$. Note that $\gamma_0 q_0$ is added to H_{20} to ensure that the right-hand side of the system for H_{02} is in the range of A (see Section 8.7 in [12] for more details).

Collecting the terms with equal components in w of order three at the homological equation gives the following equations.

$$w_0^3: AH_{30} + C(q_0,q_0,q_0) + 3B(q_0,H_{20}) - 6a_2H_{11} - 6a_3q_1 = 0, \tag{18}$$

$$w_0^2 w_1: AH_{21} + C(q_0,q_0,q_1) + 2B(q_0,H_{11}) + B(q_1,H_{20}) - 2a_2H_{02}$$
$$- 2b_2H_{11} - H_{30} - 2b_3q_1 = 0, \tag{19}$$

$$w_0 w_1^2: AH_{12} + C(q_0,q_1,q_1) + 2B(q_1,H_{11}) + B(q_0,H_{02}) - 2b_2H_{02} - 2H_{21} = 0, \tag{20}$$

$$w_1^1: AH_{03} + C(q_1,q_1,q_1) + 3B(q_1,H_{02}) - 3H_{12} = 0. \tag{21}$$

The solvability condition implies the following expressions for the cubic coefficients (see [13]):

$$a_3 = \frac{1}{6} p_1^{\mathrm{T}} \left(C(q_0, q_0, q_0) + 3B(q_0, H_{20}) - 6a_2 H_{11} \right), \tag{22}$$

$$H_{30} = -A^{\mathrm{INV}} \left(C(q_0, q_0, q_0) + 3B(q_0, H_{20}) - 6a_2 H_{11} - 6a_3 q_1 \right), \tag{23}$$

$$b_3 = \frac{1}{2} p_1^{\mathrm{T}} \left(C(q_0, q_0, q_1) + 2B(q_0, H_{11}) + B(q_1, H_{20}) - 2a_2 H_{02} - 2b_2 H_{11} - H_{30} \right), \tag{24}$$

$$H_{21} = -A^{\mathrm{INV}}(C(q_0, q_0, q_1) + 2B(q_0, H_{11}) + B(q_1, H_{20}) - 2a_2 H_{02}$$
$$- 2b_2 H_{11} - H_{30} - 2b_3 q_1), \tag{25}$$

$$H_{12} = -A^{\mathrm{INV}} \left(C(q_0, q_1, q_1) + 2B(q_1, H_{11}) + B(q_0, H_{02}) - 2b_2 H_{02} - 2H_{21} \right), \tag{26}$$

$$H_{03} = -A^{\mathrm{INV}} \left(C(q_1, q_1, q_1) + 3B(q_1, H_{02}) - 3H_{12} \right). \tag{27}$$

However, given a_3 and b_3, the solutions to the singular linear system (23), (25)-(27) are not unique. The uniqueness of the solutions can be guaranteed by requiring that (20) and (21) are solvable for H_{12} and H_{03}, respectively, *i.e.* H_{12} and H_{03} are in the range of A. Multiply the equations (20) and (21) by p_1^{T}, then the solvability condition requires that

$$p_1^{\mathrm{T}} H_{21} - \frac{1}{2} p_1^{\mathrm{T}} \left(C(q_0, q_1, q_1) + 2B(q_1, H_{11}) + B(q_0, H_{02}) - 2b_2 H_{02} \right) = 0, \tag{28}$$

$$p_1^{\mathrm{T}} H_{12} - \frac{1}{3} p_1^{\mathrm{T}} \left(C(q_1, q_1, q_1) + 3B(q_1, H_{02}) \right) = 0. \tag{29}$$

Multiply the equation (19) by p_0^{T}, Then using the substitution

$$H_{30} \mapsto H_{30} + \gamma_1 q_0 \tag{30}$$

gives

$$p_1^{\mathrm{T}} H_{21} = -p_0^{\mathrm{T}} \left(C(q_0, q_0, q_1) + 2B(q_0, H_{11}) + B(q_1, H_{20}) - 2a_2 H_{02} - 2b_2 H_{11} - H_{30} \right) + \gamma_1.$$

Substituting this into (28) with

$$\gamma_1 := p_0^{\mathrm{T}} \left(C(q_0, q_0, q_1) + 2B(q_0, H_{11}) + B(q_1, H_{20}) - 2a_2 H_{02} - 2b_2 H_{11} - H_{30} \right)$$
$$+ \frac{1}{2} p_1^{\mathrm{T}} \left(C(q_0, q_1, q_1) + 2B(q_1, H_{11}) + B(q_0, H_{02}) - 2b_2 H_{02} \right) \tag{31}$$

makes the left-hand side of (28) equal to zero. So, the substitution for H_{30} implies that (20) is solvable for H_{12}. Note that adding a scalar multiple of q_0 to H_{30} does not affect the coefficient b_3 given by (24), since $\langle p_1, q_0 \rangle = 0$. On the other hand, to ensure that (21) is solvable for H_{03}, one can use the substitution

$$H_{21} \mapsto H_{21} + \gamma_2 q_0, \tag{32}$$

then multiplying the equation (20) by p_0^{T} gives

$$p_1^{\mathrm{T}} H_{12} = -p_0^{\mathrm{T}} \left(C(q_0, q_1, q_1) + 2B(q_1, H_{11}) + B(q_0, H_{02}) - 2b_2 H_{02} - 2H_{21} \right) + 2\gamma_2. \tag{33}$$

Substitute this into (29) with

$$
\gamma_2 := \frac{1}{6}p_1^{\mathrm{T}}\left(C(q_1, q_1, q_1) + 3B(q_1, H_{02})\right) + \frac{1}{2}p_0^{\mathrm{T}}(C(q_0, q_1, q_1)
$$
$$
+ 2B(q_1, H_{11}) + B(q_0, H_{02}) - 2b_2 H_{02} - 2H_{21});
\tag{34}
$$

makes the left-hand side of (29) is equal to zero. So, this substitution implies that (21) is solvable for H_{03}. Note that the substitution for H_{21} does not affect the coefficients a_4 and b_4, as we will see in equations (35) and (37).

Finally, the homological equation implies the following expressions for the coefficients of the w^4-terms [13]:

$$
a_4 = \frac{1}{24}p_1^{\mathrm{T}}\left(D(q_0, q_0, q_0, q_0) + 6C(q_0, q_0, H_{20}) + 4B(q_0, H_{30}) + 3B(H_{20}, H_{20})\right.
$$
$$
\left. - 12a_2 H_{21} - 24a_3 H_{11}\right),
\tag{35}
$$

$$
H_{40} = -A^{\mathrm{INV}}\left(D(q_0, q_0, q_0, q_0) + 6C(q_0, q_0, H_{20}) + 4B(q_0, H_{30})\right.
$$
$$
\left. + 3B(H_{20}, H_{20}) - 12a_2 H_{21} - 24a_3 H_{11} - 24a_4 q_1\right),
\tag{36}
$$

$$
b_4 = \frac{1}{6}p_1^{\mathrm{T}}\left(D(q_0, q_0, q_0, q_1) + 3C(q_0, q_1, H_{20}) + 3C(q_0, q_0, H_{11})\right.
$$
$$
+ 3B(q_0, H_{21}) + 3B(H_{20}, H_{11}) + B(q_1, H_{30}) - H_{40} - 3b_2 H_{21}
$$
$$
\left. - 6a_2 H_{12} - 6a_3 H_{02} - 6b_3 H_{11}\right).
\tag{37}
$$

In systems (15)-(17), (23), (25), (26), (27) and (36), the expression $x = A^{\mathrm{INV}}y$ is defined by using the non-singular bordered system

$$
\begin{pmatrix} A & p_1 \\ q_0^{\mathrm{T}} & 0 \end{pmatrix} \begin{pmatrix} x \\ s \end{pmatrix} = \begin{pmatrix} y \\ 0 \end{pmatrix},
$$

where y is in the range of A.

4 Degenerate Bogdanov-Takens Bifurcation in the Gray-Scott Model

In this section, we will use the analytical results obtained in Section 3 to prove that the Gray-Scott model has two degenerate BT points at its equilibria E_1 and E_2. Recall that the Gray-Scott model (3) exhibits a BT bifurcation of the equilibrium E_2 occurring at the parameter values $(\alpha_1, \alpha_2, \varepsilon, c) = (4\alpha_2^2, \alpha_2, \varepsilon, 0)$. First, we apply the change of variables $(u, p, v, q) = E_2 + (x_1, x_2, x_3, x_4)$, which brings the equilibrium point E_2 to the origin $(0, 0, 0, 0)$. Then the Jacobian matrix evaluated at $(0, 0, 0, 0)$ is

$$
A = \begin{pmatrix}
0 & 1 & 0 & 0 \\
8\alpha_2^2 & 0 & 2\alpha_2 & 0 \\
0 & 0 & 0 & \dfrac{1}{\delta} \\
-\dfrac{4\alpha_2^2}{\delta} & 0 & -\dfrac{\alpha_2}{\delta} & 0
\end{pmatrix}.
$$

The following vectors

$$q_0 = m_1 \left(-1, \ 0, \ 4|\alpha_2|, \ 0\right)^{\mathrm{T}}, \quad q_1 = m_1 \left(0, \ -1, \ 0, \ 4|\alpha_2|\varepsilon\right)^{\mathrm{T}},$$

$$p_1 = n_1 \left(1, \ 0, \ 2\varepsilon^2, \ 0\right)^{\mathrm{T}}, \quad p_0 = n_1 \left(0, \ 1, \ 0, \ 2\varepsilon\right)^{\mathrm{T}},$$

with $m_1 = \dfrac{\frac{\alpha_2}{|\alpha_2|}}{\sqrt{16\alpha_2^2 + 1}}, \quad n_1 = \dfrac{1}{m_1}\left(\dfrac{1}{8\varepsilon^2\alpha_2 - 1}\right)$, satisfy (7)-(9). The vector-valued function $B : \mathbb{R}^4 \times \mathbb{R}^4 \to \mathbb{R}^4$ can be defined for arbitrary vectors $z, \ r \in \mathbb{R}^4$ as follows:

$$B(z, r) = \frac{4\alpha_2}{\varepsilon} \left(0, \ -z_1 r_3 - z_1 r_3 - z_3 r_3, \ 0, \ z_1 r_3 + z_1 r_3 + z_3 r_3\right)^{\mathrm{T}}.$$

Therefore, the vectors $B(q_0, q_0)$ and $B(q_0, q_1)$ can be expressed as

$$B(q_0, q_0) = \frac{16\alpha_2^2 m_1^2}{\varepsilon} \left(0, \ -\varepsilon, \ 0, \ 1\right)^{\mathrm{T}}, \quad B(q_0, q_1) = (0, \ 0, \ , \ 0, \ 0)^{\mathrm{T}}.$$

Thus, the formulas (13) and (14) give the values of the critical normal form coefficients

$$a_2 = \frac{8\alpha_2^2}{8\delta^2\alpha_2 - 1} \quad \text{and} \quad b_2 = 0.$$

These values confirm that the Gray-Scott model has a degenerate BT point of codimension ≥ 3. Similarly, one can compute the normal form coefficients at the BT of the equilibrium E_1 occurring at the parameter values $\alpha_2 = 0$, and satisfy $a_2 = -\dfrac{1}{\varepsilon^2}$ and $b_2 = \dfrac{2c\left(\varepsilon^4 + c^2\varepsilon + c^2\right)}{\varepsilon^3\left(\varepsilon^4 + c^2\right)\alpha_1}$. Therefore, the case $c = 0$ indicates a degenerate BT point for the parameter values $(\alpha_1, \alpha_2, \varepsilon, c) = (\alpha_1, 0, \varepsilon, 0)$.

5   Example

Based on the analysis carried out in Section 2, we are going to perform numerical studies of the degenerate BT bifurcation of the equilibrium E_2 [1] which occurs at $(\alpha_1, \alpha_2, \varepsilon, c) = (4\alpha_2^2, \alpha_2, \varepsilon, 0)$. To simplify, we fix the variables $\alpha_2 = 1$ and $\varepsilon = 0.1$. At the bifurcation parameter, we compute the following expressions for (13)-(17): $a_2 = \dfrac{14356}{6807}$, $b_2 = 0$ and

$$H_{20} = \left(\frac{21151}{990682}, \ 0, \ \frac{-9600}{8993}, \ 0\right)^{\mathrm{T}}, \quad H_{11} = \left(0, \ \frac{21151}{990682}, \ 0, \ \frac{-960}{8993}\right)^{\mathrm{T}},$$

$$H_{02} = \left(\frac{5423}{1079523}, \ 0, \ \frac{5807}{4623854}, \ 0\right)^{\mathrm{T}}$$

It is clear that the system (17) is solvable for H_{02}; this can be easily shown by multiplying both sides of (17) by p_1^{T} which is indeed

$$p_1^{\mathrm{T}}\left(2H_{11} - B(q_1, q_1)\right) = 0.$$

---

[1] Similar results can be derived for the BT point of the equilibrium point E_1.

Later, we compute the value of the system (22)-(27): $a_3 = \dfrac{-6441}{5329}, \quad b_3 = 0$ and

$$H_{30} = \left(\frac{-4608}{88283}, \ 0, \ \frac{73432}{36131}, \ 0 \right)^{\mathrm{T}}, \quad H_{21} = \left(0, \ \frac{-4358}{140551}, \ 0, \ \frac{12276}{60245} \right)^{\mathrm{T}},$$

$$H_{12} = \left(\frac{-1266}{253087}, \ 0, \ \frac{-633}{506174}, \ 0 \right)^{\mathrm{T}}, \quad H_{03} = \left(0, \ \frac{-3798}{253087}, \ 0, \ \frac{-2539}{6767645} \right)^{\mathrm{T}}.$$

The systems H_{21}, H_{12} and H_{03} are uniquely defined such that the solvability conditions (28) and (28) are satisfied. Finally, (35)-(37) is given by

$$a_4 = \frac{100212}{120473}, \quad H_{40} = \left(\frac{-31070}{25263}, \ 0, \ \frac{-15535}{50526}, \ 0 \right)^{\mathrm{T}}, \quad b_4 = 0.$$

Thus, our unique normal form for the Gray-Scott model is

$$\begin{cases} \dot{w}_0 &= \ w_1, \\ \dot{w}_1 &= \ \dfrac{14356}{6807} w_0^2 - \dfrac{6441}{5329} w_0^3 + \dfrac{100212}{120473} w_0^4. \end{cases}$$

6 Conclusion

In the present paper, we consider the Gray-Scott model (2), where a travel wave ansatz is introduced for which one variable describes both the spatial and the temporal behavior. This reduces the system of PDEs (2) into a system of ODEs (3). For a wide range of parameter values, the Gray-Scott model (3) possesses two degenerate BT points. The main aim of this paper is to define a unique explicit formula for the Taylor expansion of the 2D center manifold up to a term of order 4. The uniqueness of the Taylor expansion is guaranteed by applying the variables transformations (30) and (32) with the suitable choice for γ_1 and γ_2 as shown in (31) and (34), respectively. The results of this paper can be applied also for any n-dimensional system of ODEs. The theoretical results of the paper are illustrated by an example in Section 5. Natural directions for future research include developing a robust predictor for the homoclinic orbits bifurcating from a BT point in generic n-dimensional ODEs. Such a predictor needs a unique expression for the vectors H_{jk} in the Taylor expansion (12b).

References

[1] B. Al-Hdaibat, W. Govaerts, Yu. A Kuznetsov, and H. G. E. Meijer. Initialization of homoclinic solutions near Bogdanov-Takens points: Lindstedt-Poincaré compared with regular perturbation method. *SIAM J. Applied Dynamical Systems* **15** (2) (2016) 952–980.

[2] V. I. Arnold. *Geometrical Methods in the Theory of Ordinary Differential Equations.* Springer-Verlag, New York, Heidelberg, Berlin, 1983.

[3] R. I. Bogdanov. Versal deformations of a singular point on the plane in the case of zero eigenvalues. *Functional Anal. Appl.* **9** (1975) 144–145.

[4] R. I. Bogdanov. The versal deformation of a singular point of a vector field on the plane in the case of zero eigenvalues. In: *Proceedings of Petrovskii Seminar.* Moscow, Moscow State University, **2** (1976) 37–65. [Russian] (English translation: *Selecta Math. Soviet.* **1** (1981) 389–421).

[5] P. H. Coullet and E. A. Spiegel. Amplitude equations for systems with competing instabilities. *SIAM J. Appl. Math.* **43** (1983) 776–821.

[6] A. Doelman, T. J. Kaper, and P. A. Zegeling. Pattern formation in the one-dimensional Gray-Scott model. *Nonlinearity* **10** (2) (1997) 523–563.

[7] C. Elphick, E. Tirapegui, M. E. Brachet, P. H. Coullet, and G. Iooss. A simple global characterization for normal forms of singular vector fields. *Physica D* **32** (1987) 95–127.

[8] P. Gray and S. K. Scott. Autocatalytic reactions in the isothermal, continuous stirred tank reactor: Isolas and other forms of multistability. *Chemical Engineering Science* **38** (1) (1983) 29–43.

[9] P. Gray and S. K. Scott. Autocatalytic reactions in the isothermal, continuous stirred tank reactor: Oscillations and instabilities in the system A + 2B→3B; B→C. *Chemical Engineering Science* **39** (6) (1984) 1087–1097.

[10] P. Gray and S. K. Scott. Sustained oscillations and other exotic patterns of behavior in isothermal reactions. *The Journal of Physical Chemistry* **89** (1) (1985) 22–32.

[11] Yu.A. Kuznetsov. Numerical normalization techniques for all codim 2 bifurcations of equilibria in ODEs. *SIAM J. Numer. Anal.* **36** (1999) 1104–1124.

[12] Yu. A. Kuznetsov. *Elements of Applied Bifurcation Theory.* Springer-Verlag, New York, 3rd edition, 2004.

[13] Yu. A. Kuznetsov. Practical computation of normal forms on center manifolds at degenerate Bogdanov-Takens bifurcations. *International Journal of Bifurcation and Chaos* **15** (11) (2005) 3535–3546.

[14] Yu. A. Kuznetsov, H. G. E. Meijer, B. Al-Hdaibat, and W. Govaerts. Accurate approximation of homoclinic solutions in Gray-Scott kinetic model. *International Journal of Bifurcation and Chaos* **25** (09) (2015) 1550125.

[15] Y. N. Kyrychko, K. B. Blyuss, S. J. Hogan, and E. Schöl. Control of spatiotemporal patterns in the Gray-Scott model. *Chaos* **19** (4) (2009) 043126.

[16] W. Mazin, K.E. Rasmussen, E. Mosekilde, P. Borckmans, and G. Dewel. Pattern formation in the bistable Gray-Scott model. *Mathematics and Computers in Simulation* **40** (3) (1996) 371–396.

[17] J. E. Pearson. Complex patterns in a simple system. *Science*, **261** (5118) (1993) 189-192.

[18] Ai Shangbing. Homoclinic solutions to the Gray-Scott model. *Applied Mathematics Letters* **17** (12) (2004) 1357–1361.

[19] F. Takens. Forced oscillations and bifurcations. *Comm. Math. Inst., Rijksuniversiteit Utrecht* **2** (1974) 1–111. Reprinted in *Global Analysis of Dynamical Systems*, Instute of Physics, Bristol, (2001) 1–61.

[20] Daishin Ueyama. Dynamics of self-replicating patterns in the one-dimensional Gray-Scott model. *Hokkaido Mathematical Journal* **28** (1) (1999) 175–210.

[21] W. Wang, Y. Lin, F. Yang, L. Zhang, and Y. Tan. Numerical study of pattern formation in an extended Gray-Scott model. *Communications in Nonlinear Science and Numerical Simulations* **16** (2011) 2016–2026.

Dynamic Modelling of Boosting the Immune System and Its Functions by Vitamins Intervention

S. A. Alharbi [1], A. S. Rambely [2*] and A. Othman Almatroud [3]

[1] *Department of Mathematics & Statistics, College of Science, Taibah University,*
41911 Yanbu, Almadinah Almunawarah, Kingdom of Saudi Arabia
[1,2] *Mathematics Program, Faculty of Science & Technology, Universiti Kebangsaan Malaysia,*
43600 UKM Bangi, Selangor, Malaysia
[3] *Mathematics Department, Faculty of Science, University of Hail, Kingdom of Saudi Arabia*

Abstract: The purpose of this paper is to demonstrate numerically the effect of modern diet on the functions of the immune system such as modifying, identifying and inhibiting the pathogens in an unhealthy model by the intervention of vitamins within thirty days. This paper used ordinary differential equations to formulate the model which contains two populations: one of normal cells in the presence of immune cells and the other with variables of vitamins as external factors. The paper proved that switching back to a healthy diet from a modern pattern diet resulted in a decrease in the percentage of deadly diseases as well as prevention from rapid growth of pathogens. In conclusion, the immune system functionality is directly proportional to the type of diet consumed. In the case of the Western-style diet, it has a detrimental effect on the immune system.

Keywords: *dietary; weakened immune system; boost immune system; vitamins consumption; nonlinear dynamic system.*

Mathematics Subject Classification (2010): 97M60, 92B99.

---

* Corresponding author: mailto:asr@ukm.edu.my.

1   Introduction

Processed food diet is characterized by a high consumption of proteins (especially meats), sugar, salt and fat comparatively to a healthy diet comprising of an intake of fruit and vegetables [1–3]. This diet is quite common around the world and contributes heavily in the development of fatal diseases. Pre-clinical experiments indicate that a high fructose and protein diet causes cancer, insulin resistance, impaired control and damages the immune system [4–6].

A protein is one of the main macronutrients essential for immunity and general health if taken in proper quantities. The studies found mortality rate in younger people who consume more than 20% calories from protein increased to 75% whereas the percentage of people dying by cancer had increased fourfold as compared to people who imbibe less than 10% calories from proteins [7]. Other studies observed the increase in death rate associated with a diet based on animal products and a high intake of carbohydrates; contrarily, a vegetable-based diet and a low carbohydrate intake reduced the mortality rate. Furthermore, malnutrition debilitates the immune system and increases mortality rate as well as elevates the risk of contacting lethal diseases [8].

Vitro studies have revealed that simple sugars reduce the white blood cells (phagocytes) and may elevate the inflammatory cytokines in the blood [9,10]. Whereas a salty diet is associated with a risk of gastric cancer [11]. The salt in the diet causes a sodium and potassium imbalance, which can further cause a detrimental effect on the kidneys [12]. Retaining salt in the body also predominates risks of weight gain [13]. A fatty diet alters the lipids of the immune cells membranes and disrupts their function [14,15].

In addition, the intake of a high fiber diet is associated with a lower risk of not only cardiovascular diseases but also cancer and respiratory diseases as well as infectious diseases. Nutritionists recommend an intake of 25-38g of fiber per day. This average is reduced further along the societal chair [16]. It is also noted that the Africans in rural areas consume more fiber than Western people [1]. Notably, Western people have a higher chance of obesity which is directly proportional to their diet which is mainly characterized by a heavy intake of processed foods, fatty foods and a reduced intake of nutrient rich foods as fruit and vegetables [17].

The immune system plays a huge role in the defence against carcinomas. Mathematical models are used to describe how the immune system defends by inhibiting cancer cells. Researchers propose that the interaction between immune cells and the target population such as viruses, bacteria, antigens and malignant cells is a dynamic process. Marey and others succeeded to formulate a model by using ordinary differential equations to portray this process [18]. Other researchers showed that the chance of developing fatal diseases is reduced for a person who follows a healthy diet which is related to food pyramid and vice versa [19].

Mathematical models are also used for prognosis and treatment plans for cancer [20,21]. Tumor growth is a constant population in any mathematical model where cancer is studied. Several mathematical models use differential equations to prepare tumor-immune model interaction with radiation and chemotherapy [22–25]. Others focus on lifestyle and estrogen as culprit for developing cancer, especially malignant cancer in women [26–28]. Since normal cells can divide 50-60 times before dying ones, it can sometimes lead to the development of abnormal cells and cancer can occur in such a case. Thus, the mathematical model in this paper is formulated to understand the response of the immune system to prevent the growth of abnormal cells.

In this busy modern era, people are highly dependent on the Western-style diet consisting of fast food, cans and even frozen products which are readily available anytime and everywhere. One of the transparent reasons for this paper is to highlight the disadvantages of the Western-style diet to the function of the immune system. It also discusses one of the possibilities to increase the response of the immune system by modifying the diet pattern along with the intervention of vitamins within the first thirty days.

2   Materials and Methodology

Ordinary differential equations are used to describe the interaction between two populations: normal cells which begin to divide as abnormal cells and immune cells which respond to this action. The first model is formulated as

$$\begin{aligned}
\frac{dN}{dt} &= rN(1 - \beta N) - \eta IN, \\
\frac{dI}{dt} &= \sigma + \frac{\rho IN}{m + N} - \delta I - \mu IN,
\end{aligned} \tag{1}$$

where $N[0] = 1$ [28] and $I[0] = 1.22$ [29] are initial values. The first equation reveals the change of normal cell population such that N is a normal cell. The parameter r represents the growth rate, and the rate of change from normal cells to abnormal cells during division is given by the parameter β. One of the functions of the immune system is to engulf and eliminate pathogens to prevent the body from developing cancer, which is represented by η. The second equation expresses the immune efficiency, where I denotes the immune cells. The fixed value of the immune system is represented by σ. The parameter δ is the rate of natural death of the immune cells, where the immune cells usually die off after thirty days. The term $\frac{\rho IN}{\omega + N}$ exhibits the Michaelis-Menten model of the immune cells, where ρ presents the growth of the immune cells stimulated by abnormal cells and m is the threshold rate of the immune cells. Finally, the reaction between abnormal cells and immune cells leads to a reduction in the number of immune cells, and this decrease is given by μ. All values of these parameters are identified in the literature, see Table 1.

Furthermore, the modification of the model, given the intervention of vitamins in thirty days as an external factor affecting both normal and immune cells and its improvement, is given by

$$\begin{aligned}
\frac{dN}{dt} &= rN(1 - \beta N) - \eta IN + c_1 VN, \\
\frac{dI}{dt} &= \sigma + \frac{\rho IN}{m + N} - \delta I - \mu IN + c_2 VI, \\
\frac{dV}{dt} &= k_1 + k_2 V,
\end{aligned} \tag{2}$$

where the initial conditions are $N[0] = 1$ [28], $I[0] = 1.22$ [29] and $V[0] = 2$, the intervention of vitamins is denoted by V. The positive constants c_1 and c_2 show the interaction between vitamins, normal cells and immune cells, respectively. The constant rate of vitamins is represented by k_1 and the constant k_2 denotes the decreased rate of vitamins due to the reactivity between cells.

Parameter	Value	Definition and reference
r	0.431201	Rate of growth of normal cells [31]
β	$2.99 * 10^{-6}$	Rate of turn of normal cells to abnormal cells [32]
η	0.2	Rate of repaired abnormal cells [25]
σ	0.7	Fixed of immune source [33]
δ	0.57	Rate of natural death of immune cells[evaluate]
ρ	0.003	Response rate of immune cells [34]
m	0.427	Threshold rate of immune cells [33]
μ	0.82	Rate of decreasing of immune cells as a result
		of interaction with abnormal cells [31]
a	0.7	Amplitude of immune alteration [33]

Table 1: Parameters of the model and references.

3   Parameters Values

These models examine the ability of the immune system in preventing the body from pathogens without treatment. In order to achieve the aim of this paper, the values of the parameters should be selected under special conditions. The behaviour of these models has a significant relation to the parameters which demonstrate the result of an active immune system when the pathogens attack the body in the presence of abnormal cells where these parameters are represented by μ and η.

Firstly, there are no conditions for normal cells selection, where normal cells can choose any value. For example, the initial value of normal cells in [28, 30] used $N(0) = 1$ and [31] used $N(0) = 10^5$. Whereas the immune cells are especially selected in the case of a weakened immune system without any medication. For that reason, the initial value of the immune cells is selected from [29], where the main problem with a HIV patient is a weakened immune system. Then, the value which is published in [29] is close to the case study of this model. In view of the fact that the initial values of vitamins can be used for intervention, their parameters and their effect on response of the immune system and growth of normal cells are based on the hypotheses of the model (1).

Secondly, the evaluation of the rate of growth of normal cells is by reference to the results of the experiment which is illustrated in [31] where the number of cells is examined for one week. During the process of the division and growth of normal cells there is a chance for abnormal division, then the rate of turn of the normal cells to abnormal cells is given in [32]. Whereas it is difficult to find a similar study which relates to the immune cells but it can also be assumed that the rate of growth of the immune cells follows the immune efficiency which is published in [33]. The growth of immune cells in this study should be close to the immune efficiency to satisfy the hypothesis of models which describes the effect of a change in dietary pattern to be close to a Western-style diet which causes a weakened immune system. Then, it is easy to evaluate the rate of death of the immune cells as in reference [28]. The response of immune cells also should reduce as given in [34] and the threshold rate of the immune system is evaluated by using the following function $m = (\sigma - \rho t)a$, where t=30 years.

Finally, the parameters η and μ describe the behaviour of both normal cells, abnormal cells and immune cells when a pathogen attacks the body. The first parameter η

associates with the ability of immune cells in engulfing and attacking the abnormal cells. This process occurs automatically if the immune cells are absolutely healthy and its activity diminishes if the body has a weakened immune system. That means the function of immune system stimulates when the abnormal cell appearance, and the rate of this stimulation is illustrated in [25]. As a result of this process, the number of immune cells will decreased. Thus, by reference to [31], it can use the same parameter of reapplication of normal and precancerous cells where the difference is between definitions relating to the building of models. Furthermore, in this paper, the parameter of μ should be greater than η where the model formulates assuming immune efficiency.

4 Numerical Simulation

The immune system can engulf and inhabit the pathogens as well if and only if the body has a strong immune system. Then, to modify the response of the immune system in the model (1) the parameters η and μ should satisfy the following inequality:

$$\text{The rate of parameter } \eta \geq \text{ The rate of parameter } \mu.$$

The diet pattern and lifestyle (as physical activity and irregular sleep) are risk factors of the immune system. This paper is focusing on the effect of switching back to a healthy diet from the Western-style diet by consumption a regular rate of vitamins on modifying the response of the immune system in the model (1). Thus, we are simulating the parameters c_1, c_2, k_1, k_2 that are related to the effect of vitamins intervention. These parameters should satisfy the following inequalities:

$$\text{The rate of parameter } k_2 > \text{ The rate of parameter } k_1,$$

$$\text{The rate of parameter } c_1 + \text{ The rate of parameter } c_2 \leq \text{ The rate of parameter } k_2.$$

Hence, the correlation between the vitamins intake and the behaviour of the immune system and normal cells is indicated by the model (2). Here, we are simulating the specified parameters as follows

$$\eta = 0.733, \mu = 0.312, c_1 = 0.261, c_2 = 0.231, k_1 = 0.164, k_2 = 0.960.$$

Hence, the numerical result of the modification of model (1) showed that the intervention of vitamins can boost the immune system and control the division of normal cells. Thus, it prevents the development of the pathogens.
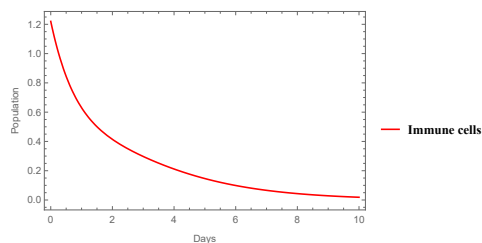

Figure 1: The behaviour of the immune system with unhealthy diet pattern within 10 days.
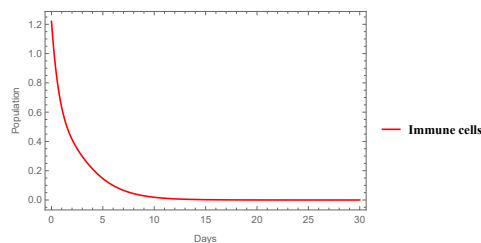
Figure 2: The behaviour of immune system with unhealthy diet pattern within 30 days.
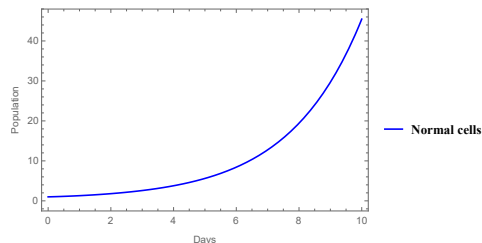
Figure 3: The behaviour of the normal cells with unhealthy diet pattern within 10 days.
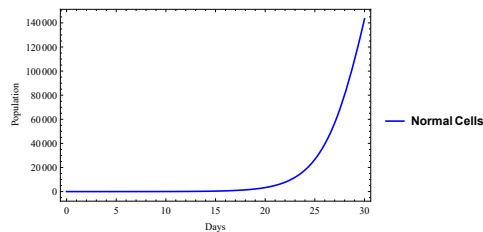
Figure 4: The behaviour of the normal cells with unhealthy diet pattern within 30 days.
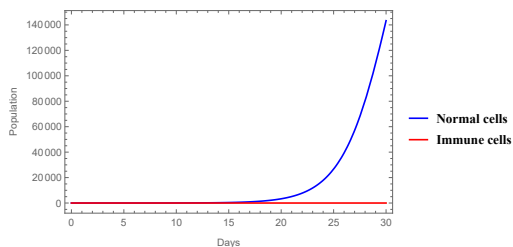
Figure 5: The behaviour of the model with unhealthy diet pattern within 30 days.
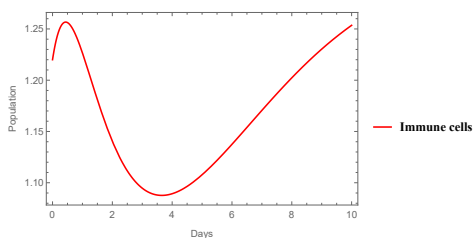
Figure 6: The behaviour of the immune system with modification of diet within 10 days.
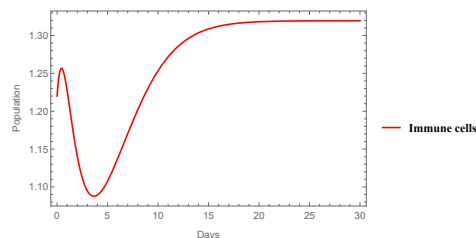
Figure 7: The behaviour of immune system with modification of diet within 30 days.

5　Results and Discussion

This paper used Mathematica 10.0 software to solve the nonlinear ordinary differential equations which described the behaviour of a weakened immune system and of that normal cells when a body is attacked by pathogens and abnormal division of cells took place. This type of division could lead to an emergence of carcinoma cells.

The numerical solution of an unhealthy model (an unhealthy diet as the Western-style diet) demonstrated the decrease in immune cells to zero within the first ten days from the appearance of abnormal cells, Figures 1, 2. This means that the immune system had a negative response and the immune cells (T cells and natural killer cells NK cells) were untenable to engulf and fight the abnormal cells. Furthermore, it may encourage the normal cells to divide and become cancerous cells. The result of previous studies such as [5, 6] support our idea that the Western-style diet
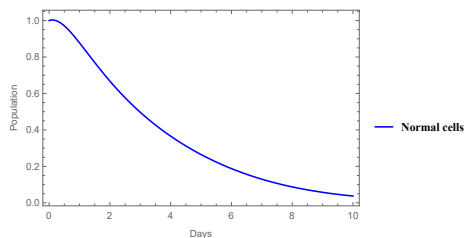
Figure 8: The behaviour of the normal cells with modification of diet within 10 days.
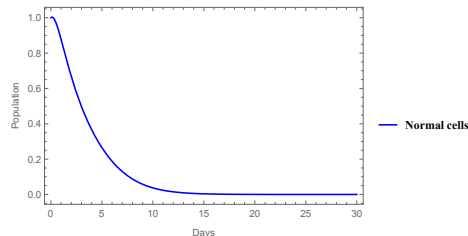
Figure 9: The behaviour of normal cells with modification of diet within 30 days.
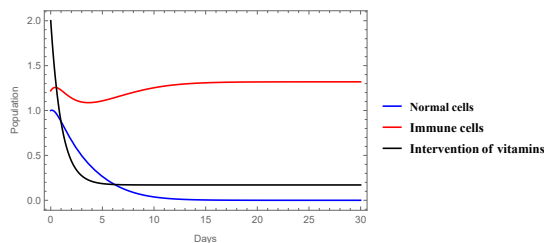

Figure 10: The behaviour of the model with modification of diet pattern within 30 days.

leads to an increase in the rate of glucose and insulin in the blood, thus causing abnormal cells to divide and grow as tumor cells.

Not only this, but the unhealthy diet has a significant impact on the behaviour of normal cells in the presence of abnormal cells in the body and the function of immune system may further weaken. The numerical solution showed that the population of normal cells elevated to 46 cells within the first ten days (Figure 3) and reached to 145000 cells approximately at the end of twenty days, Figure 4 indicated that the normal cells started to divide and grow without control. Sometimes, this way of division may cause cancer, where the growth and division of cells play an important role in protecting a human from cancer [30, 35]. The model of the unhealthy diet is illustrated in Figure 5.

Modification in the diet pattern reduces or delays the growth of tumor cells [36, 37]. In the unhealthy model, improvement was seen when intervened by vitamins. The numerical solution revealed that the intervention by vitamins affected both immune cells and normal cells. In this case, the vitamins stimulated the immune cells to increase and reach to 1.26 cells in the first day and the population of cells decreased dramatically to 1.9 cells on the fourth day. Following that, immune cells increased gradually until reaching 1.26 cells on the tenth day, Figure 6. The population of immune cells became stable at 1.32 cells, Figure 7 during the last twenty days. This result is identical to the findings of nutritionists that vitamins play an important role in boosting the immune system and supporting its functions [38, 39].

Moreover, a significant impact was observed on normal cells under the influence of vitamins. They were stable within the first twelve hours of the vitamins intake, then started to dramatically decrease to 0.1 cells in the first ten days, Figure 8. After that, the population of normal cells gradually decreases to zero within the last twenty days, Figure 9. This modification of unhealthy model is shown in Figure 10. So, an increased level of glucose, insulin resistance, obesity and cancer are disadvantages of the Western-style diet consumption. Previous studies found that

supplementation with vitamins D and C can improve glucose control and decrease serum insulin [40–43]. Other benefits of vitamin C are adipocyte lipolysis, which reduces the inflammatory response, preventing glucose metabolism, and secretion of leptin can isolate adipocyte [44–46]. Thus, consumption of vitamins can help to inhibit active abnormal cells into turning tumor cells indirectly.

Eventually, there is a complex relationship between dietary patterns and functions of the immune system which needs to be studied extensively. Our findings in this paper revealed numerically that there is a strong association between modification of the dietary pattern, boosting of the immune system and the division and growth of cells.

6 Conclusion

This paper illustrated that a modern diet (a Western-style diet) had an impact on the immune system function and the division of the normal cells when the pathogen had begun to attack the body. Consumption of a supplementary diet enabled a boost in the immune system and increased recognition of abnormal cells as foreign cells and helped eliminate them as well. Furthermore, an intake of vitamins played a huge role in getting the division of normal cells under control. Thus, an awareness must be put in motion of the concept of a healthy diet for all, especially the youth, for protecting against diseases and reducing the mortality rate due to common lethal diseases, particularly cancer.

Acknowledgment

References

[1] Y. Park, A. F. Subar, A. Hollenbeck and A. Schatzkin. Dietary fiber intake and mortality in the NIH-AARP diet and health study. *Archives of Internal Medicine* **171** (12) (2011) 1061–1068.

[2] H. Tilg and A. R. Moschen. Food, immunity, and the microbiome. *Gastroenterology* **148** (6) (2015) 1107–1119.

[3] J. A. Uranga, V. López-Miranda, F. Lombo and R. Abalo. Food, nutrients and nutraceuticals affecting the course of inflammatory bowel disease. *Pharmacological Reports* **68** (4) (2016) 816–826.

[4] A. S. Yusof, Z. M. Isa, and S. A. Shah. Dietary patterns and risk of colorectal cancer: a systematic review of cohort studies (2000-2011). *Asian Pacific Journal of Cancer Prevention* **13** (9) (2012) 4713–4717.

[5] S. E. Marwitz, L. N. Woodie and S. N. Blythe. Western-style diet induces insulin insensitivity and hyperactivity in adolescent male rats. *Physiology & Behavior* **151** (2015) 147–154.

[6] C. H. Sample, A. A. Martin, S. Jones, S. L. Hargrave and T. L. Davidson. Western-style diet impairs stimulus control by food deprivation state cues: Implications for obesogenic environments. *Appetite* **93** (2015) 13–23.

[7] M. E. Levine, J. A. Suarez, S. Brandhorst, P. Balasubramanian, C. Cheng, F. Madia, L. Fontana, M. G. Mirisola, J. Guevara-Aguirre, J. Wan and L. V. Longo. Low protein intake is associated with a major reduction in IGF-1, cancer, and overall mortality in the 65 and younger but not older population. *Cell Metabolism* **19** (3) (2014) 407–417.

[8] T. T. Fung, R. M. van Dam, S. E. Hankinson, M. Stampfer, W. C. Willett and F. B Hu. Low-carbohydrate diets and all-cause and cause-specific mortality: two cohort studies. *Annals of Internal Medicine* **153** (5) (2010) 289–298.

[9] A. Sanchez, J. L. Reeser, H. S. Lau, P. Y. Yahiku, R. E. Willard, P. J. McMillan, S. Y. Cho, A. R. Magie and U. D. Register. Role of sugars in human neutrophilic phagocytosis. *The American Journal of Clinical Nutrition* **26** (11) (1973) 1180–1184.

[10] L. B. Sórensen, A. Raben, S. Stender and A. Astrup. Effect of sucrose on inflammatory markers in overweight humans. *The American Journal of Clinical Nutrition* **82** (2) (2005) 421–427.

[11] L. DElia, G. Rossi, R. Ippolito, F. P. Cappuccio and P. Strazzullo. Habitual salt intake and risk of gastric cancer: a meta-analysis of prospective studies. *Clinical Nutrition* **31** (4) (2012) 489–498.

[12] J. van der Wijst, O. A. Z. Tutakhel, C. Bos, A. H. J. Danser, E. J. Hoorn, J. G. J. Hoenderop, and R. J. M. Bindels. Effects of a high sodium-low potassium diet on renal calcium, magnesium, and phosphate handling. *American Journal of Physiology-Renal Physiology* **315** (1) (2018) F110–F122.

[13] A. Colson, A. Brinkley, P. Braconnier, N. Ammor, M. Burnier and M. Pruijm. Impact of salt reduction in meals consumed during hemodialysis sessions on interdialytic weight gain and hemodynamic stability. *Hemodialysis International* **22** (4) (2018) 501–506.

[14] J. K. Goodrich, J. L. Waters, A. C. Poole, J. L. Sutter, O. Koren, R. Blekhman, M. Beaumont, W. Van Treuren, R. Knight, J. T. Bell and T. D. Spector. Human genetics shape the gut microbiome. *Cell* **159** (4) (2014) 789–799.

[15] P. J. Turnbaugh, V. K. Ridaura, J. J. Faith, F. E. Rey, R. Knight. and J. I. Gordon. The effect of diet on the human gut microbiome: a metagenomic analysis in humanized gnotobiotic mice. *Science Translational Medicine* **1** (6) (2009) 6ra14–6ra14.

[16] D. E. King, A. G. Mainous III and C. A. Lambourne. Trends in dietary fiber intake in the United States, 1999-2008. *Journal of the Academy of Nutrition and Dietetics* **112** (5) (2012) 642–648.

[17] L. P. Boulet. Asthma and obesity. *Clinical & Experimental Allergy* **43** (1) (2013) 8–21.

[18] H. Mayer, K. S. Zaenker and U. An Der Heiden. A basic mathematical model of the immune response. *Chaos: An Interdisciplinary Journal of Nonlinear Science* **5** (1) (1995) 155–161.

[19] S. A. Alharbi, A. S. Rambely and O. A. Alsuhaimi. Effect of dietary factor on response of the immune system numerically. Journal of Physics:Conference Series, Bangi, Malaysi, 2018,1–5.[Submitted]

[20] H. M. Byrne. Dissecting cancer through mathematics: from the cell to the animal model. *Nature Reviews Cancer* **10** (3) (2010) 221–230.

[21] W. M. Wonham. *Supervisory control of discrete-event systems.* Springer, London, 2015.

[22] A. Bratus, I. Samokhin, I. Yegorov and D. Yurchenko. Maximization of viability time in a mathematical model of cancer therapy. *Mathematical Biosciences* **294** (2017) 110–119.

[23] R. Padmanabhan, N. Meskin and W. M. Haddad. Reinforcement learning-based control of drug dosing for cancer chemotherapy treatment. *Mathematical Biosciences* **293** (2017) 11–20.

[24] F. A. Rihan and N. F. Rihan. Dynamics of Cancer-Immune System with External Treatment and Optimal Control.*Journal of Cancer Science & Therapy* **8** (2016) 256–261.

[25] M. Villasana and A. A. Radunskaya. Delay differential equation model for tumor growth. *Journal of Mathematical Biology* **47** (3) (2003) 270–294.

[26] S. Alharbi and A. S. Rambely. Stability Analysis of Mathematical Model on the Effect of Modern Lifestyles Towards the Immune System. *Journal of Quality Measurement and Analysis* **14** (2) (2018) 99–114.

[27] L. E. Green, T. A. Dinh and R. A. Smith. An estrogen model: the relationship between body mass index, menopausal status, estrogen replacement therapy, and breast cancer risk. *Computational and Mathematical Methods in Medicine* **2012** (2012).

[28] C. Mufudza, W. Sorofa and E. T. Chiyaka. Assessing the effects of estrogen on the dynamics of breast cancer. *Computational and Mathematical Methods in Medicine* **2012** (2012).

[29] L. Shan, K. Deng, N. S. Shroff, C. M. Durand, S. A. Rabi, H. Yang, H. Zhang, J. B. Margolick, J. N. Blankson and R. F. Siliciano. Stimulation of HIV-1-specific cytolytic T lymphocytes facilitates elimination of latent viral reservoir after virus reactivation. *Immunity* **36** (3) (2012) 491–501.

[30] N. I. Hammadi, Y. Abba, M. N. M. Hezmee, I. S. A. Razak, A. U. Kura and Z. A. B. Zakaria. Evaluation of in vitro efficacy of docetaxel-loaded calcium carbonate aragonite nanoparticles (DTX-CaCO3NP) on 4T1 mouse breast cancer cell line. *In Vitro Cellular & Developmental Biology-Animal* **53** (10) (2017) 896–907.

[31] F. Aziz, X. Yang, Q. Wen and Q. Yan. A method for establishing human primary gastric epithelial cell culture from fresh surgical gastric tissues. *Molecular Medicine Reports* **12** (2) (2015) 2939–2944.

[32] J. C. Roach, G. Glusman, A. F. A. Smit, C. D. Huff, R. Hubley, P. T. Shannon, L. Rowen, K. P. Pant, N. Goodman, M. Bamshad and J. Shendure. Analysis of genetic inheritance in a family quartet by whole-genome sequencing. *Science* **328** (5978) (2010) 636–639.

[33] C. Jacqueline, Y. Bourfia, H. Hbid, G. Sorci, F. Thomas and B. Roche. Interactions between immune challenges and cancer cells proliferation: timing does matter!. *Evolution, Medicine, and Public Health* **2016** (1) (2016) 299–311.

[34] Y. Aydar, P. Balogh, J. G. Tew and A. K. Szakal. Age-related depression of FDC accessory functions and CD21 ligand-mediated repair of co-stimulation. *European Journal of Immunology* **32** (10) (2002) 2817–2826.

[35] G. M. Cooper *The Cell: A Molecular Approach.* ASM Press, 2000.

[36] S. Chen, Y. Chen, S. Ma, R. Zheng, P. Zhao, L. Zhang, Y. Liu, Q. Yu, Q. Deng and K. Zhang. Dietary fibre intake and risk of breast cancer: a systematic review and meta-analysis of epidemiological studies. *Oncotarget* **7** (49) (2016) 80980–80989.

[37] M. Hatami, M. E. Akbari, M. Abdollahi, M. Ajami, Y. Jamshidinaeini and S. H. Davoodi. The relationship between intake of macronutrients and vitamins involved in one carbon metabolism with breast cancer risk. *Tehran University Medical Journal TUMS Publications* **75** (1) (2017) 56–64.

[38] P. C. Calder. Feeding the immune system. *Proceedings of the Nutrition Society* **72** (3) (2013) 299–309.

[39] K. Karacabey and N. Ozdemir. The Effect of Nutritional Elements on the Immune System. *Journal of Obesity and Weight Loss Therapy* **2** (9) (2012) 1–6.

[40] D. F. Garcia-Diaz, P. Lopez-Legarrea, P. Quintero and J. A. Martinez. Vitamin C in the treatment and/or prevention of obesity. *Journal of Nutritional Science and Vitaminology* **60** (6) 2014 367–379.

[41] S. Lim, M. J. Kim, S. Lim, M. J. Kim, S. H. Choi, C. S. Shin, K. S. Park, H. C. Jang, L. K. Billings, J. B. Meigs and S. H. Choi. Association of vitamin D deficiency with incidence of type 2 diabetes in high-risk Asian subjects. *The American Journal of Clinical Nutrition* **97** (3) (2013) 524–530.

[42] J. Mitri, B. Dawson-Hughes, F. B. Hu and A. G. Pittas. Effects of vitamin D and calcium supplementation on pancreatic β cell function, insulin sensitivity, and glycemia in adults at high risk ofdiabetes: the Calcium and Vitamin D for Diabetes Mellitus (CaDDM) randomized controlled trial. *The American Journal of Clinical Nutrition* **94** (2) (2011) 486–494.

[43] J. Rad, M. Djalali, F. Koohdani, A. A. Saboor-Yaraghi, M. R. Eshraghian, M. H. Javanbakht, S. Saboori, M. Zarei and M. J. Hosseinzadeh-Attar. The effects of vitamin D supplementation on glucose control and insulin resistance in patients with diabetes type 2: a randomized clinical trial study. *Iranian Journal of Public Health* **43** (12) (2014) 1651–1656.

[44] D. F. Garcia-Diaz, J. Campion, F. I. Milagro, N. Boque, M. J. Moreno-Aliaga and J. A Martinez. Vitamin C inhibits leptin secretion and some glucose/lipid metabolic pathways in primary rat adipocytes. *Journal of Molecular Endocrinology* **45** (1) (2010) 33–43.

[45] O. P. García, D. Ronquillo, M. C. Caamaño, M. Camacho, K. Z. Long and J. L. Rosado. Zinc, vitamin A, and vitamin C status are associated with leptin concentrations and obesity in Mexican women: results from a cross-sectional study. *Nutrition & Metabolism* **9** (1) (2012) 59–69.

[46] G. Bjørklund and S. Chirumbolo. Role of oxidative stress and antioxidants in daily nutrition and human health. *Nutrition* **33** (2017) 311–321.

A Piecewise Orthogonal Functions-Based Approach for Minimum Time Control of Dynamical Systems

S. Bichiou *, M.K. Bouafoura and N. Benhadj Braiek

Advanced System Laboratory (Laboratoire des Systèmes Avancés - LSA), Tunisia Polytechnic School - EPT, University of Carthage, BP 743, 2078 La Marsa, Tunisia.

Abstract: This paper introduces a numerical technique for solving minimum time control problems. These problems are addressed to linear time invariant systems in feedforward and feedback control. The mathematical formulation of the control problem is expanded in several piecewise orthogonal bases, namely, the Walsh, block-pulse and Haar wavelets. Operational matrices are used to transform the integration procedure into a product. A numerical optimization problem is formulated to determine the final time and the control sequence (switching times) necessary to steer the system from an initial to a target position. The used numerical method shows that the employed piecewise orthogonal function generates better results than other functions.

Keywords: *orthogonal functions; operational matrices; minimum time control; linear systems; closed loop scheme.*

Mathematics Subject Classification (2010): 93C35, 93D15.

1 Introduction

After the introduction of human operated machines, there was a need to enhance further the productivity and reduce costs. Therefore, automatic machines (i.e. robots) were designed and introduced. Today, many engineering systems, from manufacturing machines to vehicles and airplanes, require optimal control algorithms in order to operate efficiently. Pontryagin [1] developed the theoretical background needed to formulate and then solve these problems. Nevertheless, due to the nature of these engineering systems, finding a solution to these control problems remains a challenging task and requires multidisciplinary knowledge, from ordinary differential equation (ODE) discretization to optimisation so that to obtain a numerical solution. The control problems can be derived

---

* Corresponding author: `mailto:salim.bichiou@gmail.com`

in two categories: linear and nonlinear. The nonlinear problems feature nonlinear ODEs and are not the scope of this paper. This paper focuses on solving an optimal control problem for linear systems(i.e. the ODE is linear in states and control, even though the problem formulation is non-linear), and particularly, on the determination of a minimum time optimal control.

Finding a solution to the minimum time control problem is a difficult task. The intent of these problems is to steer a system from a given initial state to a target state in minimum time. Often, and due to the complexity of the mathematical formulation, it is difficult to find an analytical solution even for linear systems. In fact, very few examples have an analytical solution obtained through the Pontryagin maximum principle, it is well known that when constrains over system inputs are considered, the obtained minimum time control is necessarily of a bang-bang form [2].

Nevertheless, the minimum control problem could be undertaken with numerical approaches based on nonlinear optimization techniques like the shooting method [3]. Other approaches in literature are typically based on geometric or graphical resolution [4], however, despite of accuracy, these techniques are of limited usage to low order LTI systems.

The orthogonal functions constitue a considerable tool to solve various optimal control problems [5]. Generally, when orthogonal polynomials are used, it is called a pseudo-parametrization technique. In fact, that issue could be an interesting alternative to the securitization technique and could save considerably computational effort since it reduces unknown parameters in the nonlinear optimization problem.

There are different types of orthogonal functions:

- Piecewise functions (block-pulse, Walsh and Haar wavelets) [6, 7];

- Polynomials (Legendre, Chebyshev,...) [8];

- Trigonometric functions (sine, cosine,...) [9].

Researchers have tried to solve the minimum time control problem using the Chebyshev orthogonal functions for open loop linear systems [8], multivariable systems [10] and PID control [11].

Since the type of control is known a priori (i.e. the bang-bang control), it is suitable to use piecewise orthogonal functions thus allowing the capture of discontinuities in the inputs. This method is simpler compared to the methods proposed in [8] and [10] where the Chebyshev orthogonal polynomials had been used. In fact, in those works a set of equalities are derived where each one contains two unknown variables. Then, the authors [11] formulated a parameter optimisation problem to find the final time t_f and using the latter variables they determine the control sequence also.

In this effort, we use a simpler method that exploits the operational matrix of integration [6], and thus, there is no need to find the coefficient in [8,10] making the problem formulation easier. Furthermore, in addition to the open loop optimization, a closed loop algorithm is formulated.

This paper is organized as follows. The second section is reserved to the formulation of the minimum time control problem. In the third section, a description of the orthogonal functions used and their algebraic properties are provided. The formulation of the proposed method and simulation results are presented in the fourth section. Finally, conclusions and future works are given in the last section.

2   Time-Optimal Constrained Feedforward Control Problem

We consider an LTI system described by the following state space model:

$$\begin{cases} \dot{x}(t) & = & Ax(t) + Bu(t), \\ y(t) & = & Cx(t), \end{cases} \tag{1}$$

where $y \in \mathbb{R}^p$ is the output, $u \in \mathbb{R}^m$ is the input control signal and $x \in \mathbb{R}^n$ is the state vector. In general, if the final state is not zero, we define a new system state X given in equation (2) such that the system becomes normalized and the target remains the origin of state space. Then the system (1) can be written as

$$\begin{array}{rcl} X & = & x - x_f, \\ \dot{X} & = & AX + Bu + Ax_f, \\ X_0 & = & x_0 - x_f, \end{array} \tag{2}$$

where x_0 is the initial position of the system and x_f is the target position to reach.

To minimize the final time, the cost function is taken as [12]

$$J = t_f - t_0 = \int_{t_0}^{t_f} dt. \tag{3}$$

Applying the Pontryagin maximum principle (PMP) [1], we define the Hamiltonian [13] for (1)

$$H(.) = -1 + \lambda^T (AX + Ax_f + Bu). \tag{4}$$

The canonical equation of Hamilton is given by

$$\dot{X} = H_\lambda = AX + Ax_f + Bu, \tag{5a}$$

$$\dot{\lambda} = -H_x = -A^T \lambda. \tag{5b}$$

The target state being the origin is

$$X(t_f) = 0. \tag{6}$$

Minimizing the Hamiltonian we obtain the following control signal:

$$u(t) = sign(\lambda^T B). \tag{7}$$

This can be written as follows:

$$u(t) = \begin{cases} u_{min}, & if \quad \lambda^T B < 0, \\ u_{max}, & if \quad \lambda^T B > 0. \end{cases} \tag{8}$$

Thus, the obtained control is bang-bang.

3   Orthogonal Functions and Algebraic Properties

Using orthogonal functions to construct operational matrices was firstly proposed in the study of dynamic systems for modeling [14], identification [15] and control purposes [16].

3.1   Principle

Let $\phi_i(t)$ be a set of orthogonal polynomials, piecewise functions. Any analytical function absolutely integrable on the time interval $[0, T]$ can be approximated as follows:

$$f(t) = \sum_{i=0}^{\infty} f_i \phi_i(t), \tag{9}$$

where the coefficients f_i are evaluated by the following scalar product:

$$f_i = \int_0^T f(t) \phi_i(t) dt. \tag{10}$$

For numerical purposes, a truncation of equation (9) until a convenient number of elementary functions is considered in practice.

$$f(t) \cong \sum_{i=0}^{N-1} f_i \phi_i(t) = F_N^T \Phi_N(t), \tag{11}$$

where $\Phi_N^T = [\varphi_0(t) \varphi_1 \cdots \varphi_{N-1}(t)]$ is the orthogonal basis and $F_N^T = [f_0 f_1 \cdots \ f_{N-1}]$ is the coefficient vector.

Integrating equation (11), we obtain:

$$\int f(t) \cong F_N^T P_N \Phi_N(t), \tag{12}$$

where $P_N \in \mathbb{R}^{n \times n}$ is the operational matrix of integration depending on the considered orthogonal basis. As a result, the differential equations describing dynamic processes can be reduced into algebraic relations allowing important simplifications in the synthesis problems.

In this paper, we focus on three types of piecewise orthogonal functions, which are block-pulse, Walsh and Haar wavelets. They present different characteristics. The main difference and properties of each one will be detailed in the next section.

3.2   Block-pulse functions

Block-pulse functions constitute a complete set of orthogonal functions and are defined as follows [7, 17]:

$$b_i(t) = \begin{cases} 1, & if \ t \in [iT \ , \ (i+1)T], \\ & i = 0, ..., N-1, \\ 0, & otherwise. \end{cases} \tag{13}$$

A function $f(t)$ can be approximated by

$$f(t) \simeq \sum_{i=0}^{N-1} f_i b_i(t) = F_N^T B(t), \tag{14}$$

with: $F_N = [f_0, f_1, ..., f_{N-1}]^T$ is the coefficient vector, $B(t) = [b_0(t), b_1(t), ..., b_{N-1}(t)]^T$ is the block-pulse basis vector and f_i are given by

$$f_i = N \int_{(i-1)T}^{iT} f(t) b_i(t) dt, \tag{15}$$

where N is the order of block-pulse functions.

The operational matrix for the block-pulse functions denoted $P_{N,bp}$ is given by [5]

$$P_{N,bp} = \frac{T}{N} \begin{bmatrix} \frac{1}{2} & 1 & 1 & \dots & 1 \\ 0 & \frac{1}{2} & 1 & \dots & 1 \\ \vdots & \ddots & \frac{1}{2} & \dots & 1 \\ \vdots & & \ddots & \ddots & \vdots \\ 0 & \dots & \dots & 0 & \frac{1}{2} \end{bmatrix}. \tag{16}$$

The representation of this basis for $N = 8$ can be described in Figure 1.
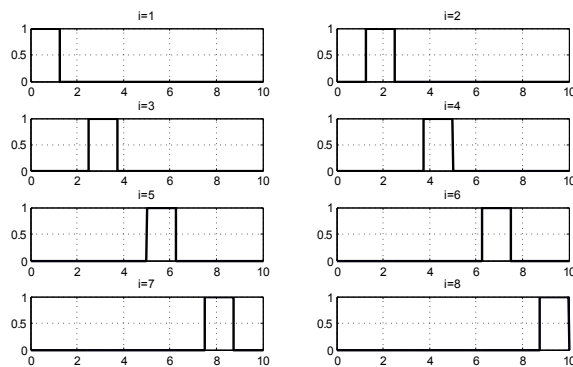
Figure 1: A set of block-pulse functions.

3.3 Walsh functions

Walsh functions belong to the family of piecewise orthogonal functions [18]. They can have only two values +1 or -1 over the interval of interest.

A function $f(t)$, absolutely integrable in $[0, 1]$, may be expanded into the Walsh series as

$$f(t) \simeq \sum_{i=0}^{N-1} f_i w_i(t) = F_N^T W(t). \tag{17}$$

The Walsh functions $w_0(t), w_1(t), \cdots, w_{N-1}(t)$ are orthonormal square waves.

To determine the operational matrix, i.e. $P_{N,w}$, of integration, the equation (18) is used:

$$P_{N,w} = \begin{bmatrix} P_{\frac{N}{2} \times \frac{N}{2}} & \frac{-1}{2N} I_{\frac{N}{2} \times \frac{N}{2}} \\ \frac{1}{2N} I_{\frac{N}{2} \times \frac{N}{2}} & 0 \end{bmatrix}, \tag{18}$$

Where I is the identity matrix. Then the same state space transformation for the block-pulse function is used.

In fact there is a matrical relation between block-pulse and Walsh operational matrix of integration [17]:

$$P_{N,w} = W_{N \times N} \times P_{N,bp} \times W_{N \times N}^{-1}, \tag{19}$$

where W denotes the transition matrix from block-pulse to Walsh basis. For $N = 4$ the Walsh transformation is

$$W_{4 \times 4} = \begin{bmatrix} 1 & 1 & 1 & 1 \\ 1 & 1 & -1 & -1 \\ 1 & -1 & 1 & -1 \\ 1 & -1 & -1 & 1 \end{bmatrix}. \tag{20}$$

This basis can be described in Figure 2 with N=8.
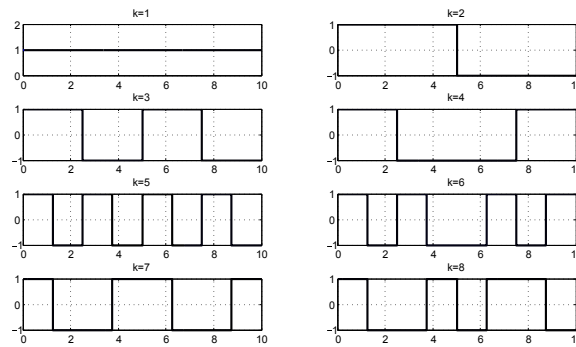
Figure 2: A set of Walsh functions.

3.4   Haar wavelets

The orthogonal set of Haar functions defined in [19] is a group of square waves with magnitude of ± 1 in some intervals and zeros elsewhere. The first function is $h_0 = 1$ $\forall x \in [0, 1]$. It is commonly referred to as the scaling function. The second is the fundamental square or the mother wavelet which spans the hole interval $[0, 1]$, for N=4, for example,

$$h_1(t) = [1 \ \ 1 \ -1 \ -1]\phi_4(t). \tag{21}$$

All the other subsequent curves are generated from $h_1(t)$ with two operations: translation and dilation. $h_2(t)$ is obtained from $h_1(t)$ with dilation, namely, $h_1(t)$ is compressed from the whole interval $[0, 1]$ to the half interval $[0, 1/2]$ to generate $h_2(t)$. $h_3(t)$ is the same as $h_2(t)$ but shifted to the right by $1/2$. Similarly, $h_2(t)$ is compressed from the half interval to the quarter interval to generate $h_4(t)$. $h_4(t)$ is translated to the right by $1/4$, $1/2$ and $3/4$ to generate $h_5(t)$, $h_6(t)$ and $h_7(t)$, respectively.

The general description of the square waves is given as follows:

$$h_0(t) = 1,$$

$$h_i(t) = \begin{cases} 2^{j/2}, \frac{k-1}{2^j} \le t < \frac{k-1/2}{2^j}, \\ \\ -2^{j/2}, \frac{k-1}{2^j} \le t < \frac{k-1/2}{2^j}, \\ \\ 0, otherwise \ in [0, 1). \end{cases} \tag{22}$$

The index $i = 1, 2, \ldots, N-1$, j and k represent the integer decomposition of i as follows: $i = 2^j + k - 1$.

The description of the Haar wavelets can be seen in Figure 3 for N=8.
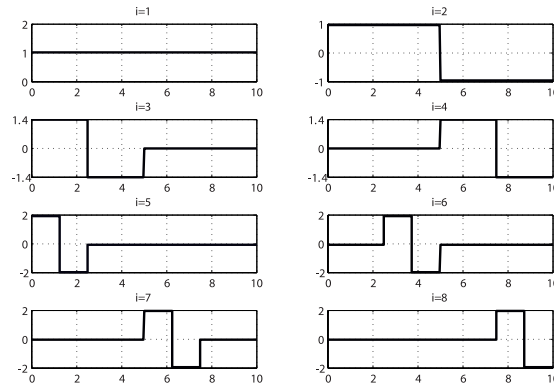
Figure 3: A set of Haar functions.

The operational matrix of integration for the Haar wavelets denoted $P_{N,h}$ is given as follows:

$$P_{N,h} = \frac{1}{2N} \begin{bmatrix} 2NP_{\frac{N}{2} \times \frac{N}{2}} & -H_{\frac{N}{2} \times \frac{N}{2}} \\ H_{\frac{N}{2} \times \frac{N}{2}}^{-1} & 0 \end{bmatrix}, \tag{23}$$

where

$$H_{N \times N} \triangleq \begin{bmatrix} h_N(t_0) & h_N(t_1) & \cdots & h_N(t_{N-1}) \end{bmatrix}.$$

As the Walsh function, the operational matrix of the Haar wavelets can be expressed by the block-pulse operational matrix [17]

$$P_{N,h} = H_{N \times N} \times P_{N,bp} \times H_{N \times N}^{-1}. \tag{24}$$

For N=4, $H_{N \times N}$ is as follows:

$$H_{4 \times 4} = \begin{bmatrix} 1 & 1 & 1 & 1 \\ 1 & 1 & -1 & -1 \\ \sqrt{2} & -\sqrt{2} & 0 & 0 \\ 0 & 0 & \sqrt{2} & -\sqrt{2} \end{bmatrix}. \tag{25}$$

4 Orthogonal Function Based Minimum Time Control Problem Formulation

4.1 The original open loop problem

Minimum time control is an open loop control problem. It is described by Figure 4, where $X(0)$ is the known initial system state and $u(t)$ is the control vector. This framework is dedicated to the class of systems described by equation (1). Here $x(t)$ is the system state trajectory that is needed to search for a prefixed target state in a minimum time t_f to be calculated.

In this work, we intent to develop a numerical method that is able to return the final time t_f and the control sequence (or precisely the control coefficient over an orthogonal function basis), while the initial $X(0)$ (i.e. its coefficients over the same basis) should be provided to the algorithm.
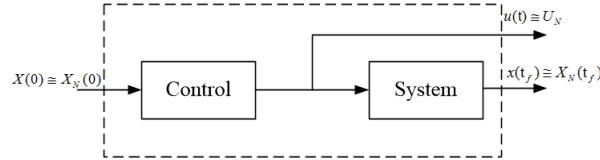
Figure 4: An open loop control structure.

4.2 Main developement

Finding the solution of (5b) means solving multiple differential equations, which is mathematically delicate. To overcome this difficulty we will make use of the set of orthogonal functions described in the last section.

In order to derive the final time, a variable change is introduced:

$$t = \tau t_f. \tag{26}$$

This change of variable allows a transformation of the time domain from $t \in [0, t_f]$ to $\tau \in [0, 1]$, then system states becomes

$$X(t) = \tilde{X}(\tau). \tag{27}$$

Notice that the latter variable change leads to a constant time interval [0,1] for the used series since the final time t_f is unknown.

Consequently, we deduce

$$\dot{X}(t) = \frac{d\tilde{X}(\tau)}{d\tau} \cdot \frac{d\tau}{dt} = \frac{1}{t_f}\dot{\tilde{X}}(\tau). \tag{28}$$

The original state equation of system (1) is now equivalent to

$$\frac{1}{t_f}\dot{\tilde{X}}(\tau) = A\tilde{X}(\tau) + B\tilde{u}(\tau). \tag{29}$$

Using orthogonal functions consists in developing both, the system states and the input over that basis:

$$\tilde{X}(\tau) = \tilde{X}_N^T \cdot \phi_N(\tau), \quad \tilde{u}(\tau) = \tilde{u}_N^T \cdot \phi_N(\tau), \tag{30}$$

where $\phi_N(\tau) \in B(\tau), W(\tau), H(\tau)$. Furthermore, integrating equation (29) leads to

$$\frac{1}{t_f}(\tilde{X}(\tau) - \tilde{X}(0)) = A \int_0^1 (\tilde{X}(\tau))d\tau + B \int_0^1 \tilde{u}(\tau)d\tau. \tag{31}$$

Introducing coefficients of $\tilde{X}(\tau)$, $\tilde{u}(\tau)$ and the operational matrix of integration we obtain

$$\int_0^1 \tilde{X}(\tau)d\tau = \tilde{X}_N \int_0^1 \phi_N(\tau)d\tau = \tilde{X}_N^T P_N \phi_N(\tau), x \tag{32}$$

then we can write

$$(\tilde{X}_N^T - \tilde{X}_{N_0}^T)\phi_N = t_f(A\tilde{X}_N^T P_N + B\tilde{U}_N^T P_N)\phi_N, \tag{33}$$

thus

$$\tilde{X}_N^T - \tilde{X}_{N0}^T = t_f(A\tilde{X}_N^T P_N + B\tilde{U}_N^T P_N), \tag{34}$$

where $\tilde{X}_{N0}$ is a projection of the initial state over orthogonal functions and depends on the chosen set of functions.

4.3   OFs Optimization problem formulation

To find the transition time from the initial to the target position, we need to solve the following nonlinear problem:

Original optimization problem

$$\mathbf{min}\ (t_f) \tag{35}$$

subject to:

$$
\begin{aligned}
&\dot{x}(t) = Ax(t) + Bu(t), \quad 0 \le t \le t_f, \\
&u \in [u_{min}, u_{max}], \\
&x(0) = x_0, x(t_f) = x_f.
\end{aligned}
\tag{36}
$$

This problem is reported to the domain $[0, \tau]$. The optimization algorithm in the orthogonal basis has the following form:

Orthogonal function optimization problem

$$\mathbf{min}\ (t_f) \tag{37}$$

subject to linear constraints: initial state expansion:

- for the block-pulse function

$$\tilde{X}_{N0,bp} = \begin{bmatrix} \tilde{X}(0) & \tilde{X}(0) & \cdots & \tilde{X}(0) \end{bmatrix},$$

- for the Walsh functions and Haar wavelets

$$\tilde{X}_{N0,w} = \tilde{X}_{N0,h} = \begin{bmatrix} \tilde{X}(0) & 0 & \cdots & 0 \end{bmatrix}$$

final state expansion:

- For the block-pulse functions:
  $\tilde{U}_{Nmin} \le \tilde{U}_N \le \tilde{U}_{Nmax}$,
  $\tilde{X}_{Nf,bp} = \begin{bmatrix} 0 & 0 & \cdots & \tilde{X}_f \end{bmatrix}$.

- For the Walsh functions:
  $\tilde{U}_{Nmin} \le \tilde{U}_N\ \phi_{N,w} \le \tilde{U}_{Nmax}$,
  $\tilde{X}_{Nf,w} = \begin{bmatrix} 0 & 0 & \cdots & \tilde{X}_f \end{bmatrix} W_{N \times N}$.

- For the Haar functions:
  $\tilde{U}_{Nmin} \le \tilde{U}_N\ \phi_{N,h} \le \tilde{U}_{Nmax}$,
  $\tilde{X}_{Nf,h} = \begin{bmatrix} 0 & 0 & \cdots & \tilde{X}_f \end{bmatrix} H_{N \times N}$,

where $\tilde{X}_{N,f}$ denotes the projection of the final sate over orthogonal functions. $W_{N \times N}$ and $H_{N \times N}$ are, respectively, the Walsh and Haar transition matrices,
nonlinear constraints:

$$\tilde{X}_N - \tilde{X}_{N0} = t_f(A\tilde{X}_N P_N + B\tilde{U}_N P_N). \tag{38}$$

To solve this optimization problem, an interior point method the same as the one implemented in the function "fmincon" of Matlab is used.

Figure 5: Example 1.
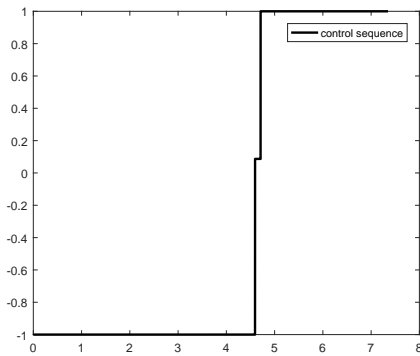
(a) Control sequence for Example 1.
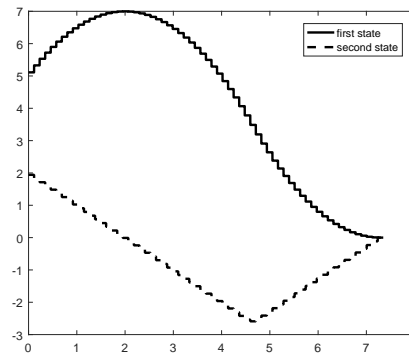
(b) System trajectory for Example 1.

4.4 Simulation and validation

In this subsection, a comparison between our results and some other results available in the literature is presented.

4.4.1 Example 1

We consider a simple double integrator system in which its analytic solution using the PMP is well known. Its state space representation is given in equation (39):

$$A = \begin{bmatrix} 0 & 1 \\ 0 & 0 \end{bmatrix}, \quad B = \begin{bmatrix} 0 \\ 1 \end{bmatrix}. \tag{39}$$

The system needs to be shifted from an initial state $x(0) = [5, 2]^T$ to the origin of state space with the input constraint $u \in [-1, 1]$. The analytical solution for this system is as follows: the system has one switching point at $t_c = 4.64$ and the final time is $t_f = 7.29$. Determining the solution of the double integrator system using optimization algorithm for a base of dimension $N = 64$, we obtain comparable results with the analytical solution. From Figure 5(a) and Figure5(b), it is clear that the system has only one switching point at $t_c = 4.594$ which is almost the same one found by the analytical solution.

We can also see that the control sequence is bang-bang and that the final time $t_f = 7.3508$ is also the same as the analytical solution.

4.4.2 Example 2

Take the example given in [10] which is a fourth order MIMO system with two real double poles $\lambda_1 = 5, 2833$ and $\lambda_2 = -0.0833$. The state space representation of the system is given as follows:

$$A = \begin{bmatrix} -\frac{1}{10} & 0 & 0 & 0 \\ 0 & -\frac{1}{15} & 0 & 0 \\ 0 & 0 & -\frac{1}{15} & 0 \\ 0 & 0 & 0 & -\frac{1}{10} \end{bmatrix}, \quad B = \begin{bmatrix} \frac{1}{2} & 0 \\ \frac{1}{2} & 0 \\ \frac{1}{2} & 0 \\ 0 & \frac{1}{2} \\ 0 & \frac{1}{2} \end{bmatrix}, \quad C = \begin{bmatrix} \frac{3}{5} & 0 & \frac{8}{15} & 0 \\ 0 & \frac{2}{3} & 0 & \frac{3}{5} \end{bmatrix}.$$

Figure 6: Example 2.
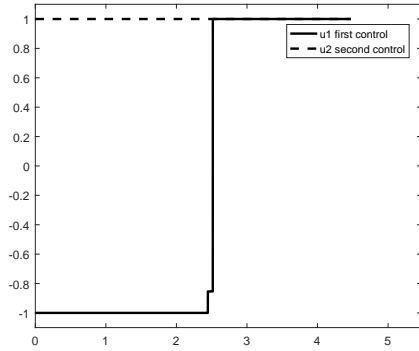
(a) Control sequence for Example 2.
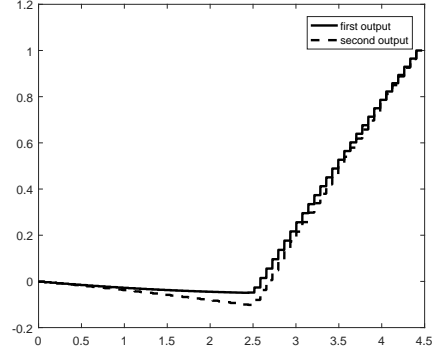
(b) System trajectory for Example 2.

This system needs to be shifted from $y = [0,0]^T$ to $y_f = [1,1]^T$, the input constraints are $u_1, u_2 \in [-1,1]^T$.

Computing the MIMO system including its constraints we obtain the control sequence described in Figure 6(a).

We can see from Figure 6(a) that the control sequence is bang-bang, that u_1 does not contain any switching time and that u_2 contains only one at $t_c = 2.5$.

This proves that our method is also effective for MIMO constrained systems. By comparing this result to the result obtained in [10] where $t_f = 54.1$ we can see from Figure 6(b) that the target is reached before at $t_f = 4.47$.

It is clear that the obtained results through the orthogonal piecewise functions using operational matrices are far better than the one obtained using the Chebyshev technique [10].

5 Closed Loop Online Suboptimal Minimum Time Control Algorithm

In the past section we have elaborated an algorithm to compute the minimum time control for open loop systems. Such solution can not recover from perturbations, so we determined an offline suboptimal control structure. In this part, we introduce an online suboptimal minimum time control.

5.1 Principle

The control problem is now described by Figure 7. Z is a perturbation that may affect the system states, $X_N^T(kh) = [x_0(kh) \ \ x_1(kh) \ \cdots \ x_{N-1}(kh)]$ is the output state vector at $t = kh$ which represents the discrete time. Besides, h is chosen as small as possible in order to take into account correctly an eventual disturbance over the system states.

The optimization problem formulation in the closed loop is similar to that in the open loop case. However, it is computed k times. The initial state is continuously actualized to the final state of the previous optimization step.
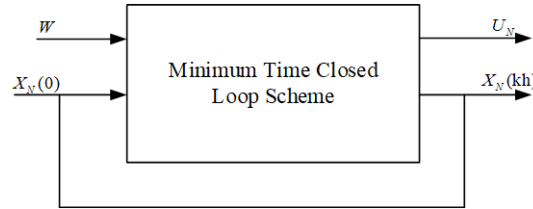
Figure 7: Feedback control scheme.

5.2 Algorithm description

Algorithm 5.1 Minimum time closed-loop algorithm

---

begin
    initialization
    $k \longleftarrow 0$
    $h \longleftarrow 10^{-2}$
    $\tilde{X}_{N0,bp} = [\tilde{X}(0)\ \tilde{X}(0)\quad \cdots \quad \tilde{X}(0)]$
    While $\tilde{x} \neq x_f$ **do**
        Find **min**(t_f)
        Subject to:
        Linear constraints:
        $\tilde{U}_{Nmin} \leq \tilde{U}_N \times \phi_N \leq \tilde{U}_{Nmax}$
        $\tilde{X}_{N0} = [\tilde{x}_0(kh)\ \tilde{x}_1(kh)\quad \tilde{x}_{N-1}(kh)]$
        $\tilde{X}_{N0,f} = [0\quad 0\quad \cdots \quad \tilde{x}_f]$
        Nonlinear constraints:
        $\tilde{X}_N - \tilde{X}_{N0} = t_f(A\tilde{X}_N P_N + B\tilde{U}_N P_N)$
        $k \longleftarrow k + 1$
    end
end

5.3 Simulation and comparison results

We consider the same system: a simple double integrator described previously.

In this section we intent to apply the closed loop optimization procedure to the system using the orthogonal block-pulse, Walsh or Haar wavelets for $N = 64$. This will be considered for various cases, namely, the system without disturbance (here the closed loop performance should meet the open loop one to prove the correctness of the algorithm), and after that the presence of perturbation case is examined. That disturbance is seen as an exterior event that discards the system state from its trajectory at time instant denoted t_p.

From Figure 8(a), it is clear that the system has only one switching point at $t_c = 4.594$ which is almost the same one found by the analytical solution.

We can also see that the control sequence is bang-bang in the closed loop and that the final time $t_f = 7.323$ is also the same as the analytical solution. It is clear from Figure 8(b) that the system without perturbations in the closed loop reaches the target at the same time of the open loop.

Figure 8: Example 1 without perturbation.
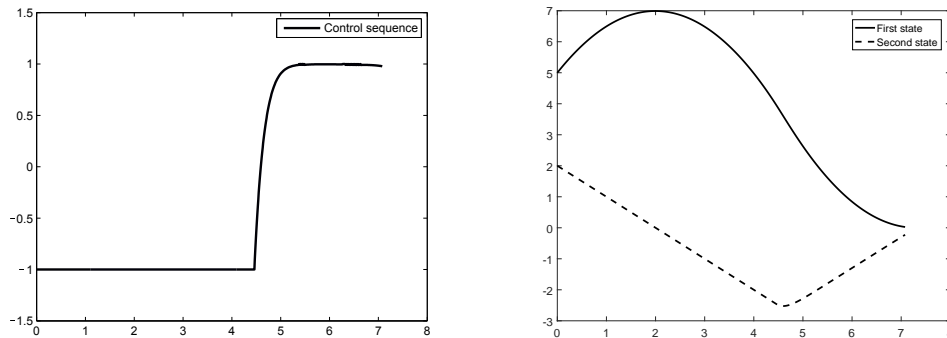
(a) Control sequence for the example 1 without perturbation.

(b) System trajectory for the example 1 without perturbation.

Figure 9: Example 1 with perturbation.
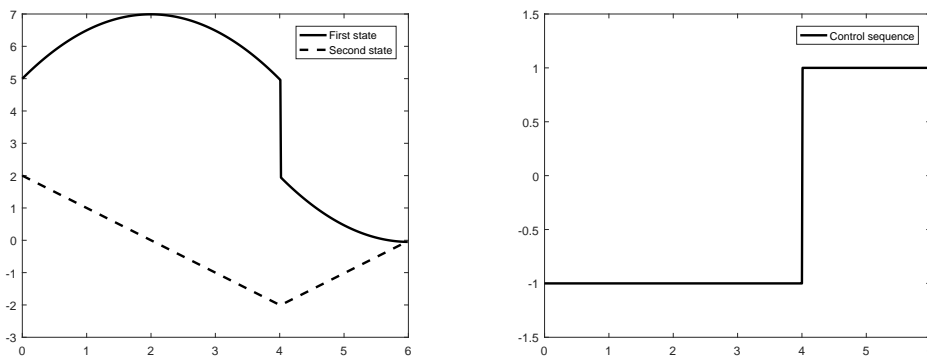
(a) System trajectory for the example 1 with perturbation on the first state.

(b) Control sequence for the example 1 with perturbation on the first state.

5.4 Example for perturbed system

In this part, the system is perturbed at $t_p = 4s$. We can see from Figure 9(b) that the control sequence is still bang-bang but there is a change of the switching time.

It is clear from Figure 9(a) that the system is able to recover from the perturbation and reaches the target faster for the case of this perturbation. In fact, the perturbation signal on the first state has brought it closer to the target. This explains why $t_f < t_{f_{ol}}$.

Another simulation context could be verified. In fact, the system described by the state space form in (39) is perturbed at $t_p = 4s$, where $x = [x_1 - 2; x_2 - 3]$.

We can see from Figure 10(b) that the control sequence is still bang-bang but the system needs two switches to steer the system to the origin.

It is clear from Figure 10(a) that the system is able to recover from the perturbation and reaches the target. In fact, the perturbation signal on the two states has made the

Figure 10: Example 1 with perturbation on two states.
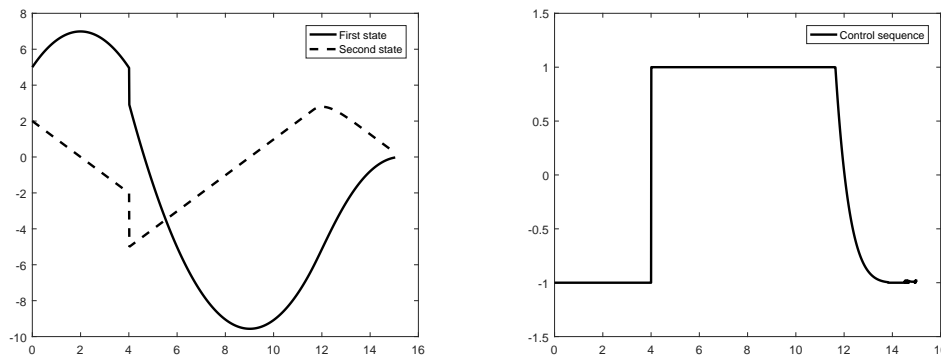
(a) System trajectory for the example 1 with perturbation on the two states.

(b) Control sequence for the example 1 with perturbation on the two states.

final time t_f bigger than the one without perturbation. Then the perturbation signal has a direct effect on the final time t_f.

6   Conclusion

In this paper, we focused on the problem of a minimum time control determination for linear systems in both cases of control structures: an open loop and a closed loop control. The key of the developed method is the approximation of the dynamic equation of the system under consideration using a complete basis of orthogonal functions and its operational properties. We have opted for the use of the piecewise orthogonal functions: block-pulse, Walsh and Haar wavelets. The results suggest that the proposed development yields a new formulation of the optimization problem which is simpler than those developed in the literature.

Other advantages of the proposed method include a better final time estimate and fewer switches for high order systems. The developed algorithm was also tested for a number of examples (i.e. SISO and MIMO systems), the results showed perfect agreement with the exact analytic results, which ensures the availability of the proposed technique. In the closed loop case, two algorithms were introduced to take into account the effects of perturbations on the system. They are: an offline algorithm which, compared to open loop results, has a great deterioration of results, and an online one which has a slight deterioration of performances even with perturbations.

In future work, we expect to generalize the proposed approach to the synthesis of minimum time control laws for nonlinear and fuzzy systems using state variable observation [20].

References

[1] L. S. Pontryagin, V. Boltyanskii, R. Gamkrelidze and E. Mischenko. *The Mathematical Theory of Optimal Processes.* Interscience Publishers, Inc. New York, 1962.

[2] L. Consolini and A. Piazzi. Generalized bang-bang control for feedforward constrained regulation. *Automatica* **45** (10) (2009) 2234–2243.

[3] R. Bulirsh, F. Montrone and H. T. Pesch. Abort landing in the presence of windshear as a minimax optimal control problem, part2: multiple shooting and homotopy. *Journal of optimization theory and applications* **70** (2) (1991) 1–23.

[4] Z. Shen, P. Huang and S. B. Andersson. Calculating switching times for the time-optimal control of single-input, single-output second-order systems. *Automatica* **49** (5) (2013) 1340–1347.

[5] B. M. Mohan and S. K. Kar. Continuous time dynamical systems state estimation and optimal control with orthogonal functions. *CRC Press*, 2012.

[6] K. B. Datta and B. M. Mohan. *Orthogonal Functions in Systems and Control.* World scientific, Singapore, 1995.

[7] M. K. Bouafoura, O. Moussi, and N. Benhadj Braiek. A fractional state space realization method with block pulse basis. *Signal Processing* **91** (3) (2011) 492–497.

[8] S. Piccagli and A. Visioli. Using a Chebyshev technique for solving the generalized bang-bang control problem. *46th IEEE Conference on Decision and Control.* New orleans, LA, December 2007, 4743–4748.

[9] M. Razzaghi and S. Yousefi. Sine-cosine wavelets operational matrix of integration and its applications in the calculus of variations. *J. Syst. Sci.* **33** (10) (2002) 805–810.

[10] S. Piccagli and A. Visioli. Using a Chebyshev approach for the minimum-time open-loop control for constrained MIMO systems. *International Conference on Control 2008 (UKACC)*, Manchester, UK, September 2008.

[11] S. Piccagli and A. Visioli. Minimum-time feedforward technique for PID control. *IET Control Theory and Applications* **3** (10) (2009) 1341–1350.

[12] D. E. Kirk. *Optimal Control Theory: An Introduction.* Dover Books on Electrical Engineering, 2012.

[13] E. R. Barnes. The Optimal Control of Hamiltonian Systems. *IBM Thomas J. Watson Research Division*, 1975.

[14] M. K. Bouafoura, P. Lanusse and N. Benhadj Braiek. State space modeling of fractional systems using Block-pulse fonction. In: *Proceedings of 15th IFAC Symposium on system Identification SYSID'2009.* St Malo, France, 6-8 July 2009.

[15] G. P. Rao and L. Sivakumar. Transfer function matrix identification in MIMO systems via Walsh functions. *IEEE Proc.* **69** (4) (1981) 465–466.

[16] B. M. Mohan and S. K. Kar. Orthogonal functions approach to optimal control of delay systems with reverse time terms. *Journal of the Franklin Institute* **347** (9) (2010) 1723–1739.

[17] J. L. Wu, C. H. Chen and C. F. Chen. A Unified Derivation of Operational Matrices for Integration in Systems Analysis. *International Symposium on Information Technology ITCC* Las Vegas, NV, USA, March 2000, 436–442.

[18] C. F. Chen, C. H. Hsiao. Design of piecewise constant gains for optimal control via Walsh functions. *IEEE Transactions on Automatic Control* **20** (5) (1975) 596–603.

[19] C. F. Chen and C. H. Hsiao. Haar wavelet method for solving lumped and distributed-parameter systems. *IEEE Proc. Control Theory Appl.* **144** (1) (1997) 87–94.

[20] A. Chibani, M. Chadli and N. Benhadj Braiek. A sum of squares approach for polynomial fuzzy observer design for polynomial fuzzy systems with unknown inputs. *International Journal of Control, Automation and Systems* **14** (1) (2016) 323–330.

Weakly Nonlinear Integral Equations
of the Hammerstein Type

A.A. Boichuk [1*], N.A. Kozlova [2] and V.A. Feruk [1]

[1] *Institute of Mathematics of the National Academy of Sciences of Ukraine,*
3, Tereshchenkivska Str., Kyiv, 01601, Ukraine
[2] *Taras Shevchenko National University of Kyiv,*
64/13, Volodymyrska Str., Kyiv, 01601, Ukraine

Abstract: By using the theory of Moore-Penrose pseudoinverse operators, the necessary and sufficient conditions for the solvability of a weakly nonlinear integral equation with a nondegenerate kernel are obtained. Equations for generating constants are constructed. A connection between the necessary and sufficient conditions has been established. The iterative procedure for finding a solution is proposed.

Keywords: *weakly nonlinear integral equations; Moore-Penrose pseudoinverse matrix; generating solution; equation for generating constants; iterative process.*

Mathematics Subject Classification (2010): 45B05, 45G10, 39B42.

1 Introduction

A lot of works are devoted to the investigation of different aspects of the theory of linear and nonlinear integral, differential and integro-differential equations [1, 2, 8–10, 12, 18, 19, 21]. A large part of such equations, in particular integral equations, belong to the equations with not everywhere invertible operator and arise in different areas of the natural science such as electrodynamics, mathematical physics, biology, economics and others [11, 22, 24]. The application of the theory of pseudoinverse operators enabled us to establish the conditions for the existence and the structure of solutions of such equations in the case where the kernel of integral equation is degenerate [5–7, 23, 25]. In the present paper, continuing the research mentioned above, we use one of possible approaches to finding the necessary and sufficient conditions for the solvability of weakly nonlinear integral equations with non-degenerate kernels and propose an algorithm for finding a solution. The obtained theoretical results can be used to study mathematical models and to create effective computational algorithms frequently encountered in applied research.

---

* Corresponding author: `mailto:boichuk.aa@gmail.com`

2   Statement of the Problem.

We consider the weakly nonlinear integral equation

$$x(t) - \int\limits_a^b K(t,s)x(s)ds = f(t) + \varepsilon \int\limits_a^b K_1(t,s)Z(x(s,\varepsilon),s,\varepsilon)ds. \qquad (1)$$

Our aim is to establish conditions for the existence of solution $x = x(t,\varepsilon)$: $x(\cdot,\varepsilon) \in L_2[a,b]$, $x(t,\cdot) \in C[0,\varepsilon_0]$, of equation (1), which turns into one of solutions $x_0(t,c_r)$ of the generating equation

$$x(t) - \int\limits_a^b K(t,s)x(s)ds = f(t) \qquad (2)$$

for $\varepsilon = 0$. In what follows, the solution $x_0(t,c_r)$ is called a generating solution of the nonlinear equation (1).

Here, $K(t,s)$, $K_1(t,s)$ are square-summable kernels in $[a,b] \times [a,b]$, $f \in L_2[a,b]$, $x \in L_2[a,b]$, $Z(x(t,\varepsilon),t,\varepsilon)$ is the function nonlinear with respect to the first component and such that

$$Z(\cdot,t,\varepsilon) \in C^1[\|x - x_0\| \le q], \quad Z(x(\cdot,\varepsilon),\cdot,\varepsilon) \in L_2[a,b], \quad Z(x(t,\cdot),t,\cdot) \in C[0,\varepsilon_0], \quad (3)$$

where q, ε_0 are sufficiently small constants, $\varepsilon << 1$ is a small parameter.

As in [17], equation (1) can be reduced to a countably dimensional system of weakly nonlinear algebraic equations. Let $\{\varphi_i(t)\}_{i=1}^{\infty}$ be a complete orthonormal system of functions in space $L_2[a,b]$. Let us introduce into consideration the following notations:

$$x_i(\varepsilon) = \int\limits_a^b x(t,\varepsilon)\varphi_i(t)dt, \quad f_i = \int\limits_a^b f(t)\varphi_i(t)dt, \qquad (4)$$

$$a_{ij} = \int\limits_a^b \int\limits_a^b K(t,s)\varphi_i(t)\varphi_j(s)dtds, \quad \tilde{a}_{ij} = \int\limits_a^b \int\limits_a^b K_1(t,s)\varphi_i(t)\varphi_j(s)dtds, \qquad (5)$$

$$m_i(\varepsilon) = m_i(x_1(\varepsilon), x_2(\varepsilon), \ldots, x_i(\varepsilon), \ldots, \varepsilon) = \int\limits_a^b Z(x(t,\varepsilon),t,\varepsilon)\varphi_i(t)dt. \qquad (6)$$

Then we pass from equation (1) to the countably dimensional system of weakly nonlinear algebraic equations

$$x_i(\varepsilon) - \sum_{j=1}^{\infty} a_{ij}x_j(\varepsilon) = f_i + \varepsilon \sum_{j=1}^{\infty} \tilde{a}_{ij}m_j(\varepsilon), \quad i = \overline{1,\infty}, \qquad (7)$$

$$\sum_{j=1}^{\infty} |x_j(\varepsilon)|^2 < +\infty, \quad \sum_{j=1}^{\infty} |m_j(\varepsilon)|^2 < +\infty, \quad \forall \varepsilon \in [0,\varepsilon_0].$$

We rewrite system (7) in the following vector form:

$$\Lambda z = g + \varepsilon \Lambda_1 V(z(\varepsilon),\varepsilon), \qquad (8)$$

where

$$z(\varepsilon) = col\left(x_1(\varepsilon), \quad x_2(\varepsilon), \quad \ldots, \quad x_i(\varepsilon), \quad \ldots \right) \in \ell_2,$$

$$g = col\left(f_1, \quad f_2, \quad \ldots, \quad f_i, \quad \ldots \right) \in \ell_2,$$

$$\Lambda = \begin{pmatrix} 1 - a_{11} & -a_{12} & \ldots & -a_{1i} & \ldots \\ -a_{21} & 1 - a_{22} & \ldots & -a_{2i} & \ldots \\ \ldots & \ldots & \ldots & \ldots & \ldots \\ -a_{i1} & -a_{i2} & \ldots & 1 - a_{ii} & \ldots \\ \ldots & \ldots & \ldots & \ldots & \ldots \end{pmatrix}, \ \Lambda_1 = \begin{pmatrix} \tilde{a}_{11} & \tilde{a}_{12} & \ldots & \tilde{a}_{1i} & \ldots \\ \tilde{a}_{21} & \tilde{a}_{22} & \ldots & \tilde{a}_{2i} & \ldots \\ \ldots & \ldots & \ldots & \ldots & \ldots \\ \tilde{a}_{i1} & \tilde{a}_{i2} & \ldots & \tilde{a}_{ii} & \ldots \\ \ldots & \ldots & \ldots & \ldots & \ldots \end{pmatrix},$$

$$V(z(\varepsilon), \varepsilon) = col\left(m_1(\varepsilon), \quad m_2(\varepsilon), \quad \ldots, \quad m_i(\varepsilon), \quad \ldots \right) \in \ell_2,$$

$$V(\cdot, \varepsilon) \in C^1[\|z - z_0\| \leq q], \quad V(z(\cdot), \cdot) \in C[0, \varepsilon_0].$$

The generating operator system for system (8) has the form

$$\Lambda z = g. \tag{9}$$

The following solvability condition is valid for system (9) [7, p. 57].

Theorem 2.1 *The homogeneous system (9) ($g = 0$) possesses an r-parameter family of solutions $z \in \ell_2$*

$$z(c_r) = P_{\Lambda_r} c_r, \quad \forall c_r \in \mathbb{R}^r.$$

The inhomogeneous system (9) is solvable if and only if r linearly independent conditions

$$P_{\Lambda_r^*} g = 0 \tag{10}$$

are satisfied. In this case, the inhomogeneous system (9) possesses an r-parameter family of solutions $z \in \ell_2$

$$z(c_r) = P_{\Lambda_r} c_r + \Lambda^+ g, \quad \forall c_r \in \mathbb{R}^r. \tag{11}$$

Here, P_{Λ_r} is a matrix composed of a complete system of r linearly independent columns of the matrix orthoprojector P_Λ, $P_{\Lambda_r^*}$ is the matrix composed of a complete system of r linearly independent rows of the matrix orthoprojector P_{Λ^*} and Λ^+ is the Moore–Penrose pseudoinverse matrix for the matrix Λ.

3   Necessary Condition for the Existence of Solution.

We now establish a necessary condition for the existence of solution $z(\varepsilon)$ of system (8), which turns into one of the generating solutions $z(c_r)$ of system (9) for $\varepsilon = 0$. The solvability condition of system (8) has the form

$$P_{\Lambda_r^*}(g + \varepsilon \Lambda_1 V(z(\varepsilon), \varepsilon)) = 0.$$

Taking into account (10), we obtain

$$P_{\Lambda_r^*} \Lambda_1 V(z(\varepsilon), \varepsilon) = 0. \tag{12}$$

Since $z(\varepsilon) \to z(c_r)$ as $\varepsilon \to 0$, by using the conditions imposed on the nonlinear function $V(z(\varepsilon), \varepsilon)$, we pass to the limit as $\varepsilon \to 0$ in (12) and obtain a necessary condition for the existence of solution of system (8)

$$P_{\Lambda_r^*} \Lambda_1 V(z(c_r), 0) = 0. \tag{13}$$

Thus, if system (13) has the root $c_r = c_r^0 \in R^r$, then c_r^0 specifies the generating solution $z(c_r^0)$, which may correspond to the solution $z(\varepsilon)$ of system (8). If system (13) has no solutions, then system (8) also does not have the required solution. Here, we speak about real solutions of system (13). We say that equation (13) is the equation for generating constants c_r^0 of the nonlinear system (8) [7]. The conditions of type (13) first emerged in the theory of periodic boundary-value problems for the systems of ordinary differential equations. In this case, the constants c_r have physical meaning: they are amplitudes of periodic solutions. Therefore, these equations are called the equations for generating amplitudes [3, 13, 20].

Theorem 3.1 *Assume that the weakly nonlinear system (8) possesses a solution $z(\varepsilon)$:*

$$z(\varepsilon) \in \ell_2, \quad z(\cdot) \in C[0, \varepsilon_0],$$

which turns into the generating solution (11) with constant $c_r = c_r^0 \in R^r$ for $\varepsilon = 0$. Then the vector of constants c_r^0 is necessarily a real root of the equation for generating constants (13).

4   Sufficient Condition for the Existence of Solution

To establish sufficient conditions for the existence of solution, we perform the following change of variables in system (8):

$$z(\varepsilon) = z(c_r^0) + y(\varepsilon),$$

where $z(c_r^0)$ is the generating solution, $c_r^0 \in R^r$ is a real root of equation (13).

We seek the conditions for the existence of a solution $y(\varepsilon)$,

$$y(\varepsilon) \in \ell_2, \quad y(\cdot) \in C[0, \varepsilon_0], \quad y(0) = 0,$$

of the following system

$$\Lambda y(\varepsilon) = \varepsilon \Lambda_1 V(z(c_r^0) + y(\varepsilon), \varepsilon). \tag{14}$$

By using the continuous differentiability of function $V(z, \varepsilon)$ with respect to z in the neighborhood of the generating solution, we separate the linear part in y and the zero-order terms with respect to ε of function $V(z(c_r^0) + y(\varepsilon), \varepsilon)$:

$$V(z(c_r^0) + y(\varepsilon), \varepsilon) = V(z_0(c_r^0), 0) + A_1 y(\varepsilon) + R(y(\varepsilon), \varepsilon), \tag{15}$$

where

$$V(z_0(c_r^0), 0) \in \ell_2, \quad A_1 = A_1(c_r^0) = \left. \frac{\partial V(z, 0)}{\partial z} \right|_{z=z(c_r^0)}, \quad R(y(\varepsilon), \varepsilon) \in \ell_2.$$

Here, we have

$$R(\cdot, \varepsilon) \in C^1(\|y\| \le q), \quad R(y(\cdot), \cdot) \in C[0, \varepsilon_0], \quad R(0, 0) = 0, \quad \frac{\partial R(0, 0)}{\partial y} = 0.$$

Thus, we consider the right-hand side of system (14) as an inhomogeneity. According to Theorem 2.1, system (14) has a solution

$$y(\varepsilon) = P_{\Lambda_r} c_r + \bar{y}(\varepsilon), \quad \forall c_r \in R^r, \tag{16}$$

$$\bar{y}(\varepsilon) = \varepsilon \Lambda^+ \Lambda_1 V(z(c_r^0) + y(\varepsilon), \varepsilon).$$

The solvability condition of system (14) takes the form

$$P_{\Lambda_r^*} \Lambda_1 V(z(c_r^0) + y(\varepsilon), \varepsilon) = 0. \tag{17}$$

We substitute expansion (15) in equality (17)

$$P_{\Lambda_r^*} \Lambda_1 (V(z_0(c_r^0), 0) + A_1 y(\varepsilon) + R(y(\varepsilon), \varepsilon)) = 0.$$

In view of equation (13) and representation (16), we obtain

$$B_0 c_r = -P_{\Lambda_r^*} \Lambda_1 (A_1 \bar{y}(\varepsilon) + R(y(\varepsilon), \varepsilon)), \tag{18}$$

where B_0 is the $(r \times r)$-dimensional matrix of the form

$$B_0 = P_{\Lambda_r^*} \Lambda_1 A_1 P_{\Lambda_r}. \tag{19}$$

The algebraic system (18) is solvable if and only if the following condition

$$P_{B_0^*} P_{\Lambda_r^*} \Lambda_1 (A_1 \bar{y}(\varepsilon) + R(y(\varepsilon), \varepsilon)) = 0 \tag{20}$$

is satisfied. If

$$P_{B_0^*} P_{\Lambda_r^*} \Lambda_1 = 0, \tag{21}$$

then equality (20) is always satisfied and system (18) possesses a solution.

Thus, we arrive at the following system of operator equations for finding the solution of system (14)

$$\begin{aligned} y(\varepsilon) &= P_{\Lambda_r} c_r(\varepsilon) + \bar{y}(\varepsilon), \\ c_r(\varepsilon) &= -B_0^+ P_{\Lambda_r^*} \Lambda_1 (A_1 \bar{y}(\varepsilon) + R(y(\varepsilon), \varepsilon)), \\ \bar{y}(\varepsilon) &= \varepsilon \Lambda^+ \Lambda_1 (V(z_0(c_r^0), 0) + A_1 (P_{\Lambda_r} c_r(\varepsilon) + \bar{y}(\varepsilon)) + R(y(\varepsilon), \varepsilon)). \end{aligned} \tag{22}$$

Introducing a new variable $u = col(y(\varepsilon), c_r(\varepsilon), \bar{y}(\varepsilon))$, we obtain the equation

$$u = Lu + Fu, \tag{23}$$

where

$$L = \begin{pmatrix} 0 & P_{\Lambda_r} & I \\ 0 & 0 & L_1 \\ 0 & 0 & 0 \end{pmatrix},$$

$$L_1 := -B_0^+ P_{\Lambda_r^*} \Lambda_1 A_1,$$

$$Fu := \begin{pmatrix} 0 \\ -B_0^+ P_{\Lambda_r^*} \Lambda_1 R(y(\varepsilon), \varepsilon) \\ \varepsilon \Lambda^+ \Lambda_1 (V(z_0(c_r^0), 0) + A_1 (P_{\Lambda_r} c_r(\varepsilon) + \bar{y}(\varepsilon)) + R(y(\varepsilon), \varepsilon)) \end{pmatrix}.$$

Since the quasitriangular block matrix operator $I - L$ always possesses the inverse operator, equation (23) can be rewritten in the form

$$u = Su, \quad S := (I - L)^{-1} F. \tag{24}$$

The operator equation (24) belongs to the class of equations, which are solved with the use of the method of simple iterations [4, 7, 13]. We obtain the following iterative process for system (22).

The first approximation $\bar{y}_1(\varepsilon)$ to the element $\bar{y}(\varepsilon)$ is obtained as a particular solution of the equation

$$\Lambda \bar{y}_1(\varepsilon) = \varepsilon \Lambda_1 V(z(c_r^0), 0).$$

This solution exists due to the choice of constant $c_r^0 \in R^r$ from the equation for generating constants (13) and has the form

$$\bar{y}_1(\varepsilon) = \varepsilon \Lambda^+ \Lambda_1 V(z(c_r^0), 0).$$

We set the first approximation $y_1(\varepsilon)$ to the solution $y(\varepsilon)$ of system (14) equal to $\bar{y}_1(\varepsilon)$:

$$y_1(\varepsilon) = \bar{y}_1(\varepsilon).$$

The second approximation $y_2(\varepsilon)$ to $y(\varepsilon)$ is obtained from the equation

$$\Lambda y_2(\varepsilon) = \varepsilon \Lambda_1 (V(z_0(c_r^0), 0) + A_1(P_{\Lambda_r} c_r^1(\varepsilon) + \bar{y}_1(\varepsilon)) + R(\bar{y}_1(\varepsilon), \varepsilon)). \tag{25}$$

Equation (25) is solvable if and only if the following condition

$$B_0 c_r^1(\varepsilon) = -P_{\Lambda_r^*} \Lambda_1 (A_1 \bar{y}_1(\varepsilon) + R(\bar{y}_1(\varepsilon), \varepsilon)) \tag{26}$$

is satisfied.

The solvability condition of equation (26) has the form

$$P_{B_0^*} P_{\Lambda_r^*} \Lambda_1 (A_1 \bar{y}_1(\varepsilon) + R(\bar{y}_1(\varepsilon), \varepsilon)) = 0. \tag{27}$$

Under condition (21), equality (27) is satisfied and the first approximation $c_r^1(\varepsilon)$ to the parameter $c_r(\varepsilon)$ is obtained from equation (26)

$$c_r^1(\varepsilon) = -B_0^+ P_{\Lambda_r^*} \Lambda_1 (A_1 \bar{y}_1(\varepsilon) + R(\bar{y}_1(\varepsilon), \varepsilon)).$$

The second approximation $y_2(\varepsilon)$ to $y(\varepsilon)$ has the form

$$y_2(\varepsilon) = P_{\Lambda_r} c_r^1(\varepsilon) + \bar{y}_2(\varepsilon),$$

where
$$\bar{y}_2(\varepsilon) = \varepsilon \Lambda^+ \Lambda_1 (V(z_0(c_r^0), 0) + A_1(P_{\Lambda_r} c_r^1(\varepsilon) + \bar{y}_1(\varepsilon)) + R(\bar{y}_1(\varepsilon), \varepsilon)).$$

The third approximation $y_3(\varepsilon)$ to $y(\varepsilon)$ is obtained from the equation

$$\Lambda y_3(\varepsilon) = \varepsilon \Lambda_1 (V(z_0(c_r^0), 0) + A_1(P_{\Lambda_r} c_r^2(\varepsilon) + \bar{y}_2(\varepsilon)) + R(y_2(\varepsilon), \varepsilon)). \tag{28}$$

Equation (28) is solvable if and only if the following condition

$$B_0 c_r^2(\varepsilon) = -P_{\Lambda_r^*} \Lambda_1 (A_1 \bar{y}_2(\varepsilon) + R(y_2(\varepsilon), \varepsilon)) \tag{29}$$

is satisfied.

The solvability condition of equation (29) has the form

$$P_{B_0^*} P_{\Lambda_r^*} \Lambda_1 (A_1 \bar{y}_2(\varepsilon) + R(y_2(\varepsilon), \varepsilon)) = 0. \tag{30}$$

Under condition (21), equality (30) is satisfied and the second approximation $c_r^2(\varepsilon)$ to the parameter $c_r(\varepsilon)$ is obtained from equation (29)

$$c_r^2(\varepsilon) = -B_0^+ P_{\Lambda_r^*} \Lambda_1 (A_1 \bar{y}_2(\varepsilon) + R(y_2(\varepsilon), \varepsilon)).$$

The third approximation $y_3(\varepsilon)$ to $y(\varepsilon)$ has the form

$$y_3(\varepsilon) = P_{\Lambda_r} c_r^2(\varepsilon) + \bar{y}_3(\varepsilon),$$

where

$$\bar{y}_3(\varepsilon) = \varepsilon \Lambda^+ \Lambda_1 (V(z_0(c_r^0), 0) + A_1(P_{\Lambda_r} c_r^2(\varepsilon) + \bar{y}_2(\varepsilon)) + R(y_2(\varepsilon), \varepsilon)).$$

Continuing the iterative process, we obtain the following procedure for finding $y(\varepsilon)$:

$$
\begin{aligned}
c_r^k(\varepsilon) &= -B_0^+ P_{\Lambda_r^*} \Lambda_1 (A_1 \bar{y}_k(\varepsilon) + R(y_k(\varepsilon), \varepsilon)), \\
\bar{y}_{k+1}(\varepsilon) &= \varepsilon \Lambda^+ \Lambda_1 (V(z_0(c_r^0), 0) + A_1(P_{\Lambda_r} c_r^k(\varepsilon) + \bar{y}_k(\varepsilon)) + R(y_k(\varepsilon), \varepsilon)), \\
y_{k+1}(\varepsilon) &= P_{\Lambda_r} c_r^k(\varepsilon) + \bar{y}_{k+1}(\varepsilon), \quad k = \overline{0, \infty}, \\
y_0(\varepsilon) &= \bar{y}_0(\varepsilon) = 0.
\end{aligned}
\tag{31}
$$

Hence, the following theorem is true.

Theorem 4.1 *Assume that, under r linearly independent conditions (10), the generating system (9) for system (8) possesses an r-parameter family of solutions $z(c_r) \in \ell_2$ (11). Then, for each real value of vector $c_r = c_r^0 \in R^r$ satisfying the equation for generating constants (13) and under the condition*

$$P_{B_0^*} P_{\Lambda_r^*} \Lambda_1 = 0,$$

system (8) possesses a solution $z(\varepsilon) \in \ell_2$ continuous in ε, which turns into the generating solution $z(c_r^0)$ for $\varepsilon = 0$. This solution can be found from the following iterative process:

$$c_r^k(\varepsilon) = -B_0^+ P_{\Lambda_r^*} \Lambda_1 (A_1 \bar{y}_k(\varepsilon) + R(y_k(\varepsilon), \varepsilon)),$$

$$\bar{y}_{k+1}(\varepsilon) = \varepsilon \Lambda^+ \Lambda_1 (V(z_0(c_r^0), 0) + A_1(P_{\Lambda_r} c_r^k(\varepsilon) + \bar{y}_k(\varepsilon)) + R(y_k(\varepsilon), \varepsilon)),$$

$$y_{k+1}(\varepsilon) = P_{\Lambda_r} c_r^k(\varepsilon) + \bar{y}_{k+1}(\varepsilon),$$

$$z_k(\varepsilon) = z(c_r^0) + y_k(\varepsilon), \quad k = \overline{0, \infty},$$

$$y_0(\varepsilon) = \bar{y}_0(\varepsilon) = 0.$$

By using the obtained results for a countably dimensional system of weakly nonlinear algebraic equations (8), we can make conclusions about the existence of solution of weakly nonlinear integral equation (1). We achieve this using the approach applied in [17].

Assume that system (8) possesses at least one solution $z(\varepsilon) = col\left(x_1(\varepsilon), \quad x_2(\varepsilon), \quad \dots, \quad x_i(\varepsilon), \quad \dots\right)$. According to the Riesz–Fischer theorem, $x_i(\varepsilon)$ are the Fourier coefficients for the element $x = x(t, \varepsilon)$: $x(\cdot, \varepsilon) \in L_2[a, b]$, $x(t, \cdot) \in C[0, \varepsilon_0]$. Thus, the following representation is true:

$$x(t, \varepsilon) = \sum_{i=1}^{\infty} x_i(\varepsilon) \varphi_i(t) = \Phi(t) z(\varepsilon), \tag{32}$$

where
$$\Phi(t) = \big(\varphi_1(t), \quad \varphi_2(t), \quad \ldots, \quad \varphi_i(t), \quad \ldots \big),$$

$\{\varphi_i(t)\}_{i=1}^{\infty}$ is a complete orthonormal system of functions in $L_2[a,b]$.

By analogy with [14, 15], we can conclude that the set of elements $x(t, \varepsilon)$, defined by the relation (32), is the required family of solutions of the original equation (1).

Hence, we can apply the results of Theorem 4.1 for system (8) to integral equation (1).

Theorem 4.2 *Assume that, under r linearly independent conditions (10), the generating equation (2) for equation (1) possesses an r-parameter family of solutions $x(t, c_r)$. Then, for each real value of vector $c_r = c_r^0 \in R^r$ satisfying the equation for generating constants (13) and under the condition*

$$P_{B_0^*} P_{\Lambda_r^*} \Lambda_1 = 0,$$

equation (1) possesses a solution $x = x(t, \varepsilon)$: $x(\cdot, \varepsilon) \in L_2[a,b]$, $x(t, \cdot) \in C[0, \varepsilon_0]$, which turns into the generating solution $x_0(t, c_r)$ for $\varepsilon = 0$. This solution can be found by using the convergent iterative process

$$
\begin{aligned}
c_r^k(\varepsilon) &= -B_0^+ P_{\Lambda_r^*} \Lambda_1 (A_1 \bar{y}_k(\varepsilon) + R(y_k(\varepsilon), \varepsilon)), \\
\bar{y}_{k+1}(\varepsilon) &= \varepsilon \Lambda^+ \Lambda_1 (V(z_0(c_r^0), 0) + A_1(P_{\Lambda_r} c_r^k(\varepsilon) + \bar{y}_k(\varepsilon)) + R(y_k(\varepsilon), \varepsilon)), \\
y_{k+1}(\varepsilon) &= P_{\Lambda_r} c_r^k(\varepsilon) + \bar{y}_{k+1}(\varepsilon), \\
z_k(\varepsilon) &= z(c_r^0) + y_k(\varepsilon), \\
x_k(t, \varepsilon) &= \Phi(t) z_k(\varepsilon), \quad k = \overline{0, \infty}, \\
y_0(\varepsilon) &= \bar{y}_0(\varepsilon) = 0.
\end{aligned}
\tag{33}
$$

Remark 4.1 If the condition $P_{B_0} = 0$ is satisfied, then, according to the Fredholm property of index zero of matrix B_0, we obtain $P_{B_0^*} = 0$ and condition (21) is automatically satisfied. In this case $det B_0 \neq 0$ and in the iterative process (33) instead of B_0^+ it will be B_0^{-1}.

Remark 4.2 In the case, where $K(t,s) = 0$, $f(t) = 0$, $\varepsilon = 1$, $K_1(t,s)$ is a piecewise continuous, symmetric, positive-definite kernel, the results introduced in this paper coincide with the results established in [14].

Example 4.1 To illustrate the proposed procedure for the analysis of integral equation of the form (1), we consider the integral equation

$$x(t) - \frac{2}{\pi} \int_0^\pi \sin(t+s) x(s) ds = \sin t - \cos t +$$

$$+ \varepsilon \int_0^\pi \cos t \sin s \left(\pi(2 - \varepsilon^2) - 4(2 + 3\varepsilon^2) x(s) + 3\pi\varepsilon x^2(s) \right) ds \tag{34}$$

and the generating equation

$$x(t) - \frac{2}{\pi} \int_0^\pi \sin(t+s) x(s) ds = \sin t - \cos t. \tag{35}$$

Let us consider the orthonormal functions $\varphi_1(t) = \frac{1}{\sqrt{\pi}}(\sin t + \cos t)$ and $\varphi_2(t) = \frac{1}{\sqrt{\pi}}(\sin t - \cos t)$, which are eigenfunctions of the operator

$$(Kw)(t) = \frac{2}{\pi} \int_0^\pi \sin(t+s)w(s)ds,$$

and correspond to the characteristic numbers $\lambda_1 = 1$ and $\lambda_2 = -1$, respectively.

We reduce equations (34) and (35) to equations (8) and (9). By using the introduced notation (4)-(6), we obtain

$$\Lambda z = g + \varepsilon\Lambda_1 V(z(\varepsilon), \varepsilon), \tag{36}$$

$$\Lambda z = g, \tag{37}$$

$$\Lambda = \begin{pmatrix} 0 & 0 \\ 0 & 2 \end{pmatrix}, \quad z = \begin{pmatrix} x_1 \\ x_2 \end{pmatrix}, \quad g = \begin{pmatrix} 0 \\ \sqrt{\pi} \end{pmatrix}, \quad \Lambda_1 = \frac{\pi}{4}\begin{pmatrix} 1 & 1 \\ -1 & -1 \end{pmatrix}, \tag{38}$$

$$x_1 = \frac{1}{\sqrt{\pi}} \int_0^\pi x(t)(\sin t + \cos t)dt, \quad x_2 = \frac{1}{\sqrt{\pi}} \int_0^\pi x(t)(\sin t - \cos t)dt,$$

$$V(z(\varepsilon), \varepsilon) = 2\sqrt{\pi}(2 - \varepsilon^2)\begin{pmatrix} 1 \\ 1 \end{pmatrix} - 4(2 + 3\varepsilon^2)\begin{pmatrix} x_1 \\ x_2 \end{pmatrix} + \frac{2\varepsilon}{\sqrt{\pi}}\begin{pmatrix} 5x_1^2 + 2x_1x_2 + x_2^2 \\ x_1^2 + 2x_1x_2 + 5x_2^2 \end{pmatrix}.$$

By using the well-known formulas [7, p. 48], [16, p. 501], we get

$$\Lambda^+ = \begin{pmatrix} 0 & 0 \\ 0 & \frac{1}{2} \end{pmatrix}, \quad P_\Lambda = P_{\Lambda^*} = \begin{pmatrix} 1 & 0 \\ 0 & 0 \end{pmatrix}. \tag{39}$$

Taking into account (38), (39), it is easy to see that the condition for the solvability (10) is satisfied in this case. According to Theorem 2.1, system (37) possesses a solution

$$z(c_r) = \begin{pmatrix} c_r \\ \frac{\sqrt{\pi}}{2} \end{pmatrix}, \quad \forall c_r \in R,$$

and equation (35) has a solution

$$x(t, c_r) = \left(\frac{c_r}{\sqrt{\pi}} + \frac{1}{2}\right)\sin t + \left(\frac{c_r}{\sqrt{\pi}} - \frac{1}{2}\right)\cos t. \tag{40}$$

In the case, the necessary condition for the existence of a solution $z(\varepsilon)$ of system (36), which turns into one of the generating solutions $z(c_r)$ of system (37) for $\varepsilon = 0$, takes the form

$$P_{\Lambda_r^*}\Lambda_1 V(z(c_r), 0) = \frac{\pi}{4}\begin{pmatrix} 1 & 0 \end{pmatrix}\begin{pmatrix} 1 & 1 \\ -1 & -1 \end{pmatrix}\begin{pmatrix} m_1(0) \\ m_2(0) \end{pmatrix} =$$

$$= \frac{\pi}{4}(m_1(0) + m_2(0)) = 2\pi\left(\frac{\sqrt{\pi}}{2} - c_r\right) = 0. \tag{41}$$

Equation (41) possesses the unique solution $c_r^0 = \frac{\sqrt{\pi}}{2}$ that specifies the generating solution $z(c_r^0)$, which may correspond to the solution $z(\varepsilon)$ of system (36).

We now establish a sufficient condition for the existence of a solution of system (36). For this purpose, we perform the following change of variables:

$$z(\varepsilon) := z(c_r^0) + y(\varepsilon), \tag{42}$$

where

$$z(c_r^0) = \frac{\sqrt{\pi}}{2}\begin{pmatrix} 1 \\ 1 \end{pmatrix} \tag{43}$$

is the generating solution of system (36).

System (14) for definition $y(\varepsilon)$ takes the form

$$\Lambda y(\varepsilon) = \varepsilon \Lambda_1 V(z(c_r^0) + y(\varepsilon), \varepsilon), \tag{44}$$

where the matrices Λ, Λ_1 have the form (38) and

$$V(z(c_r^0) + y(\varepsilon), \varepsilon) = 4\sqrt{\pi}(\varepsilon - 2\varepsilon^2)\begin{pmatrix} 1 \\ 1 \end{pmatrix} -$$

$$-4\begin{pmatrix} 3\varepsilon^2 - 3\varepsilon + 2 & -\varepsilon \\ -\varepsilon & 3\varepsilon^2 - 3\varepsilon + 2 \end{pmatrix}\begin{pmatrix} y_1(\varepsilon) \\ y_2(\varepsilon) \end{pmatrix} + \frac{2\varepsilon}{\sqrt{\pi}}\begin{pmatrix} (y_1(\varepsilon) + y_2(\varepsilon))^2 + 4y_1^2(\varepsilon) \\ (y_1(\varepsilon) + y_2(\varepsilon))^2 + 4y_2^2(\varepsilon) \end{pmatrix}.$$

That is, in this case

$$V(z_0(c_r^0), 0) = 0, \quad A_1 = -8\begin{pmatrix} 1 & 0 \\ 0 & 1 \end{pmatrix}, \tag{45}$$

$$R(y(\varepsilon), \varepsilon) = 4\sqrt{\pi}(\varepsilon - 2\varepsilon^2)\begin{pmatrix} 1 \\ 1 \end{pmatrix} +$$

$$+4\varepsilon\begin{pmatrix} 3 - 3\varepsilon & 1 \\ 1 & 3 - 3\varepsilon \end{pmatrix}\begin{pmatrix} y_1(\varepsilon) \\ y_2(\varepsilon) \end{pmatrix} + \frac{2\varepsilon}{\sqrt{\pi}}\begin{pmatrix} (y_1(\varepsilon) + y_2(\varepsilon))^2 + 4y_1^2(\varepsilon) \\ (y_1(\varepsilon) + y_2(\varepsilon))^2 + 4y_2^2(\varepsilon) \end{pmatrix}.$$

According to (19), (38), (39), (45), we obtain

$$B_0 = P_{\Lambda_r^*}\Lambda_1 A_1 P_{\Lambda_r} = -2\pi \begin{pmatrix} 1 & 0 \end{pmatrix}\begin{pmatrix} 1 & 1 \\ -1 & -1 \end{pmatrix}\begin{pmatrix} 1 & 0 \\ 0 & 1 \end{pmatrix}\begin{pmatrix} 1 \\ 0 \end{pmatrix} = -2\pi.$$

Thus,

$$B_0^+ = B_0^{-1} = -\frac{1}{2\pi}, \quad P_{B_0} = P_{B_0^*} = 0$$

and sufficient condition (21) for the existence of solution of system (36) is satisfied.

After appropriate calculations, we obtain that under condition (21), system (44) is equivalent to the system

$$c_r(\varepsilon) = \sqrt{\pi}(\varepsilon - 2\varepsilon^2) + \frac{1}{2}(4\varepsilon - 3\varepsilon^2)y_1(\varepsilon) + \frac{3\varepsilon}{2\sqrt{\pi}}(y_1(\varepsilon))^2,$$

$$\bar{y}_1(\varepsilon) = \bar{y}_2(\varepsilon) = y_2(\varepsilon) = 0, \quad y_1(\varepsilon) = c_r(\varepsilon). \tag{46}$$

In this case, algorithm (31) takes the form

$$c_r^k(\varepsilon) = \sqrt{\pi}(\varepsilon - 2\varepsilon^2) + \frac{1}{2}(4\varepsilon - 3\varepsilon^2)y_1^k(\varepsilon) + \frac{3\varepsilon}{2\sqrt{\pi}}(y_1^k(\varepsilon))^2,$$

$$\bar{y}_1^{k+1}(\varepsilon) = \bar{y}_2^{k+1}(\varepsilon) = y_2^{k+1}(\varepsilon) = 0, \quad y_1^{k+1}(\varepsilon) = c_r^k(\varepsilon), \quad k = \overline{0, \infty}, \tag{47}$$

$$y_1^0(\varepsilon) = y_2^0(\varepsilon) = \bar{y}_1^0(\varepsilon) = \bar{y}_2^0(\varepsilon) = 0.$$

Convergence of the method of simple iterations (47) can be estimated by the method of Lyapunov majorants [3, 13]. The majorizing system for system (46) takes the form

$$v = U(v, \varepsilon) = \sqrt{\pi}(\varepsilon - 2\varepsilon^2) + \frac{1}{2}(4\varepsilon - 3\varepsilon^2)v + \frac{3\varepsilon}{2\sqrt{\pi}}v^2,$$

$$\bar{u}_1 = \bar{u}_2 = u_2 = 0, \quad u_1 = v.$$

To estimate the range of convergence for ε of the iterative process (47), we construct the system

$$v = U(v, \varepsilon), \quad 1 - \frac{\partial U}{\partial v} = 0.$$

This system possesses a real positive solution

$$\varepsilon^* = -\frac{1}{3}(2 - \sqrt{10}) \approx 0,3874, \quad v^* = -\frac{\sqrt{\pi}}{3}(2 - \sqrt{10}) \approx 0,6867.$$

Hence, system (36) has a solution $z(\varepsilon)$ in a neighborhood of $\varepsilon = 0$, which turns into the generating solution $z(c_r^0)$ for $\varepsilon = 0$. This solution can be found by the use of iterative process (47) convergent for $\varepsilon \in [0, \varepsilon^*]$ and equality (42).

We construct the first few approximations of the iterative process by scheme (47)

$$y_1^1(\varepsilon) = 0,$$
$$y_1^2(\varepsilon) = \sqrt{\pi}(\varepsilon - 2\varepsilon^2),$$
$$y_1^3(\varepsilon) = \sqrt{\pi}(\varepsilon - 4\varepsilon^3 - 3\varepsilon^4 + 6\varepsilon^5), \tag{48}$$

$$y_1^4(\varepsilon) = \frac{\sqrt{\pi}}{2}(2\varepsilon - 16\varepsilon^4 - 24\varepsilon^5 + 15\varepsilon^6 + 66\varepsilon^7 + 72\varepsilon^8 - 117\varepsilon^9 - 108\varepsilon^{10} + 108\varepsilon^{11}).$$

As we see, the constructed approximate solutions in the neighborhood of $\varepsilon = 0$ lead to the vector

$$y^*(\varepsilon) = \begin{pmatrix} \sqrt{\pi}\varepsilon \\ 0 \end{pmatrix}. \tag{49}$$

One can easily verify by substitution that this vector is a solution of equation (44). Deviation of approximations (48) from the exact solution (49) is represented in the table.

Table 1: Approximation accuracy constructed by the method of simple iteration (47)

ε	$|y_1^*(\varepsilon) - y_1^1(\varepsilon)|$	$|y_1^*(\varepsilon) - y_1^2(\varepsilon)|$	$|y_1^*(\varepsilon) - y_1^3(\varepsilon)|$	$|y_1^*(\varepsilon) - y_1^4(\varepsilon)|$
0,3874	0,686648	0,532015	0,439177	0,375906
0,3000	0,531736	0,319042	0,208653	0,142307
0,2000	0,354491	0,141796	0,061823	0,027792
0,1000	0,177245	0,035449	0,007515	0,001611
0,0100	0,017725	0,000354	0,000007	0,000000

Thus, according to (42) and (49), the solution $z^*(\varepsilon)$ of system (36), which turns, for $\varepsilon = 0$, into the generating solution (43) of system (37), has the form

$$z^*(\varepsilon) = \frac{\sqrt{\pi}}{2} \begin{pmatrix} 1 + 2\varepsilon \\ 1 \end{pmatrix}.$$

And, according to Theorem 4.2, the solution of equation (34) takes the form

$$x(t) = (\varepsilon + 1)\sin t + \varepsilon \cos t. \tag{50}$$

It is easy to see that solution (50) is transformed, for $\varepsilon = 0$, into the generating solution (40) with a constant $c_r^0 = \frac{\sqrt{\pi}}{2}$. The constant $c_r^0 = \frac{\sqrt{\pi}}{2}$ is the root of the equation for generating constants (41).

5 Conclusion

We considered the weakly nonlinear integral equation of the Hammerstein type in space $L_2[a, b]$ with a parameter. The problem of existence and construction of solutions, which turn into one of solutions of the generating equation for zero value of the parameter, is investigated. The equation for generating constants is obtained and it is shown that for the existence of the required solution it is necessary that this equation possesses at least one real root. Sufficient conditions for the existence of such a solution are obtained and a constructive algorithm for its finding is proposed. An illustrative example is given. The obtained results are also valid for the case of weakly nonlinear Fredholm boundary-value problems for integral equations.

References

[1] J. Appell and T.D. Benavides. Nonlinear Hammerstein equations and functions of bounded Riesz–Medvedev variation. *Topological Methods in Nonlinear Analysis* **47** (2016) 319–332.

[2] K.E. Atkinson. *The Numerical Solution of Integral Equations of the Second Kind.* Cambridge: Cambridge University Press, 1997.

[3] A.A. Boichuk. *Constructive Methods for the Analysis of Boundary-Value Problems.* Kiev: Naukova Dumka, 1990. [Russian]

[4] A. Boichuk, J. Diblik, D. Khusainov and M. Ruzickova. Boundary-value problems for weakly nonlinear delay differential system. *Abstr. Appl. Anal.* **2011** (2011) 19 p.

[5] A.A. Boichuk and I.A. Holovats'ka. Weakly nonlinear systems of integrodifferential equations. *Nelin. Kolyvannya* **16** (3) (2013) 314–321. [Ukrainian]; English translation: Weakly nonlinear systems of integrodifferential equations. *Journal of Mathematical Sciences* **201** (3) (2014) 288–295.

[6] A.A. Boichuk and A.M. Samoilenko. *Generalized Inverse Operators and Fredholm Boundary-Value Problems.* Utrecht: VSP, 2004.

[7] A.A. Boichuk and A.M. Samoilenko. *Generalized Inverse Operators and Fredholm Boundary-Value Problems.* 2nd edition, Inverse and Ill-Posed Problems Series 59. Berlin: De Gruyter, 2016.

[8] A.A. Boichuk and V.F. Zhuravlev. Solvability Criterion for Integro-Differential Equations with Degenerate Kernel in Banach Spaces *Nonlinear Dynamics and Systems Theory* **18** (4) (2018) 331-341.

[9] T.A. Burton and B. Zhang. A NASC for Equicontinuous Maps for Integral Equations *Nonlinear Dynamics and Systems Theory* **17** (3) (2017) 247-265.

[10] A. Cabada, J.A. Cid and G. Infante. A positive fixed point theorem with applications to systems of Hammerstein integral equations. *Boundary Value Problems* **2014** (2014).

[11] O. Diekmann. Thresholds and traveling for the geographical spread of infection. *J. Math. Biol.* **6** (2) (1978) 109-130.

[12] Z. Gouyandeh, T. Allahviranloo and A. Armand. Numerical solution of nonlinear Volterra–Fredholm–Hammerstein integral equations via Tau–collocation method with convergence analysis. *Journal of Computational and Applied Mathematics* **308** (2016) 435–446.

[13] E.A. Grebennikov and Yu.A. Ryabov. *Constructive Methods for the Analysis of Nonlinear Systems.* Moscow: Nauka, 1979. [Russian]

[14] A. Hammerstein. Nichtlineare Integralgleichungen nebst Anwendungen. *Acta Math.* **54** (1930) 117–176.

[15] D. Hilbert. *Selected Papers., vol. 2.* Moscow: Factorial, 1998. [Russian]

[16] R. Horn and Ch. Johnson. *Matrix Analysis.* Moscow: Mir, 1989. [Russian]

[17] N.O. Kozlova and V.A. Feruk. Noetherian boundary-value problems for integral equations. *Nelin. Kolyvannya* **19** (1) (2016) 58–66. [Ukrainian]; English translation: Noetherian boundary-value problems for integral equations. *Journal of Mathematical Sciences* **222** (3) (2016) 266–275.

[18] T.A. Lukyanova and A.A. Martynyuk. Stability Analysis of Impulsive Hopfield-Type Neuron System on Time Scale *Nonlinear Dynamics and Systems Theory* **17** (3) (2017) 315-326.

[19] K. Maleknejad, E. Hashemizadeh and B. Basirat. Computational method based on Bernstein operational matrices for nonlinear Volterra–Fredholm–Hammerstein integral equations. *Communications in Nonlinear Science and Numerical Simulation* **17** (2012) 52–61.

[20] I.G. Malkin. *Some Problems in the Theory of Nonlinear Oscillations.* Moscow: Gostekhizdat, 1956. [Russian]

[21] A.A. Martynyuk, D.Ya. Khusainov and V.A. Chernienko. Integral estimates of solutions to nonlinear systems and their applications *Nonlinear Dynamics and Systems Theory* **16** (1) (2016) 1-11.

[22] P.K. Sahu and Ray S. Saha. Comparative experiment on the numerical solutions of Hammerstein integral equation arising from chemical phenomenon. *Journal of Computational and Applied Mathematics* **291** (2016) 402-409.

[23] A.M. Samoilenko, A.A. Boichuk and S.A. Krivosheya. Boundary-value problem for linear systems of integro-differential equations with degenerate kernel. *Ukr. Mat. Zh.* **48** (11) (1996) 1576–1579. [Ukrainian]; English translation: Boundary-value problems for systems of integro-differential equations with degenerate kernel. *Ukr. Math. J.* **48** (11) (1996) 1785–1789.

[24] I.S. Sokolnikoff. *Mathematical Theory of Elasticity.* 2nd edition. New York-Toronto-London: McGraw-Hill Book Company, Inc., 1956.

[25] V.F. Zhuravlev. Boundary-value problems for integral equations with degenerate kernel. *Nelin. Kolyvannya* **15** (1) (2012) 36–54. [Russian]; English translation: Boundary-value problems for integral equations with degenerate kernel. *Journal of Mathematical Sciences* **187** (4) (2012) 413–431.

Particle Distributions in Nucleation Lattice Models:
A Matrix Approach

O. Gutiérrez *

Universidad Autnoma de Barcelona – Campus de Bellaterra – 08193 Spain

Abstract: In this paper we use a matrix approach to investigate the distribution of particles in nucleation coalescence models with discrete lattices, both in the irreversible coagulation case and in the reversible one. In the irreversible case $(A + A \to A)$, the evolution of the particle distribution is described by means of a simple recursive procedure. In two particular cases the model is analytically solvable: with high density and particles that always fuse into one, and in the case of constant density. In the reversible case $(A + A \rightleftharpoons A)$ offspring production is allowed, and the system can reach a stationary distribution, which is jointly calculated with the equilibrium density. The particular case, in which meeting particles react with probability one, admits an exact solution.

Keywords: *coalescence models; Markov chain; exponential matrix; Poisson distribution; phase transition.*

Mathematics Subject Classification (2010): 82Cxx, 15A16, 15A18, 60J10.

1 Introduction

In the last decades, diffusion-controlled coalescence processes have attracted much research interest [1], [2], [3], [4], [5], [6] (see [7] and [8] for literature reviews). The models of these processes are applied to the analysis of phenomena involving particles in a solid, chemical species which randomly hop and react with adjacent ones, or non-equilibrium processes ranging from fluorescence to explosions. This kind of models is increasingly being used in biology, chemistry, genetics, sociology or finance, see [9], [10], [11] and [12], in which variations of the Ising model are used. We apply a simple matrix approach to the analysis of one-dimension coalescence models that usually require sophisticated mathematical tools (or Monte-Carlo simulations) to be solved.

---

* Corresponding author: `mailto:oscar.gutierrez@uab.es`

In one-dimension diffusion-limited reactions, the reaction time is much shorter than the diffusion time, so it is often assumed to be instantaneous. The physical system has a high number of particles, which can nucleate, and the distances between particles in a nucleus are negligible if compared to the distances between nuclei, which do not interact. The attractive interaction between particles is small, so the particles can diffuse into neighbor regions. Lastly, the energy of nucleated particles is very small, so reactions among the particles are neglected. Then, it is sensible to model the physical system by means of a discrete lattice where separate cells (sites) contain an integer number of particles. Two different situations can be considered: (i) In the case of irreversible coagulation, $A + A \to A$, the particle input is not allowed and particles diffuse until two of them meet and fuse (or not) into one. The fusion happens with some probability k, which reflects the fact that reactions are not necessarily instantaneous ($k = 1$ means that the reaction occurs instantaneously). (ii) If the back reaction is possible, particles can give birth to another particle (offspring production, $A \to A + A$). In the reversible coalescence process, $A + A \rightleftharpoons A$, the system can reach an equilibrium state, often characterized by the existence of a phase transition. Some well-known results in low-dimension diffusion-limited reaction models are: (i) the mean-field approximation for reaction kinetics breaks down (in the mean-field approximation, the particle density goes with the inverse of time, $\rho \sim t^{-1}$, a dependence derived from the dynamics equation $d\rho/dt \propto \rho^2$); (ii) in the irreversible case (coagulation), the system is temporarily described by the classical limit; but in the long-time regime, when the mean distance between particles is very large, it follows a diffusion limited decay, with $\rho \sim t^{-1/2}$; (iii) the one-dimensional single-species reversible reaction, $A + A \rightleftharpoons A$, is characterized by a second-order phase transition.

In this paper we use a one-dimensional discrete model to derive the particle distribution in two nucleation models: the irreversible coalescence model, and the reversible model with back reaction. J. C. Lin [3] also uses a discrete formalism, but centers his attention on the time-dependent probability that an interval with n sites is empty at time t, and Doering and Ben-Avraham [2] use the same interparticle distribution function in continuous formalism. Instead of analyzing the interparticle distribution as in [2] and [3], we propose a simple matrix approach to calculate the occupation probabilities and the particle density. The method offers a description of the system where the particle distribution can be obtained, valid whenever the particle density is not too low. This is so since we implicitly neglect spatial correlations (so, in particular, the occupation numbers in adjacent sites are uncorrelated). In the irreversible case, in which the number of particles never increases, we describe the occupation dynamics (which represents a non-equilibrium state unless $k = 0$). In the two particular cases of high density with $k = 1$, and non-reacting particles ($k = 0$, the number of particles does not vary) the steady state distribution is given in closed-form. In the reversible case, the particle input is allowed, we describe the stationary distribution. In the particular case, where particles always react ($k = 1$), the model is solved in closed-form. The appearance of a phase transition is predicted.

A matrix approach to systems of interacting particles with random dynamics is already used in [13], but applied to different phenomena (the authors analyze the one-dimensional fully asymmetric exclusion model, where the particles hop in a preferred direction with hard core interactions). J.M. Cushing [14] also applies a matrix approach to analyze a bifurcation phenomenon for a class of nonlinear matrix models, describing the evolutionary dynamics of a structured population.

Section 2 presents a simple coalescence model where the particle input is forbidden, so

the number of particles cannot increase. We analytically show some results derived in [15] by means of Monte-Carlo simulations. In Section 3, the particle input is allowed. The equilibrium distribution is obtained, and the appearance of a dynamic phase transition is analyzed. Section 4 summarizes the paper results and concludes.

2 Irreversible Coagulation: $A + A \to A$

Consider a system with N identical particles located in a lattice containing L identical sites. The initial distribution can be approximated by a Poisson one with the parameter $\rho = N/L$. The choice is natural: if each particle initially occupies a site chosen at random, the occupation number (the random number of particles in an arbitrary site) follows a binomial distribution, which tends to the Poisson one as N and L tend to $+\infty$. Particles leap from one site to an adjacent one. Then, the reaction can take place (with probability k) or not, which reflects that reactions are not instantaneous. If the reaction takes place, the number of particles in the system decreases by one unity; the occupation number in the former site of the leaping particle is one unit less; and the site, where the particle leaps, has the same occupation number since the reaction takes place and one particle disappears. If the reaction does not take place, the particle just changes its location, so the number of particles in the system remains the same. The model is more complex than the hard-core model, where sites can be occupied by only one particle, see [15]. [8] offers a simple explanation of why a particle in a many-particle quantum system can behave as a classical object that occasionally hops from one lattice cell to another.

The interval of time between two leaps is assumed to be the inverse of the number of particles: $\delta t = 1/N(t)$. We center our attention on the number of particles in a representative site, and calculate the transition probabilities associated to the representative site. The transition probabilities are put in an infinite matrix that resembles a Markov chain matrix (see the matrix below). However, probabilities depend on time since N varies with time, so we must notice that, strictly speaking, it is not a Markov chain unless $k = 0$ (N remains then constant). In spite of this limitation, we use the Markov chain formalism to describe the particle distributions in discrete one-dimensional coagulation systems. The transition matrix at time t is

$$M \equiv (M_i^j)_{i,j=0,1,2,\dots,N} = (I_i^j)_{i,j=0,1,2,\dots,N} + (A_i^j)_{i,j=0,1,2,\dots,N} \tag{1}$$

with $(I_i^j)_{i,j=0,1,2,\dots,N}$ being the identity matrix and $(A_i^j)_{i,j=0,1,2,\dots,N}=$

$$= \begin{pmatrix} -\frac{1}{L} & \frac{1}{L} & 0 & 0 & 0 & \dots \\ \frac{1}{N} & -\frac{1}{N} - \frac{1}{L}(1-k) & \frac{1}{L}(1-k) & 0 & 0 & \dots \\ 0 & \frac{2}{N} & -\frac{2}{N} - \frac{1}{L}(1-k) & \frac{1}{L}(1-k) & 0 & \dots \\ 0 & 0 & \frac{3}{N} & -\frac{3}{N} - \frac{1}{L}(1-k) & \frac{1}{L}(1-k) & \dots \\ 0 & 0 & 0 & \frac{4}{N} & -\frac{4}{N} - \frac{1}{L}(1-k) & \dots \\ \vdots & \vdots & \vdots & \vdots & \vdots & \vdots \end{pmatrix}.$$

Stricto sensu, matrix M has finite dimension. However, given that the number of particles is very large, matrix M can be thought of as defined in $\mathbb{R}^N$ with $N \to +\infty$, a vector space of infinite dimension, and the particle distribution can be taken as a Poisson one. The master equation of the system can be obtained from the transition matrix (1).

As in any stochastic matrix, the sum of elements in a row is equal to one. We observe that transitions can only occur to adjacent sites; the transition matrix is then *systolic*, like all the transition matrices in the paper. The probability that a site with $j (\geq 1)$ particles turns to be occupied by $j+1$ particles when the system contains $N(t)$ particles is equal to $P_{j \to j+1} \equiv M_j^{j+1} = (1/L)(1-k)$, independently of N, while the probability of remaining with j particles is $P_{j \to j} \equiv M_j^j = 1 - j/N - (1/L)(1-k)$. Next, we explain how the diagonal element (j, j) in matrix M (with $j \geq 1$) is obtained. Let us look at the adjacent elements: on the one hand, if the representative site has j particles at time t, the element $(j, j-1)$ in matrix M, denoted by M_j^{j-1}, which represents the probability associated to the event "the site will have $j-1$ particles at $t + \delta t$", is equal to j/N; this means that one of the j particles in the site is the one which hops between t and $t + \delta t$. On the other hand, the site can be occupied by $j+1$ particles after the next hop. Taking into account that a particle can hop from any adjacent site, and that a particular particle hops with probability $1/N$, the probability that an additional particle will occupy the site considered is $M_j^{j+1} = \frac{1-k}{N}[0.5\sum_{j=1}^N jP(j) + 0.5\sum_{j=1}^N jP(j)] = \frac{1-k}{N}\rho = \frac{1-k}{L}$. Consequently, for $j \geq 1$, the element (j, j) in M must be $M_j^j = 1 - j/N - (1/L)(1-k)$.

By means of the transition matrix M in (1) we obtain the evolution of the particle distribution, from which we calculate the particle density: the product of the initial distribution (a vector) by the time-dependent matrices (written in terms of $N(t)$) gives us the particle distribution across time (a vector), and its scalar product with vector (0,1,2,3,...) gives us the particle density $\rho(t) = \sum_{j=1}^N jP(j)$, which changes with time. The distributions are written in terms of N (or, alternatively, ρ), and are readily obtained by a simple recursive procedure. The evolution of the density and particle distribution can be explicitly written in terms of time by using the fact that $\delta N(t) = -k((1 - P(0))$ and $\delta t = 1/N(t)$. The method works when the particle density is not very low. In the long-time regime, however, the mean distance between particles is very large, so the occupation numbers are low and not independent of the occupation numbers of adjacent sites. So, correlations between the number of particles in adjacent sites are not negligible, which is confirmed by the well-known dynamics corresponding to the long-term regime, see [15], [16]. Consequently, the method proposed does not work in the long-run and in general with very low densities.

The numerical experiments performed by implementing the recursive method based on matrix M show that the time-dependent particle distribution quickly departs from the initial Poisson distribution (unless the reaction constant k is very low). In particular, the proportion of empty sites, $P(0)$, is well below the Poisson probability, while $P(j \geq 1)$ can be greater or lower than its Poisson counterpart, depending on the particular values of k, ρ and j. Let us check it for the two first probabilities. Recall that the first three probabilities of a Poisson distribution are: $P_{POI}(0) = e^{-\rho}$, $P_{POI}(1) = \rho e^{-\rho}$, $P_{POI}(2) = \rho^2 e^{-\rho}/2!$. Let us denote by $P(j|X)$ the probability that the representative cell has j particles when the system has X particles. If the system initially contains N particles, after the first iteration the probability of null occupation remains unchanged, $P(0|N - \delta N) = P_{POI}(0|N)$. However, in expectation the number of particles has decreased (from N to $N - \delta N$), so the density has also decreased (in expectation). This implies that the Poisson distribution overestimates the true probability of null occupation (so, there are more occupied cells actually than the Poisson pattern establishes). For $P(1)$, however, we obtain $P(1|N - \delta N) = P_{POI}(1|N) + k\rho e^{-\rho}/L$, so in this case the true probability $P(1|N - \delta N)$ can be above or below the Poisson one, $P_{POI}(1|N - \delta N)$ (observe that $\rho e^{-\rho}$ is not a monotone function of ρ). In general, the deviation of $P(j \geq 1)$

from the Poisson case has not a definite sign. For a typical parameter configuration, k=0.5, $L = 10^5$ and $N(0) = 3L$, for $\rho = 1.5$ we obtain $P(0)$=0.179, $P(1)$=0.391 and $P_{POI}(0)$=0.223, $P_{POI}(1)$=0.335, in concordance with the explanation above. These results are in excellent agreement with the Monte-Carlo simulations of Figs. 1 and 2 in [15].

   In two particular cases the particle distribution admits a closed-form solution.

Case 1: $\rho \gg 1$ and $k = 1$: density is high and particles always react fusing into one. Next, we show that the particle distribution obeys a Poisson distribution as long as density remains high (say, above 5). Obviously, in the distant future, inequality $\rho \gg 1$ will not hold since the number of particles decreases with time, and the approximation then fails. The proof resembles that in [17], where in a different context the authors first calculate the infinitesimal generator of the transition, and then derive the equilibrium condition of the system and the steady-state probability distribution. Condition $\rho \gg 1$ implies $P(0) \approx 0$, so N diminishes in one unity every time step with probability close to one (recall that $k = 1$), and the transition probability $P_{0\to 1}$ can be neglected. Then, the transition matrix M reduces to

$$M = (I_i^j) + \frac{1}{N} \begin{pmatrix} 0 & 0 & 0 & 0 & 0 & ... \\ 1 & -1 & 0 & 0 & 0 & ... \\ 0 & 2 & -2 & 0 & 0 & ... \\ 0 & 0 & 3 & -3 & 0 & ... \\ 0 & 0 & 0 & 4 & -4 & ... \\ \vdots & \vdots & \vdots & \vdots & \vdots & \vdots \end{pmatrix}, \text{ so the transition matrix can be ex-}$$

pressed as $M = I + G\delta t$, with I being the identity matrix, G being the infinitesimal generator of the transition, and $1/N = \delta t$ being the time step. Next, we calculate the exponential matrix $\exp(GT)$. It corresponds to the finite transformation corresponding to the time interval T, and gives the solution to the Kolmogorov forward equation when applied to the initial distribution vector. Time T is the sum of incremental time intervals: $T = \sum \delta t = \sum_{N=N(0)}^{N(T)} 1/N \approx \int_{N(0)}^{N(T)} (1/x)dx = \ln(N(0)/N(T))$. The matrix $\exp(GT)$ is calculated by diagonalizing G, which can be expressed as $G = PDP^{-1}$, where D represents the diagonal matrix constructed with the eigenvalues of G, D=diag $(0, -1, -2, -3, ...)$, and P is constructed with the eigenvectors of G. The eigenvectors form a basis under which G becomes diagonal and are obtained (up to constants) by solving a system of linear equations, whose solution gives us a possible choice for matrix P. We choose the basis written in terms of the binomial coefficients, $(P)_i^j = \binom{i}{j} \equiv \frac{i!}{j!(i-j)!}$. The inverse matrix is given by $(P^{-1})_i^j = (-1)^{i+j} \binom{i}{j}$. The exponential matrix is then written as

   $\exp(GT) = P \exp(DT) P^{-1}$ with

$$P = \begin{pmatrix} 1 & 0 & 0 & 0 & 0 & ... \\ 1 & 1 & 0 & 0 & 0 & ... \\ 1 & 2 & 1 & 0 & 0 & ... \\ 1 & 3 & 3 & 1 & 0 & ... \\ 1 & 4 & 6 & 4 & 1 & ... \\ \vdots & \vdots & \vdots & \vdots & \vdots & \vdots \end{pmatrix}, P^{-1} = \begin{pmatrix} 1 & 0 & 0 & 0 & 0 & ... \\ -1 & 1 & 0 & 0 & 0 & ... \\ 1 & -2 & 1 & 0 & 0 & ... \\ -1 & 3 & -3 & 1 & 0 & ... \\ 1 & -4 & 6 & -4 & 1 & ... \\ \vdots & \vdots & \vdots & \vdots & \vdots & \vdots \end{pmatrix},$$

$$\exp(DT) = \begin{pmatrix} 1 & 0 & 0 & 0 & 0 & \dots \\ 0 & \alpha & 0 & 0 & 0 & \dots \\ 0 & 0 & \alpha^2 & 0 & 0 & \dots \\ 0 & 0 & 0 & \alpha^3 & 0 & \dots \\ 0 & 0 & 0 & 0 & \alpha^4 & \dots \\ \vdots & \vdots & \vdots & \vdots & \vdots & \vdots \end{pmatrix}, \text{ where } \alpha := \exp(-T).$$

Finally, performing the product of the three matrices above we obtain

$$\exp(GT) = \begin{pmatrix} 1 & 0 & 0 & 0 & 0 & \dots \\ 1-\alpha & \alpha & 0 & 0 & 0 & \dots \\ 1-2\alpha+\alpha^2 & 2\alpha-2\alpha^2 & \alpha^2 & 0 & 0 & \dots \\ 1-3\alpha+3\alpha^2-\alpha^3 & 3\alpha-6\alpha^2+3\alpha^3 & 3\alpha^2-3\alpha^3 & \alpha^3 & 0 & \dots \\ \vdots & \vdots & \vdots & \vdots & \vdots & \vdots \end{pmatrix}.$$

The element j of the first column in $\exp(GT)$ obeys the form $\sum_{i=0}^{j} \binom{j}{i}(-1)^i \alpha^i$, with $j \geq 0$. The element j in the second column obeys the form $\sum_{i=1}^{j} j\binom{j-1}{i-1}(-1)^{i+1}\alpha^i$, with $j \geq 1$, et cetera. The (matrix) product of the initial distribution vector and $\exp(GT)$ gives the particle distribution at T, valid whenever $k=1$ and ρ is high. We can show that if the initial distribution follows a Poisson distribution with parameter $\rho(0)$, the time-dependent distribution of particles follows a Poisson distribution with parameter $\rho(t)$. Let us check it for the two first probabilities of the distribution. Consistently with the Poisson assumption, we take $N \to +\infty$:

$$P(0) = \sum_{j=0}^{\infty} P_{POI}(j) \sum_{i=0}^{j} \binom{j}{i}(-1)^i \alpha^i \qquad [\text{making } -\alpha \equiv \beta]$$

$$= \sum_{j=0}^{\infty} e^{-\rho_0}(\rho_0^j/j!) \sum_{i=0}^{j} \binom{j}{i}\beta^i = \sum_{i=0}^{\infty} \beta^i e^{-\rho_0} \sum_{j=i}^{\infty}(\rho_0^j/j!)\binom{j}{i}$$

$$= e^{-\rho_0} \sum_{i=0}^{\infty}(\beta^i/i!) \sum_{j=i}^{\infty} \frac{\rho_0^j}{(j-i)!} = e^{-\rho_0} \sum_{i=0}^{\infty}(\beta^i/i!)\rho_0^i e^{\rho_0}$$

$$= \sum_{i=0}^{\infty}(\beta^i/i!)\rho_0^i = e^{\rho_0\beta}.$$

Recalling that $\beta := -\alpha = -\exp(-T) = -N(T)/N(0)$, we finally obtain $P(0) = \exp(-\rho(t))$. Similarly we obtain $P(1)$:

$$P(1) = \sum_{j=0}^{\infty} P_{POI}(j) \sum_{i=1}^{j} j\binom{j-1}{i-1}(-1)^{i+1}\alpha^i = (-1)\sum_{j=1}^{\infty} \frac{je^{-\rho_0}\rho_0^j}{j!} \sum_{i=1}^{j}\beta^i \frac{(j-1)!}{(i-1)!(j-i)!}$$

$$= -e^{-\rho_0} \sum_{i=1}^{\infty} \frac{\rho_0^i\beta^i}{(i-1)!} \sum_{j=i}^{\infty} \frac{\rho_0^{j-i}}{(j-i)!} = -\sum_{i=1}^{\infty} \frac{\rho_0^i\beta^i}{(i-1)!} = -\rho_0\beta e^{\rho_0\beta} = \rho(t)e^{-\rho(t)}.$$

The rest of probabilities, $P(j \geq 2)$, are similarly obtained and correspond to a Poisson distribution of parameter ρ. In [15], the authors use Monte-Carlo simulations to show that the particle distribution is sensibly described by means of a Poisson distribution (of parameter equal to the system density) when densities are high. We have shown this result analytically.

Case 2: $k=0$ (particles never react, so $N(t)=N$). Now the transition matrix (1) is

$$(M_i^j) = (I_i^j) + \begin{pmatrix} -\frac{1}{L} & \frac{1}{L} & 0 & 0 & 0 & \cdots \\ \frac{1}{N} & -\frac{1}{N} - \frac{1}{L} & \frac{1}{L} & 0 & 0 & \cdots \\ 0 & \frac{2}{N} & -\frac{2}{N} - \frac{1}{L} & \frac{1}{L} & 0 & \cdots \\ 0 & 0 & \frac{3}{N} & -\frac{3}{N} - \frac{1}{L} & \frac{1}{L} & \cdots \\ 0 & 0 & 0 & \frac{4}{N} & -\frac{4}{N} - \frac{1}{L} & \cdots \\ \vdots & \vdots & \vdots & \vdots & \vdots & \vdots \end{pmatrix}.$$

The stationary distribution corresponds to the eigenvector with eigenvalue 1. Solving the system of equations $xM = x$ we obtain: $\delta_1 = \rho\delta_0$, $\delta_2 = \rho\delta_1/2$, $\delta_3 = \rho\delta_2/3$, ..., $\delta_j = \rho\delta_{j-1}/j$ and so on. Then, $\delta_j = \rho^j\delta_0/j!$. Condition $\sum P(j) = 1$ implies that $\delta_0 \sum_{j=0}^{\infty} \rho^j/j! = 1$, so $\delta_0 = \exp(-\rho)$: the stationary distribution is a Poisson one with parameter $\rho = N/L$, the constant density. The result is independent of the initial distribution. So, if the system initially follows a Poisson distribution, particles merely diffuse, and the particle distribution remains; otherwise, the particle distribution evolves over time towards the Poisson one.

3 Reversible Coalescence: $A + A \rightleftharpoons A$

In this section we consider that particles can give birth to another particle at rate λ: in the time interval between t and $t + \delta t$ any particle will give birth to a new particle with probability $\lambda\delta t$. Then both the offspring production ($A \to A + A$) and the coagulation processes ($A + A \to A$) coexist. We assume that the new particle stays in the same site as the generating one, in contrast with [3], where the new particle appears in an adjacent site (an assumption made for the sake of tractability in order to make the model solvable). We also assume that the particle born does not react (this is assumed without lost of generality, as parameter λ can be redefined to account for the situation where the new particle can react). We impose that inequality $\lambda < k$ must hold; otherwise, the number of particles would increase without boundary. As the time step is inversely related to the current number of particles in the system, $\delta t = 1/N$, the probability that a given particle gives birth to a new particle between t and $t + \delta t$ is λ/N. The disappearance of one particle between t and $t + \delta t$ occurs if a particle hops in such time interval and reacts. So, the probability associated to the disappearance of an arbitrary given particle in the interval δt is k/N if it jumps to a non-empty site, and 0 otherwise. In the stationary state, $P_{eq}(0)$ is calculated by imposing that the number of particles in the system does not change in expectation: $E(\delta N) = \lambda N\delta t - (1 - P_{eq}(0))k = \lambda - (1 - P_{eq}(0))k = 0$, where the minuend represents the probability of birth of a new particle in the interval $(t, t + \delta t)$, and the subtrahend represents the probability of disappearance of some particle in the same interval (a hopping particle arrives at a non-empty site and reacts). Then, at equilibrium, the probability associated to an empty site is $P(0) = 1 - \lambda/k$ with $\lambda < k$. The transition matrix is now

$$M \equiv (I_i^j) + (B_i^j) \tag{2}$$

with (I_i^j) being the identity matrix and $(B_i^j) =$

$$
= \begin{pmatrix}
-\frac{1}{L} & \frac{1}{L} & 0 & 0 & \cdots \\
\frac{1}{N} & -\frac{1}{N} - \frac{1}{L}(1-k+\lambda/\rho) & \frac{1}{L}(1-k+\lambda/\rho) & 0 & \cdots \\
0 & \frac{2}{N} & -\frac{2}{N} - \frac{1}{L}(1-k+2\lambda/\rho) & \frac{1}{L}(1-k+2\lambda/\rho) & \cdots \\
0 & 0 & \frac{3}{N} & -\frac{3}{N} - \frac{1}{L}(1-k+3\lambda/\rho) & \cdots \\
0 & 0 & 0 & \frac{4}{N} & \cdots \\
\vdots & \vdots & \vdots & \vdots & \vdots
\end{pmatrix}.
$$

The stationary particle distribution corresponds to the eigenvector with eigenvalue 1. By solving the system of equations $xM = x$, with M being the matrix given in (2), we obtain the following recursive relation: $P(1) = \rho P(0), P(2) = (\rho/2)(1 - k + \lambda/\rho)P(1), ..., P(j) = (\rho/j)[1-k+(j-1)\lambda/\rho]P(j-1)$, with $P(n)$ denoting the probabilities of the stationary distribution; the equilibrium density, ρ_{eq}, is still to be determined. Disentangling the recursive relation, the general term of the succession can be written as $P(j \geq 2) = P(0)(\rho^j/j!) \prod_{n=1}^{j-1}(1 - k + n\lambda/\rho)$.

Finally, ρ_{eq} is obtained by imposing that the sum of probabilities is one. We must observe that the system can reach an arbitrarily high population even though the birth rate is below the nucleation rate ($\lambda < k$).

A particular case deserves attention. If $k = 1$ (meeting particles always react and fuse into one), we obtain an exact solution. Let us see it. The computation of $P(j \geq 2)$ reduces to

$$
P(j \geq 2) = P(0)(\rho^j/j!) \prod_{n=1}^{j-1}(n\lambda/\rho) = \rho P(0)\lambda^{j-1}/j.
$$

The equilibrium density is calculated as follows:

$$
1 = \sum_{j=0}^{\infty} P(j) = 1 - \lambda + \rho(1 - \lambda) + \sum_{j=2}^{\infty} P(j) =
$$

$$
= (1 + \rho)(1 - \lambda) + (P(1)/\lambda)(\sum_{j=1}^{\infty} \lambda^j/j - \lambda) =
$$

$$
= (1 + \rho)(1 - \lambda) + (P(1)/\lambda)\sum_{j=1}^{\infty} \lambda^j/j - P(1).
$$

Taking into account the fact that $P(1) = \rho P(0) = \rho(1 - \lambda)$ and that

$\sum_{j=1}^{\infty} \lambda^j/j = \lambda + \lambda^2/2 + \lambda^3/3 + ... = -ln(1 - \lambda)$ if $\lambda < 1$, we finally obtain:

$$
\rho_{eq} = \frac{\lambda^2}{(1 - \lambda)[-ln(1 - \lambda)]}. \tag{3}
$$

This equilibrium density is a positive number that can be above 1 (if $\lambda > 0.606$) or below 1 (if $\lambda < 0.606$). The quantity $-ln(1 - \lambda)$, denoted by ρ^* henceforth, is necessarily smaller than ρ_{eq} (inequality $\rho^* < \rho_{eq}$ is easily shown using the fact that $-ln(1 - \lambda) = \lambda + \lambda^2/2 + \lambda^3/3 + ...$). This inequality is relevant later on.

The particular case $k = 1$ (which leads to (3)) is not as restrictive as it may seem, since the condition $k < 1$ represents that reactions are not instantaneous, so time can be re-scaled to kt. Then we can also re-scale the birth rate λ (changing it to λ/k) to have a model similar to the previous one. After re-scaling, the simpler model ($k = 1$) gives a good

approximation to ρ_{eq} when $k < 1$. Both models are not mathematically identical, but qualitatively similar. The approximation $\rho_{eq} = \dfrac{(\lambda/k)^2}{(1 - (\lambda/k))[-ln(1 - (\lambda/k))]}$ obtained from (3) is very good if the ratio λ/k is small.

An apparent paradox arises: both $\rho(t)$ and $P_t(0)$ can be increasing functions of time. Consider, for example, $L = 10^5$, $N = 0.7 \times 10^4$, $k = 1$ and $\lambda = 0.5$; then $\rho(t)$ increases from $\rho(0) = 0.7$ to $\rho_{eq} = 0.7213$ and $P(0)$ increases from $P_0(0) = e^{-\rho(0)} = 0.4966$ to $P_{eq}(0) = 1 - \lambda = 0.5$. Can both the density and the number of empty sites simultaneously increase? The answer is affirmative. The paradox is not such since the particle distribution follows a Poisson one only at $t = 0$, but in equilibrium the system has more empty sites than in the Poisson case (oppositely to the irreversible model, $A + A \rightarrow A$). A distinguishing feature of the model is that the particle density does not necessarily evolve monotonically towards the equilibrium. This fact is related to the existence of a kinetic phase transition. Let us see it.

At any time t, the system density decreases if the birth rate λ is smaller than the disappearance rate $kC(t)$, with $C(t) \equiv 1 - P(0)$ being the system concentration. Take $k = 1$ and assume $\rho_0 = \rho_{eq}$ for simplicity, with ρ_{eq} given in (3). At $t = 0$, the density decreases if $\lambda < kC(t) = 1 - e^{-\rho_0}$; recall that $k = 1$ and the initial distribution is a Poisson one. Inequality $\lambda < 1 - e^{-\rho^*}$ is equivalent to $-ln(1 - \lambda) < \rho^*$, which necessarily holds because $\rho^* \equiv -ln(1 - \lambda)$ is smaller than ρ_{eq} (see above). So, starting at $\rho_0 = \rho_{eq}$, the density initially decreases and then increases (towards ρ_{eq}). In the case where ρ_0 is below ρ^*, the density initially increases instead, since $\lambda > kC(t)$ necessarily holds. In sum: ρ^* is lower than ρ_{eq}, as in [3] and [18], and for initial densities lying between ρ^* and ρ_{eq}, $\rho(t)$ first decreases and then increases. If, for example, $\lambda = 0.2$, the equilibrium density is $\rho_{eq} = 0.2241$; if the initial density is between 0.2231 and 0.2241, equal to $-ln(1 - \lambda)$ and ρ_{eq} respectively, the system density initially decreases and then increases towards ρ_{eq}. The concentration evolves from $C(0) = 1 - e^{-\rho_0} = 0.2007$ to $\lambda = 0.2$.

Then, the system evolution depends on the initial conditions. In particular, the time until equilibrium behaves differently depending on whether the initial density is above or below ρ^*: if T denotes the time elapsed until the density first reaches ρ_{eq}, it is easy to show that in the neighborhood of ρ^*, $\partial T/\partial\rho_0 < 0$ if $\rho_0 < \rho^*$ but $\partial T/\partial\rho_0 > 0$ if $\rho_0 > \rho^*$. The discontinuity in the derivative suggests the existence of a dynamic phase transition at $\rho_0 = \rho^*$, which confirms a result in [3]: the lattice effect is not important qualitatively in predicting the transition. Equivalently, the dynamic phase transition corresponds to an initial concentration $C(0) = \lambda$. In fact, the system concentration (rather than the density) is the key to explain the system behavior, which shows a manifestation of the lattice effect. The order of the phase transition requires the calculation of the relaxation time, which is not available from the transition matrix; see [3] or [18] for its computation in a different formulation.

If we assume instead that the particle input occurs in an adjacent site to the site of the mother particle, the transition matrix is slightly different from the previous case (in which the particle input occurs in the cell of the mother particle). The matrix elements are now: $M_0^0 = 1 - (1/L)(1 + \lambda)$, $M_j^j = 1 - j/N - (1/L)(1 + \lambda)(1 - k)$ and $M_j^{j+1} = (1/L)(1 + \lambda)(1 - k)$ for $j \geq 1$, and the rest of elements are obtained by taking into account the fact that the matrix is stochastic.

If $k < 1$, from the new matrix we obtain $P(0) = 1 - \frac{\lambda}{k(\lambda+1)}$, $P(1) = \rho(1 + \lambda)P(0)$, and the recursive relation $P(j) = (\rho/j)(1 + \lambda)(1 - k)P(j - 1)$, which leads to $P(j) = \frac{[\rho(1+\lambda)(1-k)]^{j-1}}{j!}P(1)$. By imposing that the sum of probabilities is one, we obtain an

equation from which the equilibrium density ρ_{eq} can be computed. The density obtained is below the equilibrium density obtained in the previous case, because now the new particle is born in an adjacent site and can react, which is neglected by assumption in the previous model (in which the particle remains in the site of the mother particle without reacting).

If $k = 1$, then $P(j \geq 2) = 0$, and the equilibrium density reduces to $\rho_{eq} = \lambda/(1 + \lambda)$. In equilibrium, sites are either empty or occupied by one particle, so, asymptotically, the model resembles the hard-core model.

4   Concluding Remarks

In this paper we use a matrix method to analyze the particle distribution in nucleation diffusion-limited models, both in the irreversible case $(A + A \rightarrow A)$ and in the reversible one $(A + A \rightleftharpoons A)$. In the irreversible case, the number of particles in the system cannot increase with time. We focus our attention on the situation where the system density is not too low and decays with $\rho \sim t^{-1}$. In the long-time regime, however, the decay goes with $\rho \sim t^{-1/2}$, which remains out of our scope. In the reversible case particles give birth to other particles, and the density reaches an equilibrium level for some parameter configurations. According to the method proposed, the particle distribution can be calculated by using a simple recursive procedure based on Markov chains, with the density being part of the solution.

In some particular cases, exact solutions are obtained. In particular, in the irreversible coagulation case, if density is high and particles react with probability 1 (i.e., $\rho \gg 1$ and $k = 1$), then the time-dependent distribution is Poisson with parameter equal to the time-dependent density. Also, if offspring production is not allowed and particles do not react ($k = 0$, so the number of particles remains constant), the stationary distribution also follows a Poisson one, in this case independently of the initial distribution. In the reversible case, in which offspring production is allowed, an equilibrium stationary state is reached if $\lambda < k$. The model admits an exact solution when particles always react, $k = 1$. This simple model predicts a dynamic phase transition.

The matrix approach presented can be used in many other contexts. For example, it can be used to analyze situations in which the porosity of a medium depends on the particle distribution of its cells, which relates to percolation problems. It can also be used to analyze other problems from physics, chemistry, biology or social sciences.

References

[1]   C. R. Doering and D. Ben-Avraham. Interparticle distribution functions and rate equations for diffusion-limited reactions. *Physical Review A* **38** (6) (1988) 3035–3042.

[2]   C. R. Doering and D. Ben-Avraham. Diffusion-limited coagulation in the presence of particle input: Exact results in one dimension. *Physical Review Letters* **62** (21) (1989) 2563–2566.

[3]   J.C. Lin. Exact results for one-dimensional reversible coagulation in discrete spatial formalism. *Physical Review A* **45** (6) (1992) 3892–3895.

[4]   V. Privman. Exact results for diffusion-limited reactions with synchronous dynamics. *Physical Review E* **50** (1) (1994) 50–53.

[5]   D. J. Aldous. Deterministic and stochastic models for coalescence (aggregation and coagulation): a review of the mean-field theory for probabilists. *Bernoulli* **5** (1) (1999) 3–48.

[6]   G. Odor. Universality classes in nonequilibrium lattice systems. *Reviews of Modern Physics* **76** (3) (2004) 663–724.

[7]   D.C. Mattis and M.L. Glasser. The uses of quantum field theory in diffusion-limited reactions. *Reviews of Modern Physics* **70** (3) (1998) 979–1001.

[8]   H. Hinrichsen. Non-equilibrium phase transitions. *Physica A: Statistical Mechanics and its Applications* **369** (1) (2006) 1–28.

[9]   Y. W. Teh, C. Blundell, and L. Elliott. Modelling genetic variations using fragmentation-coagulation processes. In *Advances in neural information processing systems*, 2011, 819–827.

[10] S. Biswas, S. Sinha, and P. Sen. Opinion dynamics model with weighted influence: Exit probability and dynamics. *Physical Review E* **88** (2) (2013) 022152.

[11] P. Roy, S. Biswas, and P. Sen. Universal features of exit probability in opinion dynamics models with domain size dependent dynamics. *Journal of Physics A: Mathematical and Theoretical* **47** (49) (2014) 495001

[12] F. Bagnoli and R. Rechtman. Stochastic bifurcations in the nonlinear parallel Ising model. *Physical Review E* **94** (5) (2016) 052111.

[13] B. Derrida, M.R. Evans, V. Hakim, and V. Pasquier. Exact solution of a 1D asymmetric exclusion model using a matrix formulation. *Journal of Physics A: Mathematical and General* **26** (7) (1993) 1493–1517.

[14] J. M. Cushing. On the dynamics of a class of Darwinian matrix models. *Nonlinear Dynamics and Systems Theory* **10** (2)(2010) 103-116.

[15] L. A. Braunstein and R.C Buceta. Nucleation model for diffusion-limited coalescence with finite reaction rates in one dimension. *Physical Review E* **53** (4) (1996) 3414–3419.

[16] V. Privman, C.R. Doering, and H.L. Frisch. Crossover from rate-equation to diffusion-controlled kinetics in two-particle coagulation. *Physical Review E* **48** (2) (1993) 846–851.

[17] D. Yue, C. Li, and W. Yue. The matrix-geometric solution of the M/Ek/1 queue with balking and state-dependent service. *Nonlinear Dynamics and Systems Theory* **6** (3) (2006) 295–308.

[18] E. Abad, T. Masser, and D. Ben-Avraham. Lattice kinetics of diffusion-limited coalescence and annihilation with sources. *Journal of Physics A: Mathematical and General* **35** (7) (2002) 1483–1500.

Increased and Reduced Synchronization between Discrete-Time Chaotic and Hyperchaotic Systems

L. Jouini and A. Ouannas *

Department of Mathematics and Computer Sciences, University of Larbi Tebessi, Tebessa, 12002 Algeria

Abstract: In this paper, by combining generalized synchronization (GS) and inverse generalized synchronisation (IGS), new schemes for increased and reduced synchronization between different dimensional discrete-time systems are proposed. Based on the Lyapunov stability theory, two control laws are proposed to prove the co-existence of GS and IGS between the general three-dimensional drive map and the two-dimensional response map in 3D and 2D, respectively. Numerical simulation has confirmed the findings of the paper.

Keywords: *discrete chaos; generalized synchronization; inverse generalized synchronisation; co-existence; Lyapunov stability.*

Mathematics Subject Classification (2010): 93C10, 93C55, 93D05.

1 Introduction

Chaotic discrete–time systems have received a considerable attention over the last two decades due to their many applications in secure communications [1]. One of the most studied aspects in discrete-time chaotic systems is the synchronization of chaotic systems. Synchronization refers to the addition of a set of control parameters to the controlled chaotic system and adaptively updating the controls so that the states become synchronized [2–4]. Throughout the years, many studies have considered the synchronization of discrete–order chaotic and hyperchaotic systems including [5–7]. One of the most exciting synchronization types is the generalized synchronization (GS). It refers to the existence of a functional relationship between the drive states and the response states. Instead of the conventional definition of synchronization, which stipulates that

---

* Corresponding author: `mailto:ouannas.a@yahoo.com`

the difference between the drive and response trajectories tends to zero as $t \rightarrow +\infty$, GS forces the difference between the response states and a function of the drive states to zero. IGS is the natural reversal of GS, i.e. the error is the difference between the master states and a function of the slave states. The importance of GS and IGS stems from the fact that they can enrich the behavior of chaotic systems [8].

Naturally, curiosity grew as to the possibility of multiple synchronization types being achieved simultaneously for the states of the response system. This phenomenon is commonly referred to as the coexistence of synchronization types [9–11]. The present research work focuses on the coexistence of GS and IGS between chaotic and hyperchaotic systems. The next section of this paper describes the model for the drive and response systems. Section 3 presents the control law that guarantees the coexistence of GS and IGS in 3D. Section 4 presents numerically the control laws that establish the coexistence of GS and IGS in 2D. Finally, Section 5 summarizes the work carried out in this paper.

2   Drive–Response Model

We consider the following drive chaotic system:

$$
\begin{aligned}
x_1(k+1) &= f_1(x_1(k), x_2(k)), \\
x_2(k+1) &= f_2(x_1(k), x_2(k)),
\end{aligned}
\tag{1}
$$

where $(x_1(k), x_2(k))^T$ is the state vector of the drive system and $f_i : \mathbb{R}^2 \longrightarrow \mathbb{R}, 1 \leq i \leq 2$.

As the response system, we consider the following hyperchaotic system:

$$
\begin{aligned}
y_1(k+1) &= \sum_{j=1}^{3} b_{1j} y_j(k) + g_1(y_1(k), y_2(k), y_3(k)) + u_1, \\
y_2(k+1) &= \sum_{j=1}^{3} b_{2j} y_j(k) + g_2(y_1(k), y_2(k), y_3(k)) + u_2, \\
y_3(k+1) &= \sum_{j=1}^{3} b_{3j} y_j(k) + g_3(y_1(k), y_2(k), y_3(k)) + u_3,
\end{aligned}
\tag{2}
$$

where $(y_1(k), y_2(k), y_3(k))^T$ is the state vector of the response system, $(b_{ij}) \in \mathbb{R}^{3 \times 3}$ is the linear part of the response system, $g_i : \mathbb{R}^3 \longrightarrow \mathbb{R}, 1 \leq i \leq 3$, are the nonlinear functions and $u_i, 1 \leq i \leq 3$, are the controllers to be designed.

3   Synchronization in 3D

The problem of increased synchronization in 3D between the drive system (1) and the response system (2) is to find controllers $u_i, i = 1, 2, 3$, and functions $\phi, \chi : \mathbb{R}^2 \longrightarrow \mathbb{R}$, $\varphi : \mathbb{R} \longrightarrow \mathbb{R}$, such that the synchronization errors

$$
\begin{aligned}
e_1(k) &= y_1(k) - \phi(x_1(k), x_2(k)), \\
e_2(k) &= x_2(k) - \varphi(y_2(k)), \\
e_3(k) &= y_3(k) - \chi(x_1(k), x_2(k))
\end{aligned}
\tag{3}
$$

satisfy the condition $\lim\limits_{n \rightarrow +\infty} e_i(k) = 0$, for $i = 1, 2, 3$.

Remark 3.1 From the error system (3), it is clear that y_1 and $(x_1, x_2)^T$ are generalized synchronized, x_2 and y_2 are inverse generalized synchronized and y_3 is in generalized synchronization with x_1 and x_2 so that generalized synchronization and inverse generalized synchronization coexist in the synchronization of the systems (1) and (2) in 3D.

We assumed that φ is an invertible function and its inverse is noted by φ^{-1}. Hence, we have proved the following result.

Theorem 3.1 *Increased synchronization in 3D between systems (1) and (2) is achieved under the following controllers:*

$$u_1 = -\sum_{j=1}^{3} b_{1j} y_j(k) - g_1(Y(k)) + \phi\left(f_1(X(k)), f_2(X(n))\right) + \tfrac{1}{2}e_1(k) + \tfrac{2}{5}e_2(k) - \tfrac{2}{3}e_3(k),$$

$$u_2 = -\sum_{j=1}^{3} b_{2j} y_j(k) - g_2(Y(k)) + \varphi^{-1}\left(\tfrac{1}{2}e_1(k) + \tfrac{2}{5}e_2(k) + \tfrac{2}{3}e_3(k) - f_2(X(k))\right), \qquad (4)$$

$$u_3 = -\sum_{j=1}^{3} b_{3j} y_j(k) - g_3(Y(k)) + \chi\left(f_1(X(k)), f_2(X(k))\right) + \tfrac{1}{2}e_1(k) - \tfrac{4}{5}e_2(k),$$

where $X(k) = (x_1(k), x_2(k))^T$ and $Y(k) = (y_1(k), y_2(k), y_3(k))^T$.

Proof. The error system (3) can be derived as

$$
\begin{aligned}
e_1(k+1) &= \sum_{j=1}^{3} b_{1j} y_j(k) + g_1(Y(k)) + u_1 - \phi\left(f_1(X(k)), f_2(X(k))\right), & (5) \\
e_2(k+1) &= f_2(X(k)) - \varphi\left(\sum_{j=1}^{3} b_{2j} y_j(k) + g_2(Y(k)) + u_2\right), \\
e_3(k+1) &= \sum_{j=1}^{3} b_{3j} y_j(k) + g_3(Y(k)) - \chi\left(f_1(X(k)), f_2(X(k))\right).
\end{aligned}
$$

Substituting the control law (4) into (5), one can get

$$
\begin{aligned}
e_1(k+1) &= \tfrac{1}{2}e_1(k) + \tfrac{2}{5}e_2(k) - \tfrac{2}{3}e_3(k), & (6) \\
e_2(k+1) &= \tfrac{1}{2}e_1(k) + \tfrac{2}{5}e_2(k) + \tfrac{2}{3}e_3(k), \\
e_3(k+1) &= \tfrac{1}{2}e_1(k) - \tfrac{4}{5}e_2(k).
\end{aligned}
$$

We construct the Lyapunov function in the form $V(e_1(k), e_2(k), e_3(k)) = e_1^2(k) + e_2^2(k) + e_3^2(k)$, so

$$
\begin{aligned}
\Delta V &= e_1^2(k+1) + e_2^2(k+1) + e_3^2(k+1) - e_1^2(k) - e_2^2(k) - e_3^2(k) \\
&= -\left(\tfrac{1}{4}e_1^2(k) + \tfrac{17}{25}e_2^2(k) + \tfrac{1}{9}e_3^2(k)\right) < 0.
\end{aligned}
$$

It is immediate that all solutions of error system (6) go to zero as $k \to +\infty$. Therefore, systems (1) and (2) are globally synchronized in 3D.

The result of the numerical simulation of the error system (6) is plotted in (Figure 1).
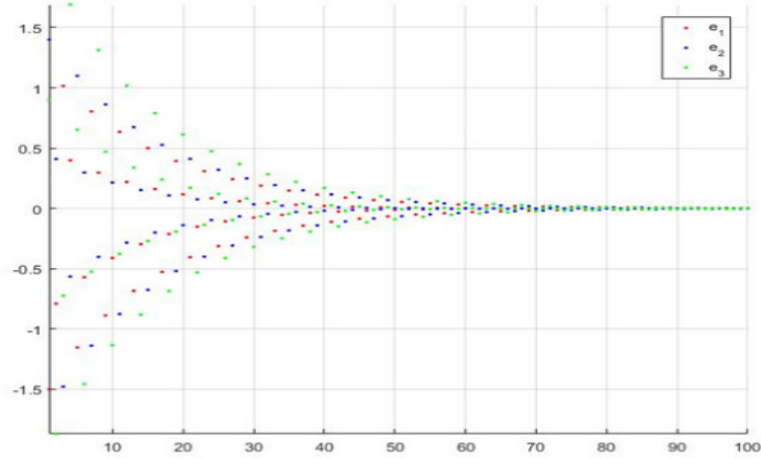
Figure 1: Time evolution of the synchronization errors 6.

4   Synchronization in 2D

The problem of reduced synchronization in 2D between the drive system (1) and the response system (2) is to find controllers u_i, $i = 1, 2, 3$, and functions $\psi : \mathbb{R}^2 \longrightarrow \mathbb{R}$, $\lambda, \omega : \mathbb{R} \longrightarrow \mathbb{R}$, such that the synchronization errors

$$
\begin{aligned}
e_1\left(k\right) &= y_1(k) - \psi\left(x_1(k), x_2(k)\right), \\
e_2\left(k\right) &= x_2(k) - \lambda\left(y_2(k)\right) - \omega\left(y_3(k)\right)
\end{aligned}
\tag{7}
$$

satisfy the condition $\lim\limits_{n \to +\infty} e_i(k) = 0,$ for $i = 1, 2$. We assume that the functions λ and ω are invertible.

Remark 4.1 From the error system (7), it is clear that y_1 is generalized synchronized with x_1 and x_2, and x_2 is inverse generalized synchronized with y_2 and y_3, so that generalized synchronization and inverse generalized synchronization coexist in the synchronization of the systems (1) and (2) in 2D.

The error system (7) can be described as

$$
\begin{aligned}
e_1\left(k+1\right) &= \sum_{j=1}^{3} b_{1j} y_j(k) + g_1(Y(k)) + u_1 - \psi\left(f_1(X(k)), f_2(X(k))\right), \\
e_2\left(k+1\right) &= f_2(X(k)) - \lambda\left(\sum_{j=1}^{3} b_{2j} y_j(k) + g_2(Y(k)) + u_2\right) \\
&\quad - \omega\left(\sum_{j=1}^{3} b_{3j} y_j(k) + g_3(Y(k)) + u_3\right).
\end{aligned}
\tag{8}
$$

In this case, the controllers can be constructed as follow:

$$
\begin{aligned}
u_1 &= -\sum_{j=1}^{3} b_{1j} y_j(k) - g_1(Y(k)) - u_1 + \psi\left(f_1(X(k)), f_2(X(k))\right) - e_1(k) - e_2(k), \quad (9) \\
u_2 &= -\sum_{j=1}^{3} b_{1j} y_j(k) - g_1(Y(k)) + \lambda^{-1}\left(e_1(k) - e_2(k)\right), \\
u_3 &= -\sum_{j=1}^{3} b_{3j} y_j(k) - g_3(Y(k)) + \omega^{-1}\left(f_2(X(k))\right),
\end{aligned}
$$

where λ^{-1} and ω^{-1} are the inverse functions of λ and ω, respectively. By substituting the control law (9) into (8), the error system can be described as

$$
\begin{aligned}
e_1(k+1) &= \frac{1}{2} e_1(k) + \frac{1}{2} e_2(k), \quad (10) \\
e_2(k+1) &= \frac{1}{2} e_1(k) - \frac{1}{2} e_2(k).
\end{aligned}
$$

We construct a Lyapunov function in the form $V\left(e_1(k), e_2(k)\right) = e_1^2(k) + e_2^2(k)$, so

$$
\begin{aligned}
\Delta V &= e_1^2(k+1) + e_2^2(k+1) - e_1^2(k) - e_2^2(k) \\
&= -\frac{1}{2}\left(e_1^2(k) + e_2^2(k)\right) < 0.
\end{aligned}
$$

Thus, from the Lyapunov stability theory, it is immediate that $\lim_{n \to +\infty} e_i(k) = 0$, $(i = 1, 2)$. Hence, we have proved the following result.

Theorem 4.1 *The drive system (1) and the response system (2) are reduced synchronization in 2D under the control law (9).*

The result of the numerical simulation of the error system (10) is plotted in Figure 2.
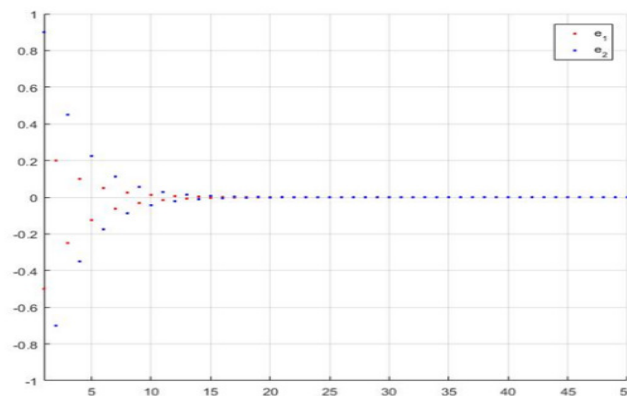

Figure 2: Time evolution of the synchronization errors (10).

5   Conclusion

In this work, we have shown that different types of synchronization can co-exist for different dimensional discrete-time chaotic systems. We assumed a two dimensional drive system and a three dimensional response system. The main results of the study were two-fold. First, we presented a control scheme whereby GS and IGS are achieved simultaneously in 3D. The stability of the zero solutions, and, consequently, the convergence of the synchronization errors were established by means of the Lyapunov stability theory. The second main result concerns the co-existence of GS and IGS in 2D. Simulations were carried out on Matlab to ensure that the errors converge to zero subject to the proposed control laws.

References

[1] Z. Kotulski, J. Szczepnski, K. Gorski, A. Paszkiewicz and A. Zugaj. Application of discrete chaotic dynamical system in cryptography-DCC method. *International Journal of Bifurcation and Chaos* **9** (6) (1999) 1121–1135.

[2] A. Y. Aguilar–Bustos, C. Cruz–Hernández, R. M. Lopez–Gutierrez, and C. Posadas–Castillo. Synchronization of different hyperchaotic maps for encryption. *Nonlinear Dynamics and Systems Theory* **8** (3) (2008) 221–236.

[3] E. Inzunza-González, and C. Cruz-Hernández. Double hyperchaotic encryption for security in biometric systems. *Nonlinear Dynamics and Systems Theory* **13** (1) (2013) 55–68.

[4] R. L. Filali, M. Benrejeb and P. Borne. On observer-based secure communication design using discrete-time hyperchaotic systems. *Communications in Nonlinear Science and Numerical Simulation* **19** (5) (2014) 1424–1432.

[5] A. Ouannas. A new synchronization scheme for general 3D quadratic chaotic systems in discrete-time. *Nonlinear Dynamics and Systems Theory* **15** (2) (2015) 163-170.

[6] A. Ouannas and G. Grassi. Inverse full state hybrid projective synchronization for chaotic maps with different dimensions. *Chiness Physics B* **25** (9) (2016) 090503-6.

[7] A. Ouannas and M. M. Al-sawalha. A new approach to synchronize different dimensional chaotic maps using two scaling matrices. *Nonlinear Dynamics and Systems Theory* **15** (4) (2015) 400-408.

[8] A. Ouannas and Z. Odibat. Generalized synchronization of different dimensional chaotic dynamical systems in discrete time. *Nonlinear Dynamics* **81** (1-2) (2015) 765–771.

[9] A. Ouannas and G. Grassi. A new approach to study co-existence of some synchronization types between chaotic maps with different dimensions. *Nonlinear Dynamics* **86** (2) (2016) 1319–1328.

[10] A. Ouannas, A. T. Azar and R. Abu-Saris. A new type of hybrid synchronization between arbitrary hyperchaotic maps. *International Journal of Learning Machine and Cybernitic* **8** (6) (2017) 1–8.

[11] A. Ouannas. Co-existence of various synchronization types in hyperchaotic maps. *Nonlinear Dynamics and Systems Theory* **16** (3) (2016) 312–321.

A New Representation of Exact Solutions for Nonlinear Time-Fractional Wave-Like Equations with Variable Coefficients

A. Khalouta* and A. Kadem

Laboratory of Fundamental and Numerical Mathematics,
Departement of Mathematics, Faculty of Sciences,
Ferhat Abbas Sétif University 1, 19000 Sétif, Algeria.

Abstract: In this paper, we give a new representation of exact solutions for nonlinear time-fractional wave-like equations with variable coefficients using a recent and reliable method, namely the fractional reduced differential transform method (FRDTM). Using the FRDTM, it is possible to find solution for this type of equations in the form of infinite series, this series in closed form gives the exact solution. It has been proven that the FRDTM is a convenient and effective method in its application. The accuracy and efficiency of the method is tested by means of three numerical examples.

Keywords: *nonlinear time-fractional wave-like equations; Caputo fractional derivative; fractional reduced differential transform method.*

Mathematics Subject Classification (2010): Primary 35R11, 26A33, Secondary 35C05, 74G10.

1 Introduction

The nonlinear fractional partial differential equations (NFPDEs) are increasingly used to model many problems in mathematical physics, including electromagnetics, fluid flow, diffusion, quantum mechanics, damping laws, viscoelasticity and other applications. Exact solutions of NFPDEs are sometimes too complicated to be attained by conventional techniques due to the computational complexities of nonlinear parts involving them. Therefore, for the study of solution of NFPDEs there are variety of analytical and approximate methods found in literature. Among them most useful and common methods are: the Adomian decomposition method (ADM) [8], variational iteration method

---

* Corresponding author: `mailto:nadjibkh@yahoo.fr`

(VIM) [10], fractional difference method (FDM) [4], generalized differential transform method (GDTM) [1], homotopy analysis method (HAM) [11], homotopy perturbation method (HPM) [9].

Recently, an efficient analytical technique for handling different types of NFPDEs has been developed called the fractional reduced differential transform method (FRDTM). The FRDTM was effectively used for finding the solution of various kinds of NFPDEs [5–7]. Further, this method does not require any discretization, linearization and therefore it reduces significantly the numerical computations compare with the existing methods such as the perturbation technique, differential transform method (DTM) and the Adomian decomposition method (ADM).

In [3], we solved the nonlinear time-fractional wave-like equations with variable coefficients by two different methods and compared between these two methods.

The main objective of this paper is to give a new representation of exact solutions for this type of equations using the FRDTM.

Consider the following nonlinear time-fractional wave-like equations:

$$
D_t^{2\alpha} u = \sum_{i,j=1}^{n} F_{1ij}(X,t,u) \frac{\partial^{k+m}}{\partial x_i^k \partial x_j^m} F_{2ij}(u_{x_i}, u_{x_j}) \tag{1}
$$
$$
+ \sum_{i=1}^{n} G_{1i}(X,t,u) \frac{\partial^p}{\partial x_i^p} G_{2i}(u_{x_i}) + H(X,t,u) + S(X,t),
$$

with the initial conditions

$$
u(X,0) = a_0(X), \ u_t(X,0) = a_1(X), \tag{2}
$$

where $D_t^{2\alpha}$ is the Caputo fractional derivative operator of order 2α, $\frac{1}{2} < \alpha \le 1$.

Here $X = (x_1, x_2, ..., x_n) \in \mathbb{R}^n, n \in \mathbb{N}^*$, $F_{1ij}, G_{1i} \ i,j \in \{1,2,...,n\}$, are nonlinear functions of X, t and u, $F_{2ij}, G_{2i} \ i,j \in \{1,2,...,n\}$, are nonlinear functions of derivatives of u with respect to x_i and $x_j \ i,j \in \{1,2,...,n\}$, respectively. Also H, S are nonlinear functions and k, m, p are integers.

These types of equations are of considerable significance in various fields of applied sciences, mathematical physics, nonlinear hydrodynamics, engineering physics, biophysics, human movement sciences, astrophysics and plasma physics. These equations describe the evolution of erratic motions of small particles that are immersed in fluids, fluctuations of the intensity of laser light, velocity distributions of fluid particles in turbulent flows.

2 Basic Definitions

In this section, we give some basic definitions and properties of the fractional calculus theory which are used further in this paper. For more details, see [4].

Definition 2.1 A real function $u(x,t), x \in I \subset \mathbb{R}, t > 0$, is considered to be in the space $C_\mu(I \times \mathbb{R}^+), \mu \in \mathbb{R}$ if there exists a real number $p > \mu$, so that $u(x,t) = t^p f(x,t)$, where $f(x,t) \in C(I \times \mathbb{R}^+)$, and it is said to be in the space C_μ^n if $u^{(n)}(x,t) \in C_\mu, n \in \mathbb{N}$.

Definition 2.2 Let $u(x,t) \in C_\mu(I \times \mathbb{R}^+), \mu \ge -1$. The Riemann-Liouville fractional integral operator of order $\alpha \ge 0$ of $u(x,t)$ is defined as follows:

$$
I_t^\alpha u(x,t) = \begin{cases} \frac{1}{\Gamma(\alpha)} \int\limits_0^t (t-\xi)^{\alpha-1} u(x,\xi)d\xi, \alpha > 0, x \in I, t > \xi \ge 0, \\ u(x,t), \qquad\qquad\qquad\quad \alpha = 0, \end{cases} \tag{3}
$$

where $\Gamma(.)$ is the well-known gamma function.

Definition 2.3 The Caputo fractional derivative operator of order α of $u(x,t)$ is defined as follows:

$$D_t^\alpha u(x,t) = \begin{cases} \frac{1}{\Gamma(n-\alpha)} \int\limits_0^t (t-\xi)^{n-\alpha-1} u^{(n)}(x,\xi)d\xi, n-1 < \alpha < n, \\ u^{(n)}(x,t), \qquad\qquad\qquad\qquad \alpha = n. \end{cases} \tag{4}$$

For the Riemann-Liouville fractional integral and Caputo fractional derivative, we have the following relation:

$$I_t^\alpha D_t^\alpha u(x,t) = u(x,t) - \sum_{k=0}^{n-1} u^{(k)}(x,0^+)\frac{t^k}{k!}, x \in I, t > 0. \tag{5}$$

3 Fractional Reduced Differential Transform Method (FRDTM)

In this section, we apply the fractional reduced differential transform method for $(n+1)-$variable function $u(x_1, x_2, ..., x_n, t)$ which has been developed in [2].

On the basis of the properties of the one-dimensional differential transform, the function $u(x_1, x_2, ..., x_n, t)$ can be represented as

$$
\begin{aligned}
u(x_1, x_2, ..., x_n, t) &= \left(\sum_{k_1=0}^\infty F_1(k_1)x_1^{k_1} \right) \left(\sum_{k_2=0}^\infty F_2(k_2)x_2^{k_2} \right) \times ... \\
&\quad \times \left(\sum_{k_n=0}^\infty F_n(k_n)x_n^{k_n} \right) \times \left(\sum_{k_m=0}^\infty F_m(k_m)t^{k_m} \right) \\
&= \sum_{k_1=0}^\infty \sum_{k_2=0}^\infty ... \sum_{k_n=0}^\infty \sum_{k_m=0}^\infty U(k_1, k_2, ..., k_n, k_m)x_1^{k_1} x_2^{k_2}...x_n^{k_n} t^{k_m},
\end{aligned}
$$

where $U(k_1, k_2, ..., k_n, k_m) = F_1(k_1) \times F_2(k_2) \times ... \times F_n(k_n) \times F_m(k_m)$ is called the spectrum of $u(x_1, x_2, ..., x_n, t)$. Next, we assume that $u(X,t), X = (x_1, x_2, ..., x_n)$ is a continuously differentiable function with respect to the space variable and time in the domain of interest.

Definition 3.1 Let $u(X,t)$ be an analytic function, then the FRDT of u is given by

$$U_k(X) = \sum_{k=0}^\infty \frac{1}{\Gamma(k\alpha+1)} \left[\frac{\partial^{k\alpha}}{\partial t^{k\alpha}} u(X,t) \right]_{t=t_0}, \tag{6}$$

where α is a parameter describing the order of time fractional derivative in the Caputo sense. Here the lowercase $u(X,t)$ represents the original function while the uppercase $U_k(X)$ stands for the fractional reduced transformed function.

Definition 3.2 The inverse FRDT of $U_k(X)$ is defined by

$$u(X,t) = \sum_{k=0}^\infty U_k(X)(t-t_0)^{k\alpha}. \tag{7}$$

Combining equations (6) and (7), we have

$$u(X,t) = \sum_{k=0}^{\infty} \frac{1}{\Gamma(k\alpha+1)} \left[\frac{\partial^{k\alpha}}{\partial t^{k\alpha}} u(X,t) \right]_{t=t_0} (t-t_0)^{k\alpha}. \tag{8}$$

In particular, for $t_0 = 0$, equation (8) becomes

$$u(X,t) = \sum_{k=0}^{\infty} \frac{1}{\Gamma(k\alpha+1)} \left[\frac{\partial^{k\alpha}}{\partial t^{k\alpha}} u(X,t) \right]_{t=0} t^{k\alpha}. \tag{9}$$

Moreover, if $\alpha = 1$, then the FRDT of equation (8) reduces to the classical RDT method. From the above definitions, the fundamental operations of the FRDTM are given by the following theorems.

Theorem 3.1 *Let $U_k(X), V_k(X)$ and $W_k(X)$ be the fractional reduced differential transform of the functions $u(X,t), v(X,t)$ and $w(X,t)$, respectively, then*

(1) if $w(X,t) = \lambda u(X,t) + \mu v(X,t)$, then $W_k(X) = \lambda U_k(X) + \mu V_k(X)$, λ, $\mu \in \mathbb{R}$.

(2) if $w(X,t) = u(X,t)v(X,t)$, then $W_k(X) = \sum_{r=0}^{k} U_r(X)V_{k-r}(X)$.

(3) if $w(X,t) = u^1(X,t)u^2(X,t)...u^n(X,t)$, then

$$W_k(X) = \sum_{k_{n-1}=0}^{k} \sum_{k_{n-2}=0}^{k_{n-1}} ... \sum_{k_2=0}^{k_3} \sum_{k_1=0}^{k_2} U_{k_1}^1(X) U_{k_2-k_1}^2(X)$$
$$\times ... \times U_{k_{n-1}-k_{n-2}}^{n-1}(X) U_{k-k_{n-1}}^n(X).$$

(4) if $w(X,t) = \dfrac{\partial^{n\alpha}}{\partial t^{n\alpha}} u(X,t)$, then

$$W_k(X) = \frac{\Gamma(k\alpha+n\alpha+1)}{\Gamma(k\alpha+1)} U_{k+n}(X), n = 1, 2, ...$$

4   FRDTM for Nonlinear Time-Fractional Wave-Like Equations

Theorem 4.1 *Consider the nonlinear time-fractional wave-like equations (1) with the initial conditions (2).*

Then, by FRDTM the solution of equations (1)-(2) is given in the form of infinite series as follows:

$$u(X,t) = \sum_{k=0}^{\infty} U_k(X)t^{k\alpha},$$

where $U_k(X)$ is the fractional reduced differential transformed function of $u(X,t)$.

Proof.   In order to achieve our goal, we consider the following nonlinear time-fractional wave-like equations (1) with the initial conditions (2).

Applying the FRDTM to equation (1), we obtain the following recurrence relation formula:

$$U_{k+2}(X) = \frac{\Gamma(k\alpha+1)}{\Gamma(k\alpha+2\alpha+1)} \left[A_k(X) + B_k(X) + C_k(X) + D_k(X)\right], \qquad (10)$$

where $A_k(X), B_k(X), C_k(X)$ and $D_k(X)$ are the transformed form of the nonlinear terms, $\sum\limits_{i,j=1}^{n} F_{1ij}(X,t,u)\frac{\partial^{k+m}}{\partial x_i^k \partial x_j^m}F_{2ij}(u_{x_i}, u_{x_j})$, $\sum\limits_{i=1}^{n} G_{1i}(X,t,u)\frac{\partial^p}{\partial x_i^p}G_{2i}(u_{x_i})$, $H(X,t,u)$ and $S(X,t)$, rerspectively.

Now, using the FRDTM under the initial conditions (2), we obtain

$$U_0(X) = a_0(X), U_1(X) = a_1(X). \qquad (11)$$

We substitute equation (11) into equation (10), we get

$$\begin{aligned}
U_0(X) &= a_0(X), \ U_1(X) = a_1(X), \\
U_2(X) &= \frac{1}{\Gamma(2\alpha+1)}\left[A_0(X) + B_0(X) + C_0(X) + D_0(X)\right], \\
U_3(X) &= \frac{\Gamma(\alpha+1)}{\Gamma(3\alpha+1)}\left[A_1(X) + B_1(X) + C_1(X) + D_1(X)\right], \qquad (12) \\
U_4(X) &= \frac{\Gamma(2\alpha+1)}{\Gamma(4\alpha+1)}\left[A_2(X) + B_2(X) + C_2(X) + D_2(X)\right]. \\
&\quad \dots
\end{aligned}$$

Then, the solution of equations (1)-(2) in the form of infinite series is given by

$$u(X,t) = \sum_{k=0}^{\infty} U_k(X)t^{k\alpha}. \qquad (13)$$

The proof is complete.

5 Numerical Examples

In this section, we describe the method explained in Section 4. Three numerical examples of nonlinear time-fractional wave-like equations with variable coefficients are considered to validate the capability, reliability and efficiency of the FRDTM.

Example 5.1 Consider the 2-dimensional nonlinear time-fractional wave-like equation with variable coefficients:

$$D_t^{2\alpha}u = \frac{\partial^2}{\partial x \partial y}(u_{xx}u_{yy}) - \frac{\partial^2}{\partial x \partial y}(xyu_x u_y) - u, t > 0, \frac{1}{2} < \alpha \le 1, \qquad (14)$$

with the initial conditions

$$u(x,y,0) = e^{xy}, u_t(x,y,0) = e^{xy}, (x,y) \in \mathbb{R}^2. \qquad (15)$$

Applying the FRDTM to equations (14)-(15), we obtain the following recurrence relation formula:

$$\begin{aligned}
U_0(x,y) &= e^{xy}, \ U_1(x,y) = e^{xy}, \qquad (16) \\
U_{k+2}(x,y) &= \frac{\Gamma(k\alpha+1)}{\Gamma(k\alpha+2\alpha+1)}\left[\frac{\partial^2}{\partial x \partial y}A_k(x,y) - \frac{\partial^2}{\partial x \partial y}B_k(x,y) - U_k(x,y)\right],
\end{aligned}$$

where $A_k(x, y)$ and $B_k(x, y)$ are the transformed form of the nonlinear terms, $u_{xx}u_{yy}$ and $xyu_x u_y$. For the convenience of the reader, the first few nonlinear terms are as follows:

$$
\begin{aligned}
A_0 &= U_{0xx}U_{0yy}, \\
A_1 &= U_{0xx}U_{1yy} + U_{1xx}U_{0yy}, \\
A_2 &= U_{0xx}U_{2yy} + U_{1xx}U_{1yy} + U_{2xx}U_{0yy},
\end{aligned}
$$

$$
\begin{aligned}
B_0 &= xyU_{0x}U_{0y}, \\
B_1 &= xyU_{0x}U_{1y} + xyU_{1x}U_{0y}, \\
B_2 &= xyU_{0x}U_{2y} + xyU_{1x}U_{1y} + xyU_{2x}U_{0y}.
\end{aligned}
$$

From the relationship in (16), we obtain

$$
\begin{aligned}
U_0(x, y) &= e^{xy}, \ U_1(x, y) = e^{xy}, U_2(x, y) = -\frac{1}{\Gamma(2\alpha + 1)}e^{xy}, \\
U_3(x, y) &= -\frac{\Gamma(\alpha + 1)}{\Gamma(3\alpha + 1)}e^{xy}, U_4(x, y) = \frac{1}{\Gamma(4\alpha + 1)}e^{xy}...
\end{aligned}
$$

So, the solution of equations (14)-(15) is given in the form of infinite series as follows:

$$
u(x, y, t) = \left(1 + t^\alpha - \frac{1}{\Gamma(2\alpha + 1)}t^{2\alpha} - \frac{\Gamma(\alpha + 1)}{\Gamma(3\alpha + 1)}t^{3\alpha} + \frac{1}{\Gamma(4\alpha + 1)}t^{4\alpha} + ...\right)e^{xy}.
$$

In particular, for $\alpha = 1$, the solution of equations (14)-(15) has the general pattern form which coincides with the following exact solution in terms of infinite series:

$$
u(x, y, t) = \left(1 + t - \frac{t^2}{2!} - \frac{t^3}{3!} + \frac{t^4}{4!} + ...\right)e^{xy}.
$$

Therefore, the exact solution of equations (14)-(15) in a closed form of elementary function will be given by

$$
u(x, y, t) = (\cos t + \sin t)\, e^{xy},
$$

which is the same result as those obtained by the NIM and NHPM [3].

Example 5.2 Consider the following nonlinear time-fractional wave-like equation with variable coefficients:

$$
D_t^{2\alpha}u = u^2\frac{\partial^2}{\partial x^2}(u_x u_{xx} u_{xxx}) + u_x^2\frac{\partial^2}{\partial x^2}(u_{xx}^3) - 18u^5 + u, \quad t > 0, \frac{1}{2} < \alpha \leq 1, \tag{17}
$$

with the initial conditions

$$
u(x, 0) = e^x, u_t(x, 0) = e^x, \quad x \in]0, 1[. \tag{18}
$$

Applying the FRDTM to equations (17)-(18), we obtain the following recurrence relation formula:

$$
\begin{aligned}
U_0(x) &= e^x, U_1(x) = e^x, \tag{19} \\
U_{k+2}(x) &= \frac{\Gamma(k\alpha + 1)}{\Gamma(k\alpha + 2\alpha + 1)}\left[A_k(x) + B_k(x) - 18C_k(x) + U_k(x)\right],
\end{aligned}
$$

where $A_k(x)$, $B_k(x)$ and $C_k(x)$ are the transformed form of the nonlinear terms, $u^2 \dfrac{\partial^2}{\partial x^2}(u_x u_{xx} u_{xxx})$, $u_x^2 \dfrac{\partial^2}{\partial x^2}(u_{xx}^3)$ and u^5. For the convenience of the reader, the first few nonlinear terms are as follows:

$$
\begin{aligned}
A_0 &= U_0^2 \frac{\partial^2}{\partial x^2}\left[U_{0x} U_{0xx} U_{0xxx}\right], \\
A_1 &= 2U_0 U_1 \frac{\partial^2}{\partial x^2}\left[U_{0x} U_{0xx} U_{0xxx}\right] + U_0^2 \frac{\partial^2}{\partial x^2}\left[U_{1x} U_{0xx} U_{0xxx}\right. \\
&\quad \left. + U_{0x} U_{1xx} U_{0xxx} + U_{0x} U_{0xx} U_{1xxx}\right],
\end{aligned}
$$

$$
\begin{aligned}
B_0 &= U_{0x}^2 \frac{\partial^2}{\partial x^2} U_{0xx}^3, \\
B_1 &= 2U_{0x} U_{1x} \frac{\partial^2}{\partial x^2} U_{0xx}^3 + 3U_{0x}^2 \frac{\partial^2}{\partial x^2}\left[U_{0xx}^2 U_{1xx}\right],
\end{aligned}
$$

$$
C_0 = U_0^5, \ C_1 = 5U_0^4 U_1.
$$

From the relationship in (19), we obtain

$$
\begin{aligned}
U_0(x) &= e^x, \ U_1(x) = e^x, \\
U_2(x) &= \frac{1}{\Gamma(2\alpha+1)} e^x, U_3(x) = \frac{\Gamma(\alpha+1)}{\Gamma(3\alpha+1)} e^x \ldots
\end{aligned}
$$

So, the solution of equations (17)-(18) is given in the form of infinite series as follows:

$$
u(x,t) = \left(1 + t^\alpha + \frac{1}{\Gamma(2\alpha+1)} t^{2\alpha} + \frac{\Gamma(\alpha+1)}{\Gamma(3\alpha+1)} t^{3\alpha} + \ldots\right) e^x.
$$

In particular, for $\alpha = 1$, the solution of equations (17)-(18) has the general pattern form which coincides with the following exact solution in terms of infinite series:

$$
u(x,t) = \left(1 + t + \frac{t^2}{2!} + \frac{t^3}{3!} + \ldots\right) e^x.
$$

Therefore, the exact solution of equations (17)-(18) in a closed form of elementary function will be given by

$$
u(x,t) = e^{x+t},
$$

which is the same result as those obtained by the NIM and NHPM [3].

Example 5.3 Consider the following one-dimensional nonlinear time-fractional wave-like equation with variable coefficients:

$$
D_t^{2\alpha} u = x^2 \frac{\partial}{\partial x}(u_x u_{xx}) - x^2(u_{xx})^2 - u, \quad t > 0, \frac{1}{2} < \alpha \leq 1, \tag{20}
$$

with the initial conditions

$$
u(x,0) = 0, u_t(x,0) = x^2, \quad x \in \,]0,1[. \tag{21}
$$

Applying the FRDTM to equations (20)-(21), we obtain the following recurrence relation formula:

$$U_0(x) = 0, U_1(x) = x^2, \tag{22}$$

$$U_{k+2}(x) = \frac{\Gamma(k\alpha+1)}{\Gamma(k\alpha+2\alpha+1)}\left[x^2\frac{\partial}{\partial x}A_k(x) - x^2 B_k(x) - U_k(x)\right],$$

where $A_k(x)$ and $B_k(x)$ are the transformed form of the nonlinear terms, $u_x u_{xx}$ and u_{xx}^2. For the convenience of the reader, the first few nonlinear terms are as follows:

$$A_0 = U_{0x}U_{0xx},$$
$$A_1 = U_{0x}U_{1xx} + U_{1x}U_{0xx},$$
$$A_2 = U_{0x}U_{2xx} + U_{1x}U_{1xx} + U_{2x}U_{0xx},$$

$$B_0 = U_{0xx}^2,$$
$$B_1 = 2U_{0xx}U_{1xx},$$
$$B_2 = 2U_{0xx}U_{2xx} + U_{1xx}^2.$$

From the relationship in (22), we obtain

$$U_0(x) = 0, U_1(x) = x^2, U_2(x) = 0,$$
$$U_3(x) = -\frac{\Gamma(\alpha+1)}{\Gamma(3\alpha+1)}x^2, U_4(x) = 0...$$

So, the solution of equations (20)-(21) is given in the form of infinite series as follows:

$$u(x,t) = \left(t^\alpha - \frac{\Gamma(\alpha+1)}{\Gamma(3\alpha+1)}t^{3\alpha} + \frac{\Gamma(\alpha+1)}{\Gamma(5\alpha+1)}t^{5\alpha} + ...\right)x^2.$$

In particular, for $\alpha = 1$, the solution of equations (20)-(21) has the general pattern form which coincides with the following exact solution in terms of infinite series:

$$u(x,t) = \left(t - \frac{t^3}{3!} + \frac{t^5}{5!} + ...\right)x^2.$$

Therefore, the exact solution of equations (20)-(21) in a closed form of elementary function will be given by

$$u(x,t) = x^2 \sin t,$$

which is the same result as those obtained by the NIM and NHPM [3].

6   Numerical Results and Discussion

In this section the numerical results for all Examples 5.1, 5.2 and 5.3 are presented. Figures 1, 3 and 5 represent the surface graph of the exact solution and the 6−term approximate solution at $\alpha = 0.6, 0.8, 1$. Figures 2, 4 and 6 represent the behavior of the exact solution and the 6−term approximate solution at $\alpha = 0.7, 0.8, 0.95, 1$ in the case when $x = y = 0.5$ for Example 5.1 and $x = 0.5$ for Examples 5.2 and 5.3. Tables 1, 2 and 3 show the absolute errors between the exact solution and the 6−term approximate solution at $\alpha = 1$ and different values of x, y and t. The numerical results affirm that when α approaches 1, our results obtained by the FRDTM approach the exact solutions.
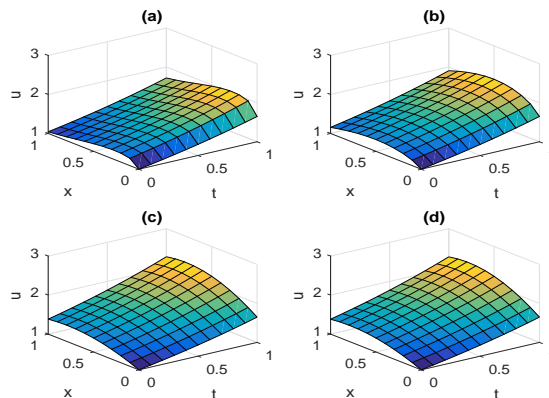
Figure 1: The surface graph of the exact solution and the 6−term approximate solution by the FRDTM for Example 5.1 when $y = 0.5$: (a) u when $\alpha = 0.6$, (b) u when $\alpha = 0.8$, (c) u when $\alpha = 1$, and (d) u is exact.
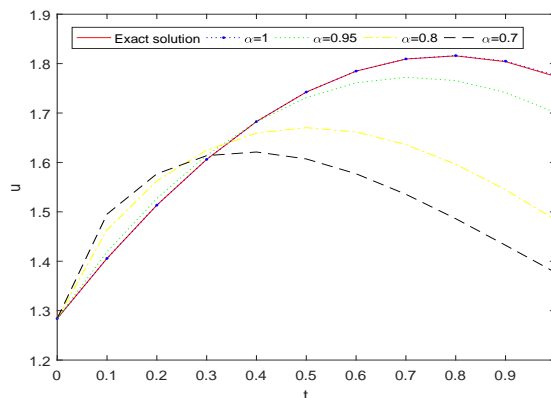

Figure 2: The behavior of the exact solution and the 6−term approximate solution by the FRDTM for different values of α for Example 5.1 when $x = y = 0.5$.

$t/x, y$	0.1	0.3	0.5	0.7
0.1	1.4226×10^{-9}	1.5411×10^{-9}	1.8085×10^{-9}	2.2991×10^{-9}
0.3	1.0648×10^{-6}	1.1535×10^{-6}	1.3536×10^{-6}	1.7208×10^{-6}
0.5	2.3382×10^{-5}	2.5330×10^{-5}	2.9725×10^{-5}	3.7787×10^{-5}
0.7	1.8000×10^{-4}	1.9499×10^{-4}	2.2882×10^{-4}	2.9089×10^{-4}
0.9	8.2963×10^{-4}	8.9872×10^{-4}	1.0547×10^{-3}	1.3407×10^{-3}

Table 1: Comparison of the absolute errors for the obtained results and the exact solution for Example 5.1, when $n = 6$ and $\alpha = 1$.
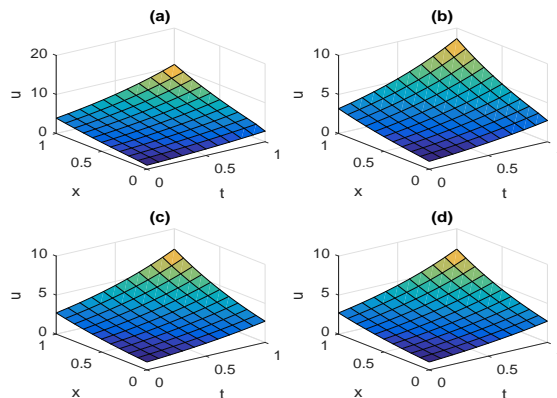
Figure 3:   The surface graph of the exact solution and the 6−term approximate solution by the FRDTM for Example 5.2 : (a) u when $\alpha = 0.6$, (b) u when $\alpha = 0.8$, (c) u when $\alpha = 1$, and (d) u is exact.
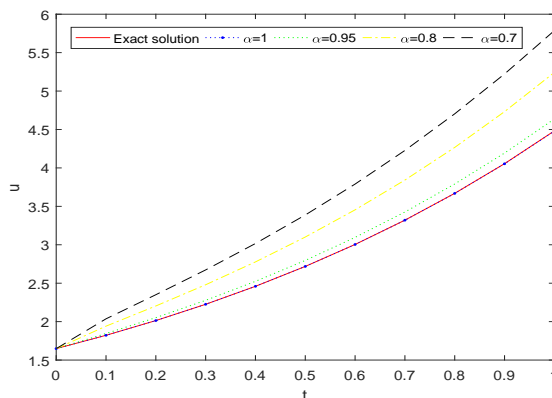

Figure 4:   The behavior of the exact solution and the 6−term approximate solution by the FRDTM for different values of α for Example 5.2 when $x = 0.5$.

t/x	0.1	0.3	0.5	0.7
0.1	1.5572×10^{-9}	1.9019×10^{-9}	2.3230×10^{-9}	2.8373×10^{-9}
0.3	1.1688×10^{-6}	1.4276×10^{-6}	1.7436×10^{-6}	2.1297×10^{-6}
0.5	2.5810×10^{-5}	3.1525×10^{-5}	3.8504×10^{-5}	4.7029×10^{-5}
0.7	2.0036×10^{-4}	2.4472×10^{-4}	2.9890×10^{-4}	3.6507×10^{-4}
0.9	9.3372×10^{-4}	1.1404×10^{-3}	1.3929×10^{-3}	1.7013×10^{-3}

Table 2: Comparison of the absolute errors for the obtained results and the exact solution for Example 5.2, when $n = 6$ and $\alpha = 1$.
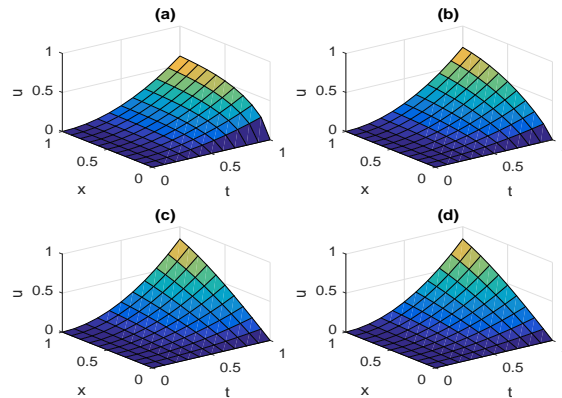
Figure 5:   The surface graph of the exact solution and the 6−term approximate solution by the FRDTM for Example 5.3 : (a) u when $\alpha = 0.6$, (b) u when $\alpha = 0.8$, (c) u when $\alpha = 1$, and (d) u is exact.
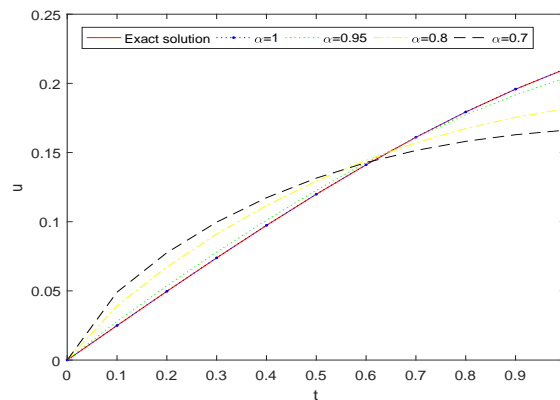

Figure 6:   The behavior of the exact solution and the 6−term approximate solution by the FRDTM for different values of α for Example 5.3 when $x = 0.5$.

t/x	0.1	0.3	0.5	0.7
0.1	1.9839×10^{-13}	1.7855×10^{-12}	4.9596×10^{-12}	9.7209×10^{-12}
0.3	4.3339×10^{-10}	3.9005×10^{-9}	1.0835×10^{-8}	2.1236×10^{-8}
0.5	1.5447×10^{-8}	1.3903×10^{-7}	3.8618×10^{-7}	7.5692×10^{-7}
0.7	1.6229×10^{-7}	1.4606×10^{-6}	4.0574×10^{-6}	7.9524×10^{-6}
0.9	9.3840×10^{-7}	8.4456×10^{-6}	2.3460×10^{-5}	4.5982×10^{-5}

Table 3: Comparison of the absolute errors for the obtained results and the exact solution for Example 5.3, when $n = 6$ and $\alpha = 1$.

7 Conclusion

In this paper, a new representation of exact solutions for nonlinear time-fractional wave-like equations with variable coefficients was presented by using the fractional reduced differential transform method (FRDTM). The method was applied to three numerical examples. In the numerical examples, our method gave us the solutions in the form of infinite series, this series in closed form gives the corresponding exact solutions for these equations without any transformation, discretization and any other restrictions, therefore it reduces significantly the numerical computations compare with the existing methods such as the perturbation technique, differential transform method (DTM) and the Adomian decomposition method (ADM). Also, our results obtained in this paper are in a good agreement with the exact solutions; hence, this technique is powerful and efficient as an alternative method for finding approximate and exact solutions for many other nonlinear fractional partial differential equations.

Acknowledgment

References

[1] D. Das and R.K. Bera. Generalized Differential Transform Method for non-linear Inhomogeneous Time Fractional Partial Differential Equation. *International Journal of Sciences & Applied Research* **4** (7) (2017) 71–77.

[2] Y. Keskin and G. Oturanc. Reduced differential transform method for fractional partial differential equations. *Nonlinear Sci. Lett.* A. **1** (2) (2010) 61–72.

[3] A. Khalouta and A. Kadem. Comparison of New Iterative Method and Natural Homotopy Perturbation Method for Solving Nonlinear Time-Fractional Wave-like Equations with Variable Coefficients. *Nonlinear Dynamics and Systems Theory* **19** (1-SI) (2019) 160-169.

[4] I. Podlubny. *Fractional Differential Equations.* Academic Press, New York, 1999.

[5] M. Rawashdeh. A reliable method for the space-time fractional Burgers and time-fractional Cahn-Allen equations via the FRDTM. *Advances in Difference Equations* **99** (2017) 1–14.

[6] B.K. Singh and P. Kumar. FRDTM for numerical simulation of multi-dimensional, time-fractional model of Navier–Stokes equation, *Ain Shams Engineering Journal* (2016) 1–8.

[7] B.K. Singh and V.K. Srivastava. Approximate series solution of multidimensional, time fractional-order (heat-like) diffusion equations using FRDTM. *R. Soc. Open. Sci.* **2** (2015) 1–13.

[8] A.M. Shukur. Adomian Decomposition Method for Certain Space-Time Fractional Partial Differential Equations. *IOSR Journal of Mathematics* **11** (1) (2015) 55-65.

[9] M. Hamdi Cherif, K. Belghaba and D. Ziane. Homotopy Perturbation Method For Solving The Fractional Fisher's Equation. *International Journal of Analysis and Applications* **10** (1) (2016) 9–16.

[10] Y. Zhang. Time-Fractional Generalized Equal Width Wave Equations: Formulation and Solution via Variational Methods. *Nonlinear Dynamics and Systems Theory* **14** (4) (2014) 410–425.

[11] X.B. Yin, S. Kumar and D. Kumar. A modified homotopy analysis method for solution of fractional wave equations. *Advances in Mechanical Engineering* **7** (12) (2015) 1–8.